https://ntrs.nasa.gov/search.jsp?R=19700003072 2020-03-12T04:42:22+00:00Z

N 70 12376

NASA CR 18

RESEARCH ON DIGITAL TRANSDUCER PRINCIPLES

Volume VI

THE PHOTODIELECTRIC EFFECT IN CADMIUM SULFIDE

CASE FILE COPY

ELECTRONIC MATERIALS RESEARCH LABORATORY

THE UNIVERSITY OF TEXAS

COLLEGE OF ENGINEERING

AUSTIN

RESEARCH ON DIGITAL TRANSDUCER PRINCIPLES

Volume VI

THE PHOTODIELECTRIC EFFECT IN CADMIUM SULFIDE

for the

NATIONAL AERONAUTICS AND SPACE ADMINISTRATION

GRANT NGR-44-012-043

Covering the Period

July 1, 1967 - June 30, 1968

by

James J. Hinds

William H. Hartwig

The University of Texas at Austin

Austin, Texas 78712

PREFACE

Previous work by this laboratory on photodielectric effect in semiconductors has led to a digital transducer which converts analog light intensity to change in frequency of a superconducting cavity. This is a digital behavior in a practical sense since the frequency is a naturally countable output. The work reported on was of a wide bandwidth detector consisting of a silicon or germanium wafer in the cavity. The optically induced free-carrier effect had a lifetime of less than a microsecond. When the light was removed the frequency change dropped to zero with that time-constant.

It is evident greater sensitivity could be realized if the lifetime was extended. In the limit the free carriers might become trapped and the effect could then be one of the change in polarization between a valence-band electron and a trapped electron. At low temperature the lifetime would become essentially infinite, or the effect could be considered as "photographic" in nature. With this hope in view, research was started on Cadmium Sulfide with Aluminum and Silver as possible impurities. If successful the detector which could be built would have a memory in the sense that it would integrate the total light flux and hold it in the form of a permenant frequency change. The frequency change would not decay when the optical stimulus was removed.

Of even greater interest was the possible device application of the little-known "tap effect". When CdS and other optically sensitive crystals are given a mechanical shock the change in polarization is removed by some mechanism that is not well understood. There appeared to be a possible

digital transducer which would convert impulse to frequency or which could be used to reset the photodielectric effect. Both the photodielectric effect and the "tap effect" are regarded as fruitful areas for digital transducer concepts.

ABSTRACT

In cadmium sulfide single crystals at cryogenic temperatures, the photodielectric effect is a result of the trapping of optically generated electrons. A change in both the real and imaginary parts of the dielectric constant is observed when the semiconductor sample is placed in a superconducting microwave resonant cavity and illuminated. The resonant frequency of the cavity decreases due to an increase in the real part of the dielectric constant, while a change in the imaginary part is detected as an increase in the amount of microwave power absorbed in the cavity. Using a simple harmonic oscillator to represent trapped electrons, equations are derived which accurately predict the change in the dielectric constant due to those electrons.

It is shown that the magnitude of the photodielectric effect due to a single trapped electron is proportional to E^{-3}, where E is the separation of the trapping level from the conduction band. There is a minimum useable value of E, however, found to be about 0.001 eV. For smaller energies, the electron acts like a free electron. Other parameters which affect the size of the cavity frequency change are the density of trapped carriers, the sample volume and the resonant frequency of the cavity. For example, a 0.143 cm^3 CdS:Al sample yields a frequency change of 730 kHz in an 830 MHz cavity due to the filling of 0.127 eV traps, with a concentration of about 1.7×10^{17} cm^{-3}.

Using simultaneous power absorption and frequency change data, it is possible to separate photoconductivity and photodielectric effects in the sample. The harmonic oscillator model predicts a larger amount of power absorption for free electrons than for bound carriers, and this relation is experimentally confirmed. A large change in the slopes of Δf and ΔP vs time, for a constant applied light, indicates the approximate time at which the electron traps become saturated and the formation of a persistent photocurrent begins.

It is further shown that the photodielectric effect has a sensitive dependence on the tap effect. The frequency change can be partially reset by applying mechanical energy. For example, the frequency recovered 20 kHz due to the weak vibration associated with a liquid helium transfer process. The results here agree with the popular model of the tap effect, attributing the phenomenon to the freeing of trapped holes. Further investigation is proposed.

Uses of the CdS-microwave cavity system operated in the photodielectric mode fall into two categories: (1) study of material properties, and (2) detection of steady weak lights. For studying trap depths and densities, as well as the tap effect and infrared quenching, the photodielectric method is easier to use than the TSC method, and provides results which are more readily analyzed, for the case when traps are shallow and not too closely spaced.

A photodielectric detector using CdS has a minimum detectable power level of 5×10^{-12} watts, assuming an integration time of one

hour and a minimum detectable frequency change of 1 Hz. Suggestions for improving the sensitivity include the use of larger samples with shallower traps, and a higher cavity frequency.

TABLE OF CONTENTS

Preface		iii
Abstract		iv
List of Figures		ix
List of Tables		xi
List of Plates		xii
CHAPTER		PAGE
I.	Introduction	1
	A. The Photodielectric Effect in Semiconductors	1
	B. Early Investigations	2
	C. Expected Photodielectric Response in CdS	3
II.	Physics and Chemistry of Cadmium Sulfide	6
	A. Crystal Structure	6
	B. Energy Bands	9
	C. Sensitization	17
	D. Other Factors Affecting the Model	24
	1. Storage Effect	24
	2. Infrared Quenching	27
	3. Tap Effect	29
	4. Absorption Edge	30
	5. Electric Field Effects	31
III.	The Photodielectric Effect	32
	A. The Change in the Dielectric Constant	32
	B. Free Electron Contribution	46
	C. Cavity Perturbation Theory	46

CHAPTER		PAGE
	D. Power Absorption	49
IV.	Determination of Electron Trap Energy	54
	A. Thermally Stimulated Conductivity	54
	B. Initial Rise of TSC Curve	59
	C. Decayed TSC	59
	D. Relative Optical Absorption	60
V.	Experimental Techniques	67
	A. Preparing Cadmium Sulfide Samples	67
	B. Preparing the Cavity	69
	C. Photodielectric Effect Apparatus	71
	D. Light Source and Calibration	76
	E. Thermally Stimulated Conductivity Apparatus	86
VI.	Results	91
	A. The Photodielectric Effect	91
	1. Aluminum Doped Samples	91
	2. Nominally Pure Cadmium Sulfide	99
	3. High Purity Cadmium Sulfide	100
	B. Power Absorption	100
	C. The Tap Effect	103
	D. Photodielectric Optical Detector	105
	E. Summary and Recommendations	106
Bibliography		109
Additional References		113
Vita		121

LIST OF FIGURES

Figure		Page
II-1a	Zincblende Crystal Structure	7
II-1b	Wurtzite Crystal Structure	7
II-2	E_g vs T in CdS	10
II-3	Temperature dependence of edge emission in cadmium Sulfide	13
II-4	Energy level model for sensitization	18
II-5	Expected curve of conductivity vs time	21
II-6	Photoconductivity and Luminescence in CdS:Ag	22
II-7	Excitation characteristics of a typical sample of CdS	23
II-8a	Comparison of the action of 3μ irradiation and 1μ irradiation on photoconductivity of CdS:Ag at 77°K	28
II-8b	Simple energy model to describe infrared quenching in CdS:Ag	28
III-1	Dependence of $\Delta\varepsilon_r'$ on binding energy	40
III-2	Re-entrant Coaxial Cavity	47
III-3	Dependence of $\Delta\varepsilon_r''$ on binding energy	51
IV-1	Shape of theoretical TSC curve.	60
IV-2	Observed TSC peak for a single trap	61
IV-3	Change in the shape of the TSC curve due to the emptying of more than one electron trap	62
IV-4	Comparison of normal and decayed TSC results	63
IV-5	Relation between photon energy and trap energy	64
IV-6	Trap distribution derived from relative optical absorption measurement	65
IV-7	TSC peak current vs wavelength for cadmium sulfide sample 6	66

Figure		Page
V-1	Block diagram of the apparatus used to study the photodielectric effect	73
V-2	Cavity assembly in place in the dewar assembly	74
V-3	Transmission coefficient for typical fiber optic bundles	78
V-4	Collection efficiency for a silicon solar cell	79
V-5	Current-voltage characteristic of a silicon solar cell for low light conditions	81
V-6	Circuit representation of a silicon solar cell connected to an ammeter	83
V-7	TSC apparatus	87
V-8	TSC sample holder	89
V-9	Heating rate for TSC apparatus	90
VI-1	Typical photodielectric results	92
VI-2	Comparison of photoconductivity and photodielectric responses	94
VI-3	Energy level model for CdS:Al sample 4	95
VI-4	Comparison of power absorption and frequency change	101
VI-5a	Comparison of the changes in frequency and power absorption in CdS:Al sample 4 due to a single 5 sec pulse of 4 milliwatt white light	102
VI-5b	Photoconductive response of sample 4 at 4.2°K, predicted from power absorption data	102
VI-6	Comparison of the changes in absorbed power and frequency as trap saturation is approached	104

LIST OF TABLES

Table		Page
II-1	Energy levels in CdS	11
II-2	Impurity concentrations in three nominally pure samples of CdS and one sample of CdS:Na	16
V-1	Specific characteristics of ideal tungsten filaments	82
VI-1	Characteristics of photodielectric samples	93

LIST OF PLATES

Plate		Page
1	Photodielectric effect apparatus	72
2	Disassembled cavity assembly	75

Chapter I

INTRODUCTION

A. The Photodielectric Effect In Semiconductors

In materials such as Ge and Si, the photodielectric effect is a decrease in the real part of the complex dielectric constant which follows the optical excitation of the crystal. This decrease is a reflection of the dynamic response when a number of bound electrons (in the valence band) become free and experience inertia forces, resulting in a phase shift between the carrier velocity and an applied RF electric field. The effect is normally short-lived, however, due to free carrier lifetimes of the order of 10^{-7} sec in Si and Ge. Arndt, Hartwig and Stone[1*] have shown that these semiconductors have relatively wide bandwidth characteristics and make relatively insensitive detectors of light, suitable for detecting high frequency amplitude modulated lasers. These materials are not sensitive detectors of steady, weak light, however.

Analysis showed that the gain-bandwidth product of a semiconductor photodielectric detector is a constant. Thus, sensitivity may be increased only at the expense of bandwidth. For steady, weak light, wide bandwidth is not needed, and sensitivity may be maximized. Since photoconductor gain is proportional to the free carrier lifetime, it would be expected that semiconductors with long free carrier lifetimes would tend to be sensitive optical detectors when operated in either the photoconductive or photodielectric mode.

---

* References listed in bibliography.

Cadmium sulfide is one of the most sensitive semiconductor photodetectors at room temperature, and its speed of response is on the order of 10^4 to 10^6 slower than for Ge or Si. Thus it was apparent that perhaps the photodielectric effect in CdS or other II-VI compounds at low temperatures would be suitable to allow the use of these materials in a slow but sensitive optical detector.

B. Early Investigations

Although the photoconductivity of semiconductors has been well studied, relatively little work had been done before 1960 on the corresponding photodielectric effects. The possibility of observing the photodielectric effect in silicon and germanium at low temperatures was proposed by Hartwig[2] and Genz[3]. Experiments showed that the noise level at 77°K, due to thermally generated carriers, masked whatever photodielectric effect might have been present. Arndt[4] repeated the measurements at 4.2°K and was able to observe a frequency shift of 90 kHz in the resonant frequency of a 810 MHz superconducting resonant cavity containing silicon. Stone[5] carried the analysis of the system further, and also designed and successfully operated a laser detector with a 1 MHz bandwidth, using the photodielectric effect in silicon.

A summary by Bube[6] of photodielectric effects in CdS-type materials revealed three possible explanations for observed apparent changes in the dielectric constants of those materials, given as follows. (1) In photoconductors with parallel plate electrodes, the change may actually represent a change in the effective distance between the electrodes, due to an increase

in the conductivity. (2) It might be a reflection of the formation of a space charge at grain boundaries in powders. (3) It may be the result of an actual change in the polarizability of the crystal, due to the trapping of electrons. Bube's conclusion was that each of the three explanations is possible, depending on the various physical conditions of the sample and its environment.

C. Expected Photodielectric Response in Cadmium Sulfide

Library research proved that CdS, and especially silver doped CdS (CdS:Ag), may in some cases be characterized by long free carrier lifetimes. Lambe[7] reported a photocurrent decay time of about 0.3 ms in CdS:Ag at 77°K. In another CdS:Ag sample at 77°K, Lambe[8] described photocurrent decay times of about 10 minutes. Kulp[9] reported photocurrents which did not decay at temperatures below 208°K in a Na-doped CdS crystal. Decay times greater than 1 minute in CdS at 276°K were observed by Bube[10]. Time dependence of capacitive decay in a capacitor with a ZnS-CdS powder dielectric, observed by Kronenberg and Accardo[11], had a two minute decay time at liquid air temperature. Matthews and Warter[12] reported photoconductivity decay times greater than 10^{-3} sec in CdS at 188°K. Many others observed similar long decay times. It must be remembered that lifetime and decay time are not the same, due to trapping effects. For example, a photoconductor with a density of n free carriers and n_t trapping sites has a response time given by

$$\tau_{on} = (1 + \frac{n_t}{n})\tau_n \qquad (1-1)$$

where τ_n is the free carrier lifetime, and thus the actual free carrier

lifetime may be much less than the response time [A complete analysis of this problem is given by Rose[13]]. Even considering this difference between lifetime and response time, the free carrier lifetime in CdS is still considerably longer than in Ge or Si at low temperatures.

The difference in the photosensitivities of cadmium sulfide and silicon is a result of certain trapping effects in the cadmium sulfide. Sensitive crystals of cadmium sulfide have a large concentration of deep hole traps. These traps slow the rate of recombination of free holes and electrons, and therefore allow the electrons to have a longer free lifetime.

Cadmium sulfide may have a photoconductive gain greater than unity. The photoconductivity gain is defined as the ratio of the number of charge carriers passing between the photoconductor electrodes in a unit time to the number of electron-hole pairs generated in a unit of time. In other words it is the ratio τ_L/T, where τ_L is the free carrier lifetime and T is the carrier transit time between the electrodes. According to Bube[14], electrons are always the majority carriers in cadmium sulfide, due to the large amount of hole trapping. Photoconductivity gains, due to long free electron lifetimes, may easily be made as large as 10^4 to 10^5.

It should now be obvious why a photodielectric detector using a cadmium sulfide sample was expected to be sensitive and slow in response. Since the rate of recombination is greatly reduced, the free electrons generated by the first few photons in a pulse of light are still free at the end of the light pulse, and thus the density of free carriers is large. If the same pulse of light were applied to silicon, however, the electrons freed by the first few photons would quickly recombine so that no trace

of them would be left at the end of the pulse. Therefore, the photosensitivity of silicon is smaller than that of cadmium sulfide.

The speed of response of silicon, on the other hand, is higher than that of cadmium sulfide. Since the free electron lifetime of silicon is shorter, the conductivity is able to follow more rapid changes in the amplitude-modulated light. The maximum modulation frequency which the photoconductor is able to follow is approximately equal to $1/\tau_L$.

To investigate the photodielectric effect in cadmium sulfide at $4.2^{\circ}K$ and to evaluate its usefulness as an optical detector when operated in the photodielectric mode, a series of experiments was proposed using the superconducting resonant cavity described by Hartwig and his co-workers.[1,2,3,4,5] It was hoped that the experimental technique would yield new insight into optical effects in cadmium sulfide by giving simultaneous dielectric and absorption measurements. In particular it was hoped that the change in the lattice polarization could be observed, when electrons were excited from the valence band to traps. The sensitivity and usefulness of a photodielectric detector using cadmium sulfide was to be determined and evaluated, and methods of maximizing the performance of the system were desired. The final goal was to develop a model and analytical procedure to explain observed effects and predict photodielectric behavior in cadmium sulfide.

Chapter II

PHYSICS AND CHEMISTRY OF CADMIUM SULFIDE

The optical and electronic processes which occur in cadmium sulfide tend to be quite complex, due to the physical and chemical nature of the substance. Many phenomena have been explained in a satisfactory manner; others are still under study. The following chapter presents a brief discussion of some of the properties of CdS necessary for the explanation of the photodielectric effect.

A. Crystal Structure

Cadmium sulfide may crystallize in either the zincblende structure or the wurtzite structure, which are both shown in figure II-1. It is seen that the zincblende structure would be the diamond structure if the atoms were all the same. Every atom is surrounded by four nearest neighbor atoms of the other kind, located at the vertices of a tetrahedron. In the sublattice of atoms of the same kind, there are twelve nearest neighbors. Six of these are located at the vertices of a hexagon surrounding the original atom. Three more are above, and three are below, at the corners of a tetrahedron. Due to this arrangement, there is no center of symmetry or inversion, and the CdS layers have unique orientations. Zincblende crystals are therefore polar, and opposed faces and opposed directions, in general, have different physical and chemical properties. For example, zincblende crystals are piezoelectric.

The wurtzite structure differs slightly from the zincblende. Each Cd atom is bonded to four S atoms, approximately at the corners of a tetrahedron, but they do not have the same spacing. The twelve next to

● - Cd

○ - S

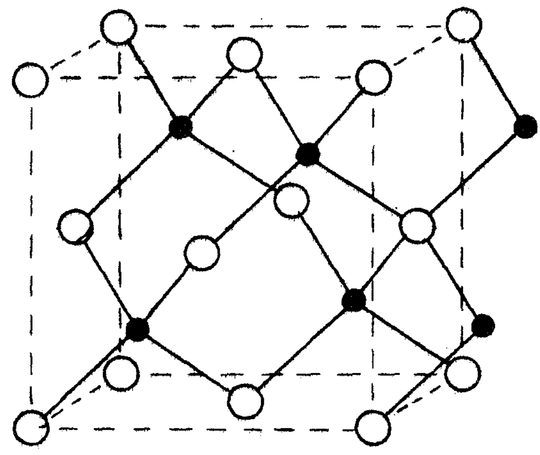

Fig. II - Ia. Zincblende crystal structure.

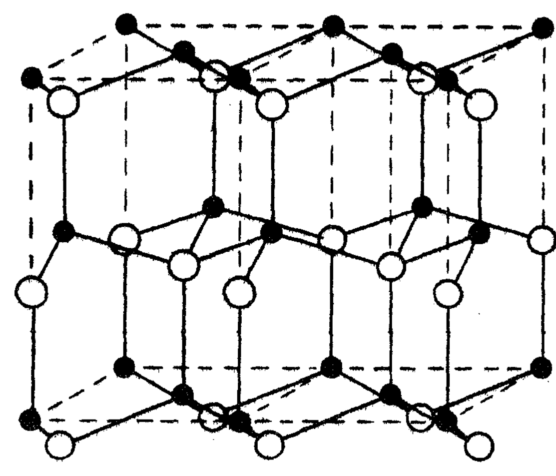

Fig. II - Ib. Wurtzite crystal structure.

nearest neighbors are arranged as in the zincblende structure. The wurtzite structure may also be viewed as two interlaced hexagonal close-packed lattices. Wurtzite likewise has no center of symmetry and the Cd and S atoms can be visualized as forming a network of permanent dipoles. In zincblende, the network is balanced, but in wurtzite there is no balance. The result is that wurtzite may be pyroelectric as well as piezoelectric. For additional details concerning crystal structure, the reader is referred to Smith[15]. Lattice parameters for CdS are given by Segall[14].

Either form of CdS may be prepared, depending on the method of preparation. According to Newberger[16], the hexagonal wurtzite form is the stable modification between 25°C and 900°C. The zincblende structure reverts to the wurtzite when the crystal is heated above 100°C.

Due to the type of crystal structure, many of the physical properties of CdS depend on the crystal orientation. Those which are of major concern here are the absorption coefficient, the dielectric constant, the effective masses, energy bands, mobility, and the reflection coefficient. Values for these parameters are normally given for alignment either perpendicular to or parallel to the c axis, which is the axis normal to the plane of the hexagon. The ratio of $\varepsilon_{r\perp}$ to $\varepsilon_{r\parallel}$ may be as great as 1.4 according to Czyzak[17]. The corresponding ratio for the electron effective mass is given as 1.05 by Hopfield and Thomas[18], while the ratio for the hole effective mass may be as high as 7.0. Zook and Dexter[19] found that there is a single conduction band minimum at k = 0, so the band gap transition is direct. Dutton[20] shows that the anisotropy of the absorption coefficient follows approximately the relation $\alpha_{\parallel}(\lambda) \approx \alpha_{\perp}(\lambda + 300\ \text{Å})$ over a

wide range of temperatures, while for the reflection coefficient, Lempicki[21] gives $\rho_{\perp}/\rho_{\parallel} = 1.15$. In the following analysis, only the anisotropy of the dielectric constant may cause difficulties.

B. Energy Bands

The energy band structure of pure and doped CdS has been studied by many observers; a complete picture is given by Cardona and Harbeke[22]. For this paper, only the energy gap between the conduction band and the valence band will be of interest. The fact that this band to band transition is direct has already been mentioned. Cardona and Harbecke give $E_g = 2.53$ eV at 300°K, and Hopfield and Thomas[18] give $E_g = 2.5826$ eV at 4.2°K. Using the latter value and data given by Colbow[23] results in a plot of E_g vs T, given as figure II-2.

The energy levels which appear within the CdS bandgap are also well studied. The only levels which can be predicted accurately are those donor levels which are due to group 3 or group 7 impurities, and those due to Cd vacancies. Calculations based on a hydrogenic model give $E_d = 0.032$ eV, while the observed values tend to be closer to 0.030 eV, as reported by Bube[6]. Other data concerning energy levels is given in Table II-1. In using this data, it should be realized that in general the origins of some of the energy levels are not definitely known.

Since the value of the band gap energy varies with temperature, it might be expected that the same is true for the energy levels. A curve of edge emission vs temperature in CdS, indicating levels down to 0.25 eV, is given by Kulp, et. al. [24] and is reproduced in figure II-3. The most noteworthy feature is that for temperatures below 100°K, any change in the position

Fig. II - 2. E_g vs T in CdS.

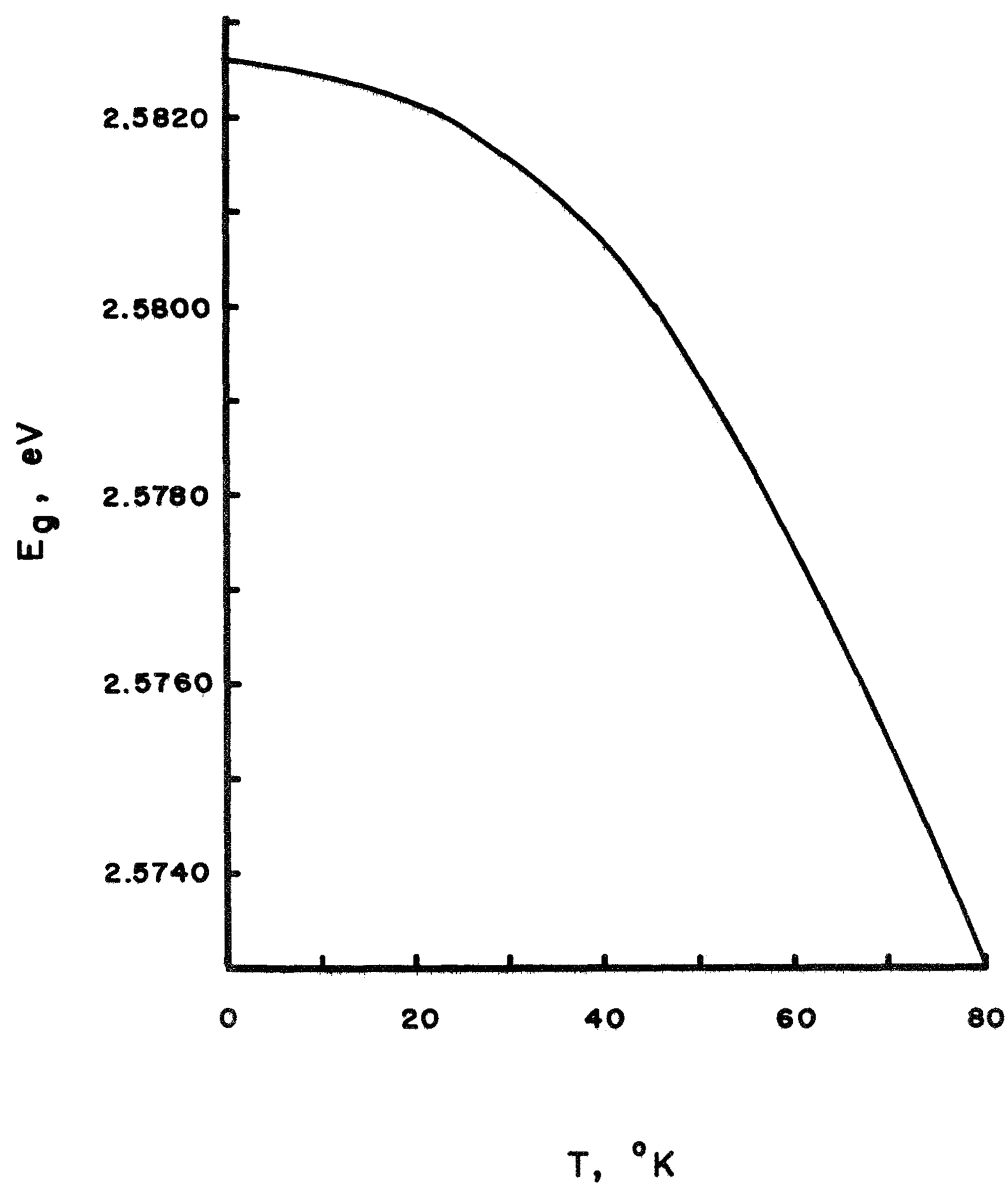

Table II-1

Energy Levels in CdS

$E_c - E$ (eV)	Probable Origin	Reference	Type*	Note*
.0011		9		a
.005		25		a
.007		9		a
.0095	Cr	16		
.0107	In	16		
.02	Cl	9		
.03	Al,Cl	23	D	
.03	Group III,VII	6	D	
.14		9	e	
.152	Ca,Mg	16	A	
.158	Ni	16		
.16		26	A	
.170		27	A	b
.173	Ni	16		
.20	S	28	A	
.23		25	e	
.24		26	A	
.25	S	28	A	
.25		9	e	
.25		29	e	a
.33		9	e	
.35	$CuCl_2$	30		
.35	Surface	31	e	
.39		10	e	
.40	Ag	32	e	
.40	Surface	31	e	
.41	Cd	28	A	
.43	$CuCl_2$	30		
.43	Surface	31	e	
.44	Cd	28	A	
.45		26		
.46		9	e	
.50	Ag	32	e	
.51	S	28	A	
.57		9	e	

.58	Cd	28	A	
.60	$CuCl_2$	30		
.62		12		
.63	Cd	28	A	
.63		26	D	
.72		33	e	c
.78	V_s	34	e	
.78		6	D	
.82		26	D	
.83		29	e	d
.86		35		
.91	Adsorbed O_2	36		
1.0	Fe	16		

$E - E_v$	Probable Origin	Reference	Type*	Note*
.025		25		
.14	I_S	25	h	
.18	V_{Cd}	23	A	
.8	Group I	9	e	a
.8		37	e	
1.0	Ag,Cu	6		
1.0		32	h	
1.0	V_{Cd}	23	h	
1.0	"	7	h	
1.1	"	10	h	
1.3	"	34	h	

* e - electron trap
h - hole trap
D - donor
A - acceptor
V_{Cd} - Cd vacancy
V_S - S vacancy
I_S - S interstitial

a - in special samples
b - doubly ionized
c - cannot be filled for $T < 180^{\circ}K$
d - cannot be filled for $T < 210^{\circ}K$

Fig. II - 3. Temperature dependence of edge emission in cadmium sulfide. From Kulp, et. al.(24).

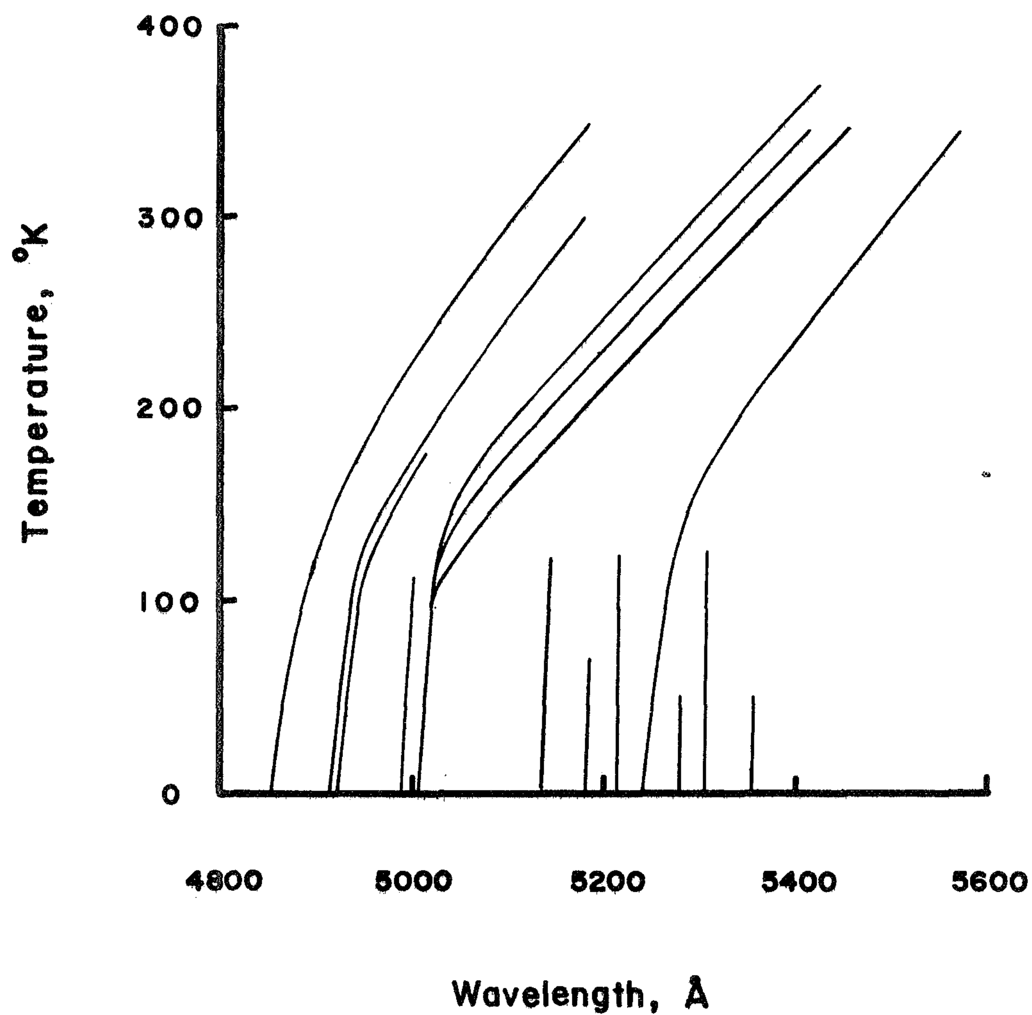

of the energy level is small, and the energy may be considered constant in the first approximation.

A question which arises is: What are the natures of the various energy levels within the forbidden band? At first glance, it might seem advisable to divide the states into the two categories of traps and recombination centers, as is normally done by Rose[8] and others. A center is classified as a recombination center if, on the average, carriers captured there have a higher probability of recombining than being re-excited. A center is a trap if the re-excitation probability is greater. Both of these terms are meant to be applied to room temperature semiconductors and insulators. It may be seen that either term is vague at low temperatures. For certain sites, the probability that a captured carrier will either recombine or be re-excited from the center within some "reasonable" amount of time, approaches zero. That is, there is very little thermal energy at low temperatures, and therefore the probabilities of both recombination and re-excitation are greatly reduced. For the present purposes, a site will be called a trap if it tends to capture and hold a carrier for a time which is long, compared to the time it spends in the conduction band.

In semiconductors and insulators, traps and recombination centers are the results of the presence of lattice imperfections, or departures from the perfect lattice. There are many types of imperfections; two of the more common ones are crystal structure defects and foreign atom impurities. The presence of free carriers and thermal motion may also be considered as imperfections, but these two defects do not contribute permanent, discrete levels in the forbidden band.

All crystals have defects; the surface is itself a departure from perfect crystalline structure. Other imperfections may involve a whole plane of atoms, as in the case of edge and screw dislocations, or may only involve discrete atoms or ions in such imperfections as Schottky defects, Frenkel defects, vacancies, and interstitials. Since a crystal without any non-surface defects cannot exist, there will always be energy levels in the forbidden band. (The explanation of how a defect generates a level in the forbidden band is covered in most solid state physics texts; for example, see chapter 3 of Wang[38].) Whether the number of various imperfections is large enough to affect the properties of the crystal depends on many factors, principally the details of the preparation of the crystal.

In general, in CdS there are always a sufficient number of defects present to contribute energy levels within the forbidden band. In the literature, dislocation defects are rarely mentioned; energy levels in cadmium sulfide are usually attributed to point defects or to several defects clustered at some point in the lattice (se Bube and MacDonald, ref. 39) Likewise, nominally pure CdS samples tend to have amounts of impurities with concentrations of several parts per million. An example of the density of impurity atoms in CdS is given in table II-2, reproduced from Kulp[9]. The samples were all nominally pure except for number 4, which was sodium doped. Here it is seen that any given sample of CdS is likely to have a large density of impurities. Certain impurities in CdS do not seem to produce levels in the forbidden band; carbon is an example.

Cadmium sulfide crystals tend to be non-stoichiometric in either direction. According to Bube[6], anion (sulfur) vacancies act as donors, and cation (cadmium) vacancies act as acceptors. Sensitive materials

Table II-2. Impurity concentrations in three nominally pure samples of CdS and one sample of CdS:Na. Concentrations are in ppm. From Kulp[9].

Element	CdS Sample #1	CdS Sample #2	CdS Sample #3	CdS:Na Sample #4	Detection Limits
Li	70	3.4	19	40	0.3
C	27	36	30	110	1.0
N	20	5	5	300	2.0
O	ND	ND	ND	ND	200
Na	460	45	570	4200	0.5
Cl	ND	17	ND	ND	3.0
K	50	1.4	63	12	0.3
Ca	3.8	1.3	0.25	0.5	0.6
Si	4.5	ND	ND	ND	1.0
Ni	12	ND	ND	3.0	1.0
In	ND	ND	ND	10	0.6
Mg	ND	2.5	2	ND	0.3

contain compensated cation vacancies (vacancies containing one or two captured electrons). Bube[10] and others believe that the acceptor sites arise due to the perturbation of the four sulfur atoms surrounding the vacant cadmium site. It is possible that for materials with moderate doping concentrations, native defects supply the major portion of the sensitization.

It is fairly easy to adjust the stoichiometry of CdS crystals. Woods[40] has found that excess Cd may be achieved by heating in a vacuum to temperatures up to 700°C. To remove excess cadmium, Colbow[23] anealed his crystals for 24 hours at 539^{0}C under equilibrium cadmium vapor pressure.

Although the acceptor sites tend to be common to most CdS crystals, donor sites depend for the most part on doping. Energy levels due to various dopants have already been listed in table II-1. It must be remembered that a great deal of speculation is involved in assigning energy levels to various imperfections. Even the level due to silver, claimed by Lambe[7,8] to be around 0.4 eV, is still disputed. Bube[41] claims that traps with depth of about 0.4 eV are fundamentally characteristic of the CdS crystal. In fact, there appears to be a quasi-continuum of levels in the range between 0.1 and 0.8 eV which may be characteristic of all CdS [see ref. 42]. The only general agreement is that cadmium vacancies generate hole traps about one electron-volt above the valence band, and columns III and VII impurities generate donor levels about 0.03 eV below the conduction band.

Other impurity effects in CdS involve various substances adsorbed on the surface, primiarily oxygen and water vapor. When the crystals are irradiated in an oxygen atmosphere, many observers[33,43,44] find that the electron lifetime is reduced by a factor of three to seven, depending on the temperature. Subsequent heating to 120°C in a helium atmosphere restores the lifetime to the original value. These changes are attributed to the photo-adsorption of oxygen. It is thought that the oxygen diffuses into sulfur vacancies and thereby destroys the sensitivity.

C. Sensitization

The main reason that cadmium sulfide is a sensitive photodetector is that it may be sensitized by impurity incorporation. The mechanism of sensitization is discussed fully by Rose[13] and involves the compensated cadmium vacancies discussed earlier. First, assume there exists a crystal with electron traps at the level E_a, as shown in figure II-4a. The sites

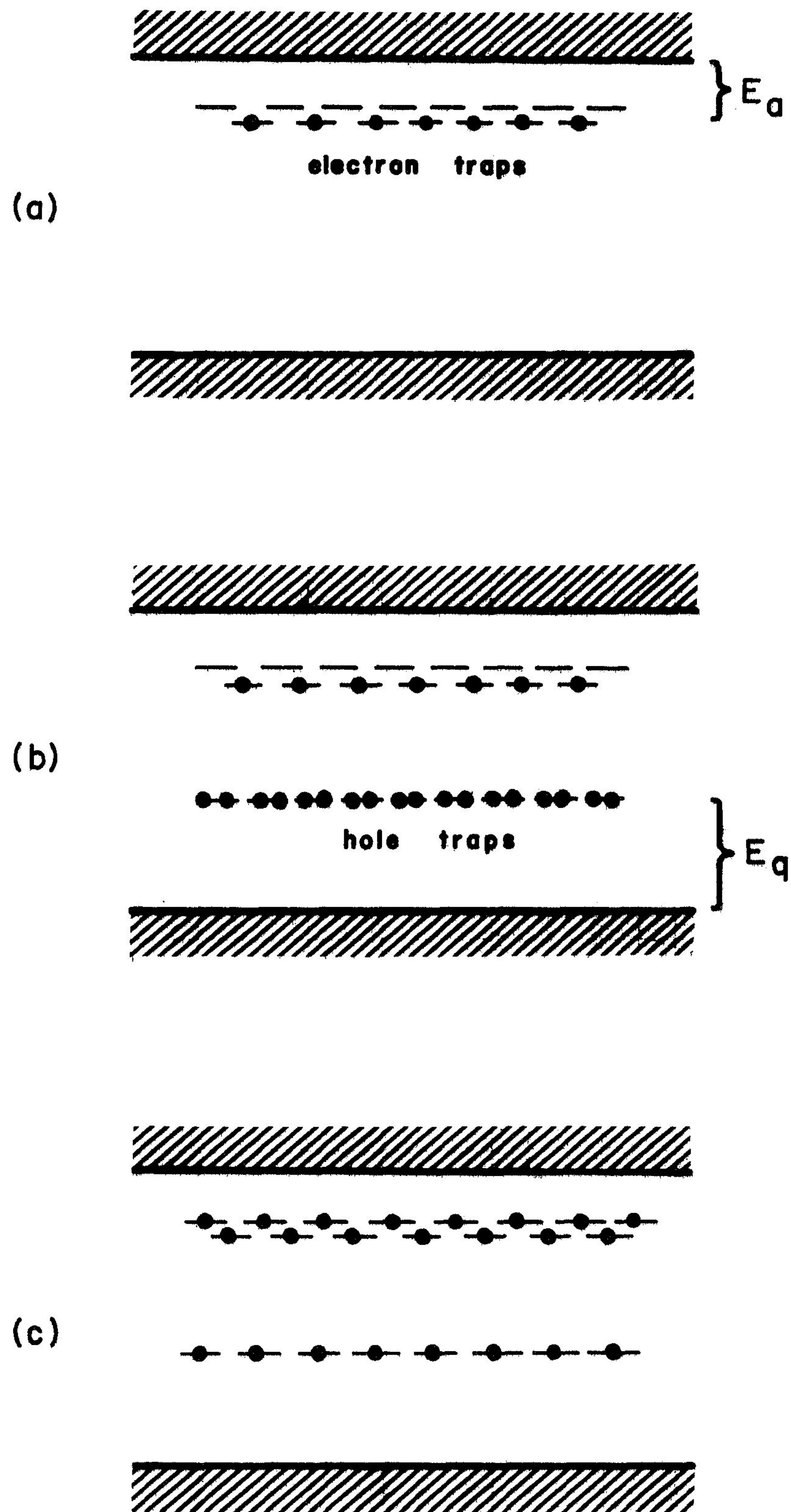

Fig. II - 4. See text.

are assumed to be partially filled with electrons. Next, let a number of compensated cadmium vacancies be introduced. Each vacancy is assumed to have two captured electrons, and thus has a double negative charge, due to the absence of the Cd^{+2} ion. The resulting level is located E_q above the valence band as shown in figure II-4b. With the energy levels in this state, assume some bandgap light is applied. The light takes electrons from the valence band to the conduction band, and normally the electron would soon suffer recombination at one of the sites in the forbidden band. This is not the case in properly prepared CdS, however, due to the nature of the cadmium vacancies (which will be called quenching sites for reasons which will be made clear later). The quenching sites, since they have captured two electrons, have a very large capture cross section for holes and a small capture cross section for electrons. The hole created by the light is immediately captured at a quenching site, reducing the charge at the site to -1. The electron formerly in the quenching site is now located in the valence band, while the electron formerly in the valence band is located in the conduction band. Since the quenching site still has a negative charge, the capture cross section there for electrons is still quite small, and the free electron tends to be captured at the activation site. This situation is presented in figure II-4c. Note that the net effect of the light is to irreversably transfer electrons from the quenching level to the activator level.

It is further evident that the presence of the conduction and valence bands is not required. If light with sufficient energy is applied, it would be expected that some electrons are transferred directly between the two levels, if the impurity sites are located physically close to each

other. For sites located farther apart, one or both of the bands would be necessary to provide the electrons and holes with a means of travel between sites.

The model presented above is thought to be the correct model for sensitized CdS. The activator element, such as Ag in CdS:Ag, provides one or more electron traps located close to the conduction band. Even without intentional doping, there are always a number of trapping levels.

It is interesting to consider a special case in which $N_q >> N_a$; i.e., there are more quenching levels than activator levels. Here, it is expected that all holes are immediately trapped, and the electrons begin filling the electron traps, filling the deepest ones first. Soon, however, all the electron traps become filled, and there remain no other places for the other electrons except the conduction band. Assuming no recombination takes place, quite a large density of electrons can be stored in the conduction band. Finally, however, all the hole traps also become filled, and any subsequently generated holes then remain free for recombination. If one were to represent this procedure in a plot of conductivity vs integrated photon flux, the curve of figure II-5 would be the expected approximate result.

The first portion of figure II-5 represents the time during which both hole and electron traps are filling. No appreciable increase in the number of free electrons is expected here. When the time reaches t_1, however, the electron traps will all be filled, and thus the electrons produced after $t = t_1$ must remain in the conduction band. At the same time, the holes are still proceeding to the hole traps. Finally, the hole traps begin to saturate at $t = t_2$, and any electron-hole pairs generated are

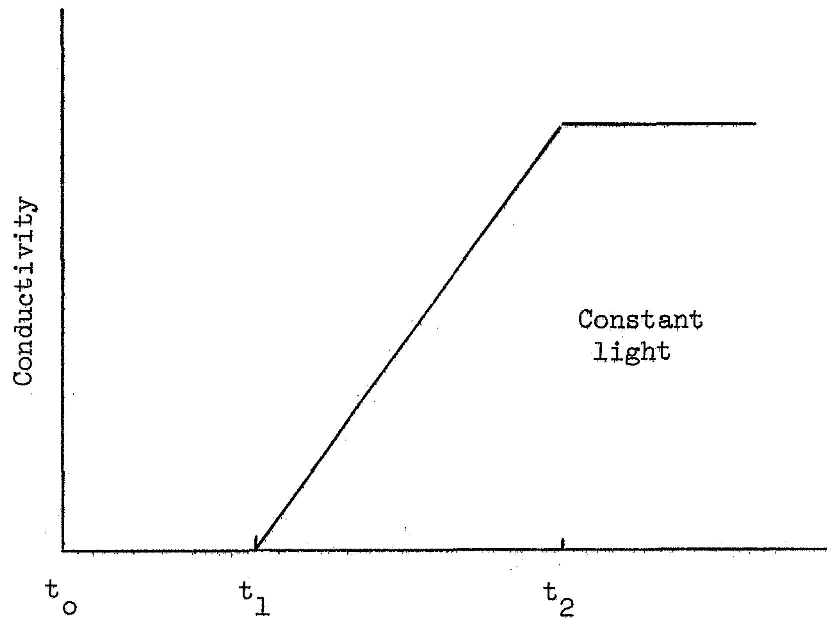

Fig. II-5. Expected curve of conductivity vs time.

then available for recombination halting the increasing conductivity.

In the preceding discussion, recombination in the early stages has been ignored. It can easily be shown that if all of the activation centers are initially empty, and an electron is then excited to one, that electron will have a very small probability of escape if the temperature is low enough. In fact, this specific feature is the basis of the thermally stimulated conductivity technique, which is discussed later. Therefore, it is felt that a recombination-free model is actually quite accurate.

The effect discussed above has been aptly termed "storage", and storage effects have been reported by many workers[7,9,11,45,46]. Most

experimenters make observations after the activator traps have been saturated, so that the only evidence of the storage phenomenon is a persistent photocurrent at low temperatures. Lambe[7], for example, observed the photoconductivity and luminescence curves reproduced in figure II-6. At a temperature of 77°K, the photoconductivity in CdS:Ag is seen to have a rapidly decaying component and a persistent component. The initial decay is accompained by orange emission, which is attributed to the recombination of free holes with trapped electrons. Electron traps are kept filled at the expense of the free electron density, causing the photoconductivity to drop. Both the decay and the luminescence cease when the supply of free holes is exhausted.

In CdS films at 4.2°K, Eastman and Brodie[45] observed persistent photocurrents whose magnitudes depended directly on the period of illumination over a suitable range of time. The half-life of the storage current was

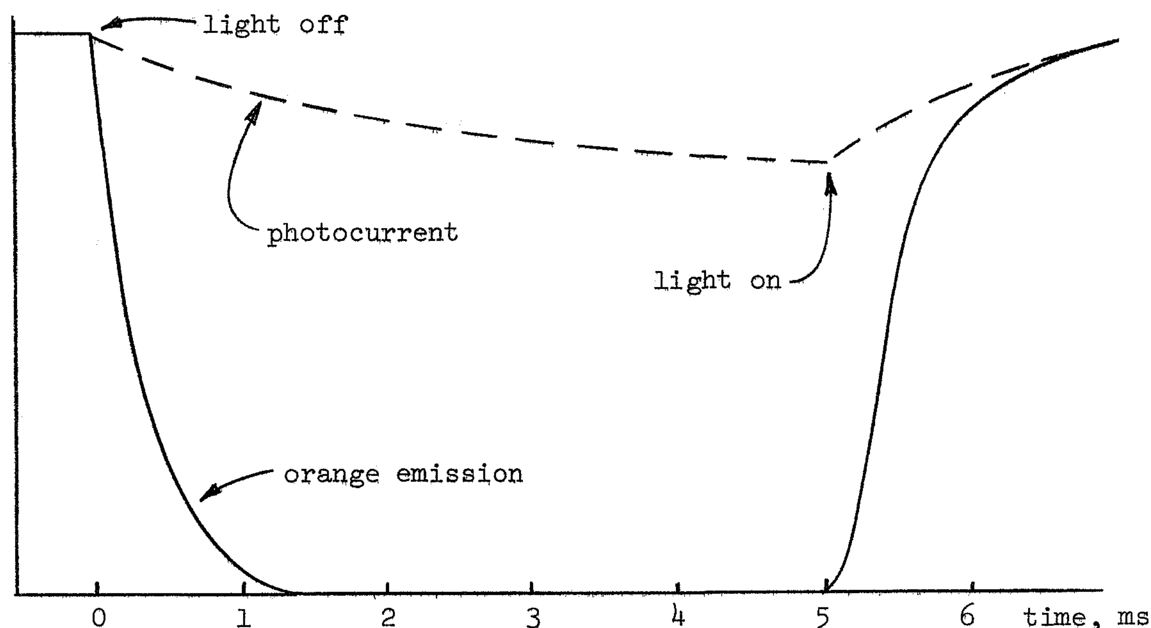

Fig. II-6. Photoconductivity and luminescence in CdS:Ag. From Lambe[7].

reported as 120 hours , and the effective wavelength was anywhere in the range 4500 Å < λ < 6500 Å. At liquid nitrogen temperature, the same effects were noted, expect the half life dropped to 24 hours.

Kronenberg and Accardo[11] measured both the photodielectric effect and the photoconductivity in CdS at 77°K, and discovered that storage effects were only noted in those crystals which showed an apparent change in dielectric constant at the low temperature. They attributed both effects to trapped electrons, but did not analyze the problem in detail.

Kulp[9] observed the same effects, and more. His plot of the initial rise of the storage current at 77°K is reproduced here as figure II-7.

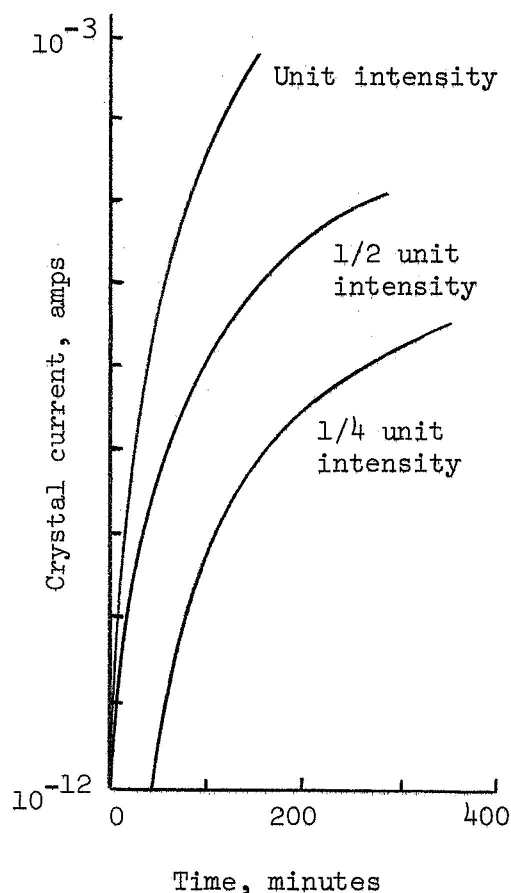

Fig. II-7. Excitation characteristics of a typical sample of CdS. From Kulp[4].

A comparison of figure II-7 and figure II-5 shows that to the first approximation, Kulp's crystal fits the model discussed earlier. For the lower light intensities, a considerable delay was experienced before any current at all could be observed. When a current did come into view, however, the rise was very rapid, and in each case, the current finally saturated. It was further noted that the decay of the current depended on the temperature; for temperatures below about 200°K, there was no decay, while for gradually increasing temperatures, the decay time dropped sharply. Later, it is seen that the specific CdS:Al crystals analyzed in this thesis behave nearly identically to those used by Kulp.

D. Other Factors Affecting The Model

The simple model presented in the previous section contains only enough features to explain a few experimental results, such as long life-times and high sensitivity. There are other phenomena occurring in CdS which must also be explained, and the model for these new effects must at least be consistent with the previous model.

1. Storage Effect

Many experimenters have observed the decay of the persistent photoconductivity at various temperatures. In general, the current begins to decay rapidly in the vicinity of 200°K, being essentially fixed at lower temperatures. Thermal quenching of the persistent photocurrent should be distinguished from thermal quenching of photo-sensitivity, which normally occurs near 400°K in CdS. The latter effect is no doubt due to the rapid thermal excitation of holes from the quenching levels, leaving them available for rapid recombination. Bube[34] has reported that infrared quenching, which

depends on the presence of trapped holes, drops sharply at temperatures above 400°K.

Although persistent photoconductivity quenching is reported by many, there appears to be no consistent way to explain the drop in current near 200°K if the holes still remain securely trapped up to 400°K. It has been assumed that any free holes are rapidly used up in either the trapping or recombination process. Free holes are always being generated at any finite temperatures, but the number of thermally generated holes would not increase rapidly relative to the number of free electrons in the vicinity of 200°K.

One solution to the preceding problem may be found in the work of Bube, et. al.[33], and Woods and Nicholas[29]. Using CdS and CdS-CdSe, Bube noted the presence of a 0.72 eV electron trap which cannot be filled at temperatures below 180°K. It always appears together with a 0.43 eV trap which can always be filled, and at temperatures above 180°K has a capture cross section of about 10^{-14} cm^2. The density of the traps appeared to be a constant, unaffected by any combination of heating, ambient atmosphere, or illumination.

Woods and Nicholas observed a trap at 0.83 eV which could not be filled at temperatures below 210°K. It was always associated with a trap at 0.41 eV which could always be filled, and its capture cross section was also about 10^{-14} cm^2. They also noted, however, that the unfillable trap was always found in both Cd-rich and S-rich crystals, and could be created or destroyed, apparently reverting to a 0.25 eV trap, following certain combinations of heating and intense illumination. The interpretation of the

0.83 eV trap was that it is not a normal trap, but rather a complex imperfection which dissociates when the trapped electron is thermally freed, and must be recreated by photoexcitation through a photochemical process.

Bube's crystals did not exhibit the same behavior, and he argues in favor of a normal trap surrounded by a Coulomb replusive barrier, extending above the conduction band (see ref. 47). At low temperatures, the capture cross section drops to such a low value that filling is no longer possible. It is evident that although the details of the capture process are still not clear, there is widespread agreement that such a trap exists in the general case. It may possibly be related to the sensitizing centers themselves, which have a small capture cross section for electrons at low temperatures, but are able to hold one or two electrons at room temperatures.

The decay of the persistent current near 200°K may now be explained, using the repulsive traps. After the current is generated by low temperature excitation, the 0.72 eV traps still remain empty. Heating to about 200°K causes the capture cross section of that trap to grow until the free electrons begin to fall into the deep traps, causing the current to drop. If the 0.72 eV traps are related to the deep hole traps, this heating would open a broad avenue to recombination, effectively resetting the crystal for the next excitation period. Evidence in favor of the last proposition includes the previously mentioned fact that thermal quenching of photosensitivity tends to occur near 400°K, but an excited crystal can be reset by a short period of warming to room temperature. Also, the repulsive traps can be created and destroyed in exactly the same manner as deep hole traps, namely by the addition or removal of excess Cd.

Several investigators[9,32,47] have discussed the presence of excited states of various trapping levels. For example, in explaining the presence of a distribution of trapping levels from 0.7 to 0.1 eV, Dussel and Bube[47] tend to favor the situation in which an electron may be captured by an excited state of a trap, and then gradually decay to the ground state though the emission of several phonons. The decay process can take place if the electron is able to give off the phonons before being thermally re-excited; at low temperatures in CdS, it is clear that the decay is a certainty.

2. Infrared Quenching

Infrared quenching effects must also fit comfortably into the model for sensitive CdS. The variety of infrared effects is too extensive to allow complete coverage here. The effects depend on the temperature (ref 33,34) the excitation and warming history of the sample (ref 9), and of course, on the doping and wavelength. The best descriptions of infrared quenching in sensitive CdS are found in the works of Lambe[7,32,48]. His plot of the response of CdS:Ag to infrared light at $77^{\circ}K$ is given in figure II-8, together with the simple energy model. The conditions under which the curves were obtained require first that the crystal be illuminated long enough to create a presistent photoconductivity. No infrared response is observed unless this is first done.

Next if light with $\lambda \approx 3\mu$ is applied, a definite enhancement of current is observed as long as the light is left on, and is shown in the figure. Actually, any light with $2\mu < \lambda < 6\mu$ produces these results, but the effect is greatest near 3μ. Note that the 3μ light adds nothing to the persistent photoconductivity. If 1μ light is then applied, a slow but complete quenching of the persistent photoconductivity takes place.

Fig. II-8a. Comparison of the action of 3μ irradiation and 1μ irradiation on photoconductivity of CdS:Ag at 77°K. From Lambe and Klick[32].

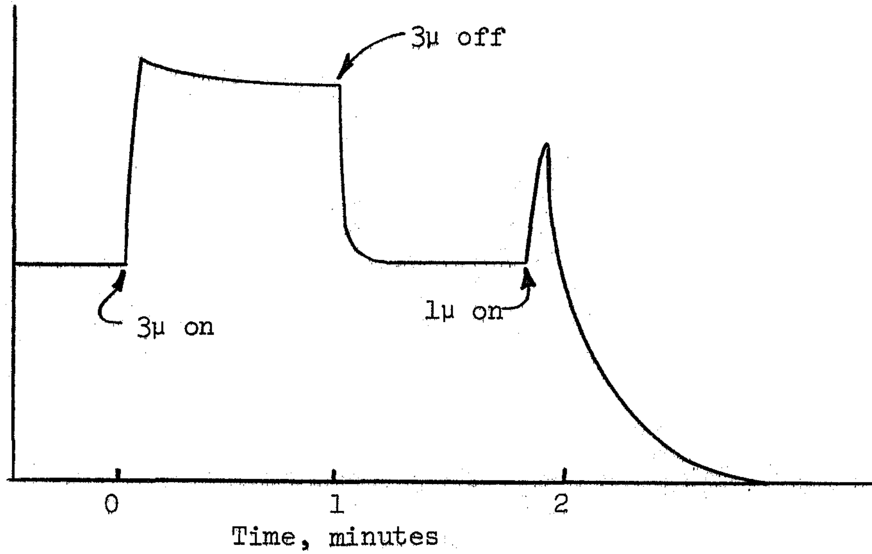

Fig. II-8b. Simple energy model to describe infrared quenching in CdS:Ag.

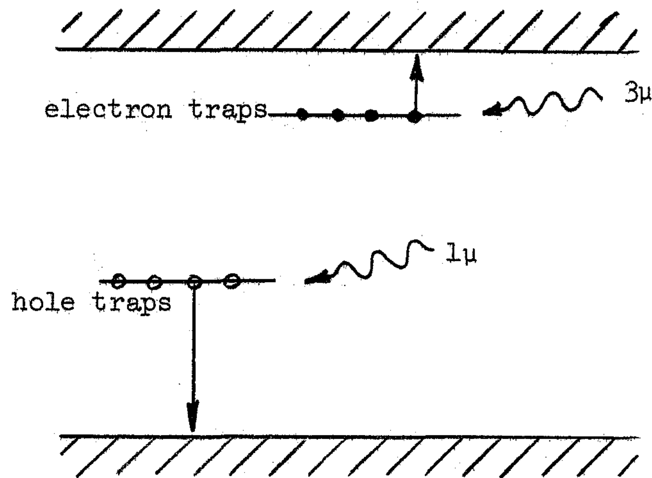

Referring to the energy model, the preceding results are easily explained. The bandgap light transfers electrons from the quenching sites to the activator sites, as was discussed earlier. Assuming there are more quenching sites than activator sites, some excess electrons are left in the conduction band, giving rise to the persistent photoconductivity. When 3μ light is applied, it is energetic enough to excite electrons from the activator sites to the conduction band, and these electrons are quickly retrapped when the light is removed. The 1μ light, however, has sufficient energy to excite holes from the quenching sites to the valence band. Free holes then combine with the trapped electrons, producing a burst of orange luminescence. Free electrons then drop into the traps to take the place of the electrons which recombined, and thus the persistent photoconductivity is quenched. This quenching by 1μ light leads to the practice of calling the hole traps "quenching centers".

Some care must be used in selecting the temperature and wavelength for infrared quenching experiments. Bube[6] shows that some wavelengths have both excitation and quenching effects, yielding a decreased net result. He also shows that another lower band of quenching wavelengths develops near room temperature. Although Lambe[32] observed quenching at 77°K, he was not able to detect any at 4.2°K, indicating that these transitions are to excited states of the center from which thermal energy frees the electron.

3. Tap Effect

Another effect associated with the freeing of trapped holes is the so-called "tap effect", reported by Kulp[9], and summarized by Halsted in reference 14. When some CdS crystals are cooled in the dark and then optically excited, a flash of green luminescence may be produced by tapping the crystal with a hard object. The luminescence is accompained by an irreversable decrease in the persistent photoconductivity. Although tap

crystals are also storage crystals (i.e., crystals which may have persistent photoconductivity), the opposite does not seem to be true. The doping requirements for producing a tap crystal are not well defined, but it is apparently desirable to tap the crystal parallel to the c-axis. The most popular explanation of the effect is that the mechanical stimulation somehow produces free holes, which then quench the photocurrent and give rise to luminescence by recombining with trapped electrons.

4. The Absorption Edge

Many parameters and effects in CdS depend on the wavelength of the applied light. Except for infrared quenching, which has already been discussed, the wavelength-dependent parameters of major concern here are the absorption coefficient and the photoconductive response. Many experimenters have observed that although the bandgap energy of CdS corresponds to a wavelength of about 4900 Å, and absorption reaches a peak near that wavelength, the photoconductivity response has a maximum close to 5150 Å (normally referred to as the absorption edge). The explanation lies in the fact that the shorter wavelength light is absorbed mainly at the surface, while the longer wavelength light is absorbed in the bulk. Thus, although part of the 5150 Å light passes through the crystal without being absorbed, there are other factors which reduce the effects of radiation absorbed at the surface. Due to the large number of imperfections at the surface of a crystal, the photoresponse can be limited by a lower lifetime or lower mobility in this region. Both Lambe[7] and Bube[41] considered this phenomenon and concluded that the photoresponse due to surface excitation was hindered by the lower lifetime brought about by the extra number of recombination

states near the surface. Unfortunately, the nature of the surface states is still a puzzle, and the corresponding dependence of the photodielectric effect in CdS on wavelength cannot be predicted. In fact, data obtained in low temperature experiments such as the photodielectric experiment may lead to a better understanding of the nature of the surface states.

5. Electric Field Effects

Previous discussions have pointed out that there are ways to empty electron traps at low temperature by freeing trapped holes, either optically or mechanically. There is some evidence that the same result may be achieved by applying a suitable electric field. Dussel and Bube[47] have analyzed the various mechanisms by which an applied field can affect the trapping process in CdS. They concluded that Coulomb attractive traps can be field emptied through a decrease in the depth and capture cross section of the trap. At 77°K, using a field of 3×10^{3} V/cm, they noted a decrease of 1.9kT in the barrier height, and the combined effects of the reduced barrier height and reduced capture cross section produced a shift of 0.055 eV in the electron quasi-Fermi level. Kallman and Mark[49] have demonstrated that both high a-c and d-c fields accelerate the de-excitation of ZnS and ZnCdS phosphors at room temperature. Electric field effects, taken together with optical or mechanical quenching, may constitute a method of "resetting" a storage crystal at low temperatures.

Chapter III

THE PHOTODIELECTRIC EFFECT

A. The Change In The Dielectric Constant

A change in the dielectric constant of cadmium sulfide may be the result of several different changes in the electron distribution within the crystal. The dielectric constant may be calculated from first principles if a few reasonable simplifying assumptions are made. First, the dielectric constant of a perfect crystal is assumed to be independent of the strength of the applied field but dependent on the frequency. Second, the applied field is taken to be independent of the space coordinates. And third, it is assumed that the density of imperfections in the crystal is so low that the dielectric constant does not differ from that of a perfect crystal.

In a perfect dielectric, the net charge is zero, so

$$\sum_i q_i = 0 \tag{3-1}$$

where the q_i are the elementary charges which make up the crystal. The electric dipole moment of one of these charges relative to any given point is $q_i\vec{\ell}_i$, where $\vec{\ell}_i$ is the vector from the point to the charge. The total moment of the crystal is

$$\vec{M} = \sum_i q_i\vec{\ell}_i \tag{3-2}$$

Considering some other point displaced from the original point by the

vector distance $\vec{b}$, the new moment is

$$\vec{M}' = \sum_i q_i(\vec{\ell}_i + \vec{b}) = \sum_i q_i\vec{\ell}_i + \vec{b}\sum_i q_i \qquad (3\text{-}3)$$

Thus if equation (3-1) holds, $\vec{M}' = \vec{M}$, and $\vec{M}$ is independent of the position of the point of reference.

Next, assume that the dipole moment vanishes when the system is in its lowest possible energy state. If $\vec{\ell}_{io}$ is the corresponding position vector, then

$$\vec{M}_o = 0 = \sum_i q_i\vec{\ell}_{io} \qquad (3\text{-}4)$$

In any other energy state, the displacement of the charge q_i from its equilibrium position is denoted by $\vec{r}_i$ and moment of the system is

$$\vec{M} = \sum_i q_i\vec{\ell}_i = \sum_i q_i(\vec{\ell}_{io} + \vec{r}_i) = \sum_i q_i\vec{r}_i \qquad (3\text{-}5)$$

This may vanish only when all charges have the same $\vec{r}_i$, which is not the general case.

If the dielectric sample has two parallel sides and the applied electric field is normal to these sides, then the surface charge density induced by the field is $\pm\vec{P}$, and the moment is

$$\vec{M} = \vec{P}Ad = \vec{P}V \qquad (3\text{-}6)$$

where A is the surface area and d is the sample thickness. But electrostatic considerations give the well know relations,

$$\vec{D} = \varepsilon_o\vec{E} + \vec{P} = \varepsilon_o\vec{E} + \varepsilon_o\chi_e\vec{E} \qquad (3\text{-}7)$$

$$= \varepsilon_o\varepsilon_r\vec{E}$$

$$\vec{P} = \varepsilon_o(\varepsilon_r - 1)\vec{E} \qquad (3\text{-}8)$$

$$\varepsilon_o(\varepsilon_r - 1) = \vec{M}/V\vec{E} = \vec{P}/\vec{E} \qquad (3\text{-}9)$$

$$\varepsilon_r = \vec{M}/V\vec{E}\varepsilon_o + 1 \qquad (3\text{-}10)$$

$$= \frac{1}{VE\varepsilon_o} \sum_i q_i\vec{r}_i + 1 \qquad (3\text{-}11)$$

It appears that the relative dielectric constant depends on both the magnitude of the applied field and the displacement of each charge. Relations between these two quantities exist, however, and they are determined next.

The equation of motion for a charged particle in any type of force field may be given by

$$m^* \frac{d^2\vec{r}}{dt^2} + \frac{m^*}{\tau}\frac{d\vec{r}}{dt} + k\vec{r} = \vec{F} \qquad (3\text{-}12)$$

where $\vec{F}$ is the applied force, m^* is the effective mass, $\vec{r}$ is the displacement of the particle from equilibrium, τ is a momentum relaxation time, and k is an effective spring constant. Here the first term represents the acceleration force, and the second gives the viscous damping force, and the

third is the elastic binding force, all of which oppose the driving force. If an alternating electric field in the x direction is taken to be the origin of the applied force, we may rewrite the preceeding equations as

$$\frac{d^2x}{dt^2} + \frac{1}{\tau}\frac{dx}{dt} + \frac{kx}{m^*} = \frac{qE'}{m^*} e^{j\omega t} \tag{3-13}$$

where $E' e^{jwt}$ is the internal field, which is assumed to be equal to the external field. Nozieres and Pines[50,51] have shown, with the aid of quantum mechanics, that local field corrections are not necessary in the calculation of dielectric constants if the solid is highly polarizable.

For a harmonic oscillator, the resonant frequency ω_o is given by Levine[52] as $\omega_o = \sqrt{k/m^*}$, so

$$\frac{d^2x}{dt^2} + \frac{1}{\tau}\frac{dx}{dt} + \omega_o^2 x = \frac{qE'}{m^*} e^{j\omega t} \tag{3-14}$$

The solution of this equation, with the transient behavior removed, is

$$x = \frac{(q/m^*)E' e^{j\omega t}}{\omega_o^2 - \omega^2 + j\omega/\tau} \tag{3-15}$$

$$= (q/m^*)E' e^{j\omega t} \frac{(\omega_o^2 - \omega^2 - j\omega\tau\ )}{(\omega_o^2 - \omega^2)^2 + (\omega/\tau)^2} \tag{3-16}$$

$$\varepsilon_r = \sum_i \frac{q_i^2}{m_i^* V \varepsilon_o} \left[\frac{\omega_o^2 - \omega^2 - j\omega/\tau}{(\omega_o^2 - \omega^2)^2 + (\omega/\tau)^2}\right]_i + 1 \tag{3-17}$$

This equation may be further simplified. First, the summation of the charges is taken on a per-unit-volume basis, so the V may be dropped. Second, we anticipate that only the <u>change</u> in the dielectric constant due to the application of light will be of interest, so charges whose position vectors do not change when light is applied are dropped from the summation. This includes all of the ions and all but a few of the electrons. The electrons have the same charge e_i and the same effective mass m_i^*, so these terms are taken outside the sum. Finally, the electrons which do remain in the sumation fall into a small number of classes, such as free, trapped in deep traps, trapped in shallow traps, and so forth; these classes are represented by a new index j, and the change in ε_r is written

$$\Delta\varepsilon_r = \frac{e}{m^*\varepsilon_o} \sum_j \Delta n_j \left[\frac{\omega_o^2 - \omega^2 - j\omega/\tau}{(\omega_o^2 - \omega^2)^2 + (\omega/\tau)^2} \right]_j \qquad (3\text{-}18)$$

where Δn_j represents the net change in the density of electrons in the j-th class. Thus, the relative dielectric constant may be represented by

$$\Delta\varepsilon_r = \varepsilon_{ro} + \Delta\varepsilon_r \qquad (3\text{-}19)$$

where $\Delta\varepsilon_r$ includes only those particles which, because of optical excitation, move from one class of states to another. The other term, ε_{ro}, accounts for all other particles, and is a constant.

It is seen that $\Delta\varepsilon_r$ has real and imaginary parts. If $\Delta\varepsilon_r = \Delta\varepsilon_r' - j\Delta\varepsilon_r''$ then

$$\Delta\varepsilon_r' = \frac{e}{m^*\varepsilon_o} \sum_j \Delta n_j \left[\frac{\omega_o^2 - \omega^2}{(\omega_o^2 - \omega^2)^2 + (\omega/\tau)^2} \right]_j \qquad (3\text{-}20)$$

$$\Delta\varepsilon_r'' = \frac{e^2}{m^*\varepsilon_o} \sum_j \Delta n_j \left[\frac{\omega/\tau}{(\omega_o^2 - \omega^2)^2 + (\omega/\tau)^2}\right]_j \qquad (3\text{-}21)$$

For a given state j, the two terms in brackets in equations (3-20) and (3-21) are constant. It should be noted that in general, ω_o and τ change in going from one state to another, while ω is the frequency of the applied field and is therefore constant for all j. Also, it is seen that $\Delta\varepsilon_r'$ exhibits a resonance for $\omega = \omega_o$. The next requirement is to calculate ω_o.

The classical frequency of an oscillator is

$$\omega_o = \sqrt{k/m^*} \qquad (3\text{-}22)$$

where k is the spring constant. The restoring force on an oscillator whose displacement is r is

$$F = kr \qquad (3\text{-}23)$$

and the potential energy is

$$E = 1/2kr^2 = 1/2m^*\omega_o{}^2r^2 \qquad (3\text{-}24)$$

Thus, the total energy of the oscillator must be

$$E = 1/2m^*\omega_o{}^2r^2{}_{max} \qquad (3\text{-}25)$$

where r_{max} is the maximum outward excursion, for which the kinetic energy is zero.

The attractive force between two opposite charges of magnitude e and separation r is

$$F = \frac{1}{4\Pi\varepsilon_o} \frac{e^2}{r^2} \quad \text{newtons} \qquad (3\text{-}26)$$

Here, the potential energy is

$$E = \frac{1}{4\Pi\varepsilon_o} \frac{e^2}{r} \tag{3-27}$$

Solving for r gives

$$r = \frac{1}{4\Pi\varepsilon_o} \frac{e^2}{E} \tag{3-28}$$

Substituting equation (3-28)into equation (3-25), ω_o^2 may be expressed in terms of E,

$$\omega_o^2 = \frac{2}{m^*} \frac{(4\Pi\varepsilon_o)^2}{e^4} E^3 \tag{3-29}$$

$$= 1.70 \times 10^{29} \left(\frac{m}{m^*}\right) E^3 \text{ (eV)} \tag{3-30}$$

where E (eV) is the energy expressed in electron-volts. The energy of electron traps is measured from the conduction band. Thus as long as $\omega \simeq 5\times 10^9$ radians per second, $\omega_o >> \omega$ for $E > 0.01$ eV. For an example, assume $m^*/m = 0.2$, and $E = 0.4$ eV. Then $\omega_o^2 = 5.44\times 10^{28}$, or $\omega_o = 2.33\times 10^{14}$.

The momentum relaxation time τ for bound electrons depends on many things, and a precise calculation is not possible. Factors affecting the relaxation time are the presence of crystal imperfections and thermal vibrations. However, if the orbit of the electron is large enough to allow it to be influenced by many atoms, it may be argued that the relaxation time should be essentially the same as that of a free electron. A very enlightening discussion of the relaxation process for free electrons is given by Kittel[53]. The correct expression for the momentum relaxation time

for a free electron is

$$\tau = m^*\mu/e \tag{3-31}$$

where μ is the mobility. If μ is taken as 10 cm^2/volt-sec (10^{-3} m^2/V-s) and $m^*/m = 0.2$, then $\tau = 10^{-15}$ sec. If $\omega = 5\times 10^9$, then $\omega/\tau = 5\times 10^{24}$, which is negligible compared to $\omega_o^2 = 5\times 10^{28}$ as calculated earlier. Thus for certain cases, equation (3-18) may be substantially simplified. The value of 10^{-15} for τ represents a lower limit of τ for electrons with large orbits. This characteristic time should lengthen as the orbit shrinks, due to a decrease in the number of atoms within the orbit. Thus, the ω/τ term in the denominator of equation (3-18) can probably be neglected for all cases.

According to equation (3-20) the real part of $\Delta\varepsilon_r$ is proportional to $\omega_o^2 - \omega^2$, and it has been shown that when $\omega_o >> \omega$, $\Delta\varepsilon_r'$ increases as the binding energy of the electron decreases. We know, however, that $\Delta\varepsilon_r'$ should be negative when the binding energy reaches zero. The relative absolute value of $\Delta\varepsilon_r'$ is plotted vs the binding energy in figure III-1 using the representative values of parameters calculated earlier, and four areas of interest are readily apparent. For the first, the bracketed term in equation (3-20) may be replaced by $(1/\omega_o)^2$ and thus $\Delta\varepsilon_r'$ rises as the binding energy drops. For the second region, $\Delta\varepsilon_r'$ decreases as E is reduced, since $\omega/\tau > \omega_o^2$, and

$$\Delta\varepsilon_r' \propto \left[\frac{\omega_o^2}{(\omega/\tau)^2}\right] \tag{3-32}$$

Fig. III-1. Dependence of $\Delta\epsilon_r'$ on binding energy.

$\tau = 10^{-15}$ sec

$\omega = 5 \times 10^{9}$ Hz

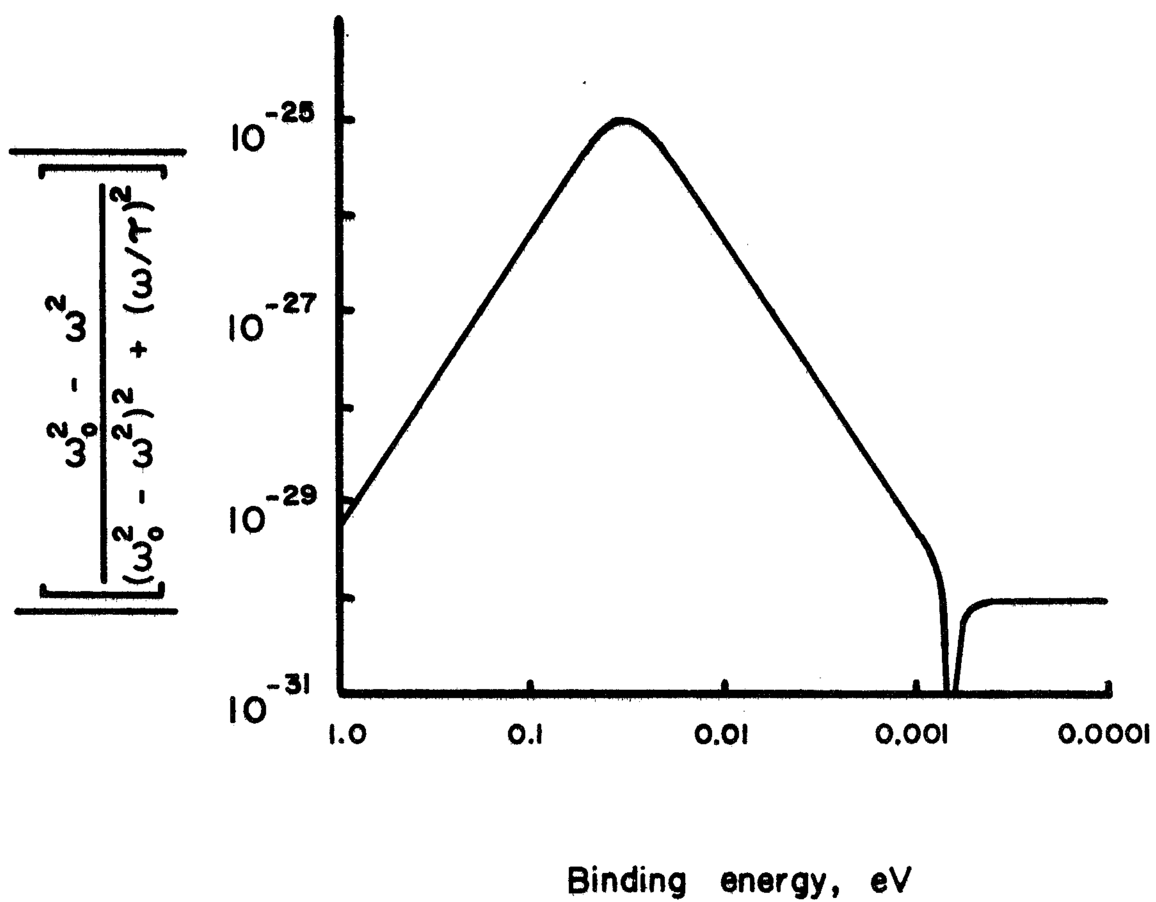

Binding energy, eV

In the third region, $\Delta\varepsilon'_r$ drops quickly to zero and then rises to a constant negative value, as $(\omega_o^2 - \omega^2)$ goes from a positive quantity to zero and then to a negative quantity. The bracketed term in this region is

$$\Delta\varepsilon'_r \propto \left[\frac{\omega_o^2 - \omega^2}{(\omega/\tau)^2}\right] \qquad (3\text{-}33)$$

For the final region, $\omega^2 >> \omega_o^2$ and $\Delta\varepsilon'_r$ is negative. Here, the bound electron takes on the behavior of a free electron, and $\Delta\varepsilon'_r$ becomes

$$\Delta\varepsilon_r = - \frac{e^2}{m^*} \frac{n\tau^2}{\varepsilon_o} \qquad (3\text{-}34)$$

If we choose to keep ω in the equation in spite of its small size relative to $1/\tau$, $\Delta\varepsilon'_r$ is

$$\begin{aligned} \Delta\varepsilon'_r &= - \frac{e^2 n}{m^*\varepsilon_o} \frac{\omega^2}{\omega^4 + \omega^2/\tau^2} \\ &= - \frac{e^2 n}{m^*\varepsilon_o} \frac{1}{\omega^2 + 1/\tau^2} \end{aligned} \qquad (3\text{-}35)$$

But equation (3-35) is recognized as the change in the dielectric constant brought about by exciting electrons from the valence band to the conduction band, as described by Arndt[4].

Differentiation of equation (3-20) shows that the maximum of $\Delta\varepsilon'_r$ occurs for $\omega_o^2 = \omega^2 + \omega/\tau$. For the sample calculation being used, this corresponds to $E = 3.1\times10^{-2}$ eV. Unfortunately, the optimum value of E depends on τ, a quantity which is not easily evaluated. The important thing

to note is that as τ increases above 10^{-15} sec, the peak of curve III-1 increases in height and shifts toward lower energies. For example, using the assumptions on curve III-1, it is found that the peak comes at the energy for which $\omega_o^2 - \omega^2 = 0$ when τ is chosen to be about 10^{-10} seconds. As τ becomes increasingly larger, the only method of maximizing $\Delta\varepsilon_r'$ is to increase ω so that it approaches ω_o. If $\omega_o >> \omega$, the dielectric constant change cannot be optimized by varying ω.

Only one quantity in equation (3-18) remains unspecfied, and it is Δn_j. In order to give Δn_j, a model for the system must assumed, with each effective electronic energy level having a separate index. The simplest case involves only two levels, such that $\Delta n_2 = -\Delta n_1$; that is, a certain number of electrons leave level 1 and enter level 2. It is shown later that this case is the one expected in CdS:Al, so it is treated here.

The net density of electrons excited from level 1 to level 2 is proportional to the intensity of the applied stimulus, which is assumed to be light, and to the length of time that the electron remains in the excited state before returning to the first state. Thus, Δn_j may be written

$$\Delta n_j = f_j \tau_{nj} / V_s \tag{3-36}$$

where f_j is the rate at which electrons are excited to the state j, τ_{nj} is the average time an electron spends in state j and V_s is the sample volume. This equation represents the steady state value of Δn_j. If, on the other hand, the light removes electrons from the state, f_j should be given a negative sign, and τ_{nj} represents the average time an electron remains out of the state.

The generation rate f_j is related to the incident light intensity, the absorption coefficient, and many other factors. In general

$$f_j = \alpha \phi_j \tag{3-37}$$

where ϕ_j is the flux of photons which are sufficiently energetic to affect Δn_j, and α is a conversion efficiency which accounts for reflection, imcomplete absorption, and any other factors which cause f_j to be less than ϕ_j. Thus,

$$\Delta n_j = \alpha \phi_j \tau_{nj} / V_s \tag{3-38}$$

One special case is of great importance, and that is when τ_{nj} approaches infinity. For this situation, equation (3-36) does not apply because the steady state can never be reached as long as f_j is non-zero. The proper equation is then

$$\begin{aligned} \Delta n_j(t') &= \frac{1}{V_s} \int_o^{t'} f_j(t)\, dt \\ &= \frac{\alpha}{V_s} \int_o^{t'} \phi_j(t) dt \end{aligned} \tag{3-39}$$

In choosing the limits of integration, it is assumed that $\Delta n(0) = 0$ and $f_j(t) = 0$ for all $t < 0$. Thus Δn_j at some time t may be found by integrating ϕ_j up to that time. All of the quantities in equation (3-39) may be measured.

The foregoing discussion amounts to a prediction that if light were applied to a CdS sample under the proper temperature and wavelength conditions,

a real change in the dielectric permittivity would be the result. Several observers have searched for such a change in ε_r in CdS at temperatures between $77^{\circ}K$ and room temperature, and have come to the conclusion that any apparent change could be explained by a change in the conductivity.

Pure CdS crystals were tested at $370^{\circ}K$ and 1000 Hz in a General Radio 650-A impedance bridge by Kallmann, Kramer, and Mark[54]. A large change in capacity (nearly 10^6) was observed and attributed entirely to a large change in the conductivity. It was concluded that traps played no part in the change in the dielectric constant because $\Delta\varepsilon_r$ decayed rapidly following the cessation of excitation while the traps remained filled for several hours. Kallmann, Kramer, and Spruch[55] repeated the same tests using CdS:Cu powders at room temperature, and came to the same conclusions.

Sixfold changes in the capacity of CdS single crystals were reported by Broser, Brumm, and Reuber[56] for temperatures above $78^{\circ}K$ and frequencies to 300 kHz. Here again, measurements indicated that the apparent dielectric change was actually a result of a change in the conductivity.

Kronenberg and Accardo[6] experimented with powders of ZnCdS:Ag, ZnCdS:AgCu, and ZnS:Ag at temperatures down to $77^{\circ}K$ and frequencies to 100 kHz. They also found large capacitance changes, but concluded that for some powders the capacity change could not be explained solely by photoconductivity. In general, those phosphors which had only photoconductivity had decay times which were nearly temperature independent, whereas for the other crystals, the decay constant at $77^{\circ}K$ was much longer than at $300^{\circ}K$. These photodielectric powders also possessed a constant capacity much higher than the dark value at $77^{\circ}K$. It was found that the

capacity could be returned to the dark value by warming the crystal to about 180°K. A model featuring both the photodielectric and photoconductive effects was suggested to explain the observations.

In ZnS (ref. 46) and ZnS:Cu, $SrSiO_3$:Eu, and Zn_2SiO_4:Mn (ref. 57), Garlick and Gibson found a change in the dielectric constant. Crystals exhibiting dielectric changes proved to be both luminescent and photoconductive, implying the presence of trapping sites. The phosphor was the dielectric in a parallel plate capacitor, which in turn was part of the frequency control circuitry of a 0.1 - 10 MHz oscillator. Changes in capacitance of the order of 1 part in 10^4 were observable over a temperature range of 90 to 600°K. Simultaneous measurements of fluorescent emission and the dielectric constant proved that the conductivity and dielectric constant exhibited completely different behaviors when light was applied and afterward. The conclusion was that in ZnS at low temperatures the dielectric changes are due to the properties of trapped electrons and that electrons in the conduction band make no significant contribution [see p 423, Bube[6]].

Reasons for the failure of some observers to detect a real change in the dielectric constant of CdS may be made more apparent by a study of the properties of CdS, especially doped CdS. A review of Chapter 2 shows that the main factors are 1) doping and 2) temperature. It was seen that if a large photodielectric effect is desired, the crystal would be doped with impurities which produce many traps, and the temperature should be low enough to minimize thermal excitation of an electron from the trap, once it is captured.

B. Free Electron Contribution

Hartwig[2], Arndt[4], and Stone[5] have described a photodielectric effect in come semiconductor crystals due to the presence of an excess of free carriers. Arndt, in a very complete analysis of the free carrier contribution, derived the dependence of $\Delta\varepsilon_r'$ on light given in the following equation:

$$\Delta\varepsilon_r = \frac{\alpha\phi\tau_L}{V_s} \frac{e^2}{m^*\varepsilon_o} \frac{\tau^2}{(1 + \omega^2\tau^2)} \qquad (3\text{-}40)$$

where α is the conversion efficiency, ϕ is the photon flux, τ_L is the free carrier lifetime and V_s is the sample volume. This equation is essentially the same as equation (3-35), and should be compared with equation (3-20) for the bound electron contribution. Maximization in either case requires $\omega > 1/\tau$, and if $\omega_o^2 = 2\omega^2$, the expressions for $\Delta\varepsilon_r'$ for the two cases are equivalent, except for the factor of n. This means that the lifetime of the photoeffect is the parameter which determines the photosensitivity of a given material which is used to tune a resonsnt cavity.

C. Cavity Perturbation Theory

A sensitive method of detecting changes in the dielectric constant of a material is to place a sample of the material on the stub of a re-entrant coaxial cavity. According to perturbation theory, any changes in the dielectric constant of the sample will show up as changes in the cavity Q and resonant frequency. The use of a superconducting cavity allows the frequency to be precisely determined with a frequency counter which is

accurate to one part in 10^9. The cavity perturbation model has been analyzed by Arndt[4] and therefore only the highlights of the theory are reproduced here.

The re-entrant coaxial cavity with a dielectric sample in place is shown in figure III-2. It may be shown[4] that for a high Q cavity of this type, the change in the resonant frequency, when the sample characterized by $\varepsilon_r = \varepsilon_1/\varepsilon_o$ is initially placed on the stub, is

$$\frac{\omega_1 - \omega_o}{\omega_1} = \frac{\Delta\omega_1}{\omega_1} = \frac{\frac{\varepsilon_o - \varepsilon_1}{\varepsilon_1} \int_{V_s} 2\varepsilon_o \left|\vec{E}_{o\ rms}\right|^2 dV}{\int_{V_c} (\varepsilon_o \vec{E}_o \cdot \vec{E}_1 - \mu_o \vec{H}_o \cdot \vec{H}_1)\, dV} \tag{3-41}$$

where V_s is the sample volume and V_c is the cavity volume. The right side of equation (3-41) is not easily calculated because of the difficulty in measuring the fields. However, if ε_1 is known, the ratio of the integrals may be measured, and it is a constant for any given sample.

Fig. III-2. Re-entrant Coaxial Cavity

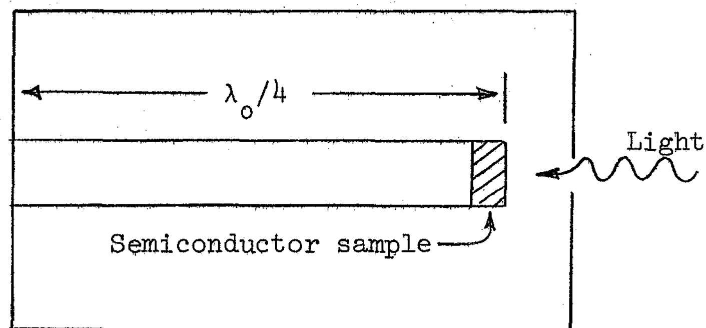

Equation (3-41) may be rewritten

$$\frac{\Delta\omega_1}{\omega_1} = \frac{\varepsilon_o - \varepsilon_1}{\varepsilon_1} \quad G \tag{3-42}$$

where the ratio of the integrals has been replaced by the symbol G, which is commonly referred to as the geometry factor. The physical significance of G is that it is a measure of the fraction of the electromagnetic energy inside the cavity which is stored in the dielectric sample.

If the dielectric constant of the sample is now changed from ε_1 to ε_2, similar equations may be written. However, if we may assume that this dielectric change has no effect on the cavity fields, G will remain unchanged and we may write

$$\frac{\omega_2 - \omega_o}{\omega_2} = \frac{\Delta\omega_2}{\omega_2} = \frac{\varepsilon_o - \varepsilon_2}{\varepsilon_2} \quad G \tag{3-43}$$

The shift in frequency obtained when ε_1 changes to ε_2 is then

$$\begin{aligned} \frac{\omega_2 - \omega_o}{\omega_2} &= \varepsilon_o G \left[\frac{1}{\varepsilon_2} - \frac{1}{\varepsilon_1} \right] \\ &= \varepsilon_o G \left[\frac{\varepsilon_1 - \varepsilon_2}{\varepsilon_1 \varepsilon_2} \right] \end{aligned} \tag{3-44}$$

Since the changes in ω and ε_r are normally very small, equation (3-44) may be rewritten,

$$\frac{\Delta\omega}{\omega} = -G \frac{\Delta\varepsilon_r}{\varepsilon_r^2} \tag{3-45}$$

The minus sign indicates that if ε_r increases, ω decreases.

D. Power Absorption

The photodielectric effect may also be observed by noting the relative power absorbed in the insulator crystal in the presence of an optical stimulus. A complete treatment of the power absorption in insulators in a re-entrant coaxial cavity is given by Arndt[4]. The well-known expression for the electromagnetic power absorbed by an insulator is

$$P_{abs} = 1/2\omega\varepsilon'' E_e^{\ 2} \qquad (3\text{-}46)$$

where ε'' is the imaginary part of the complex dielectric constant, and E_e is the electric field, assumed to be constant throughout the sample. Once again, we will only consider the change in absorbed power, ΔP_{abs}, which is

$$\Delta P_{abs} = 1/2\omega\Delta\varepsilon_r''\varepsilon_o E_e^{\ 2} \qquad (3\text{-}47)$$

But equation (3-20) gives

$$\Delta\varepsilon_r'' = \frac{e^2}{m^*\varepsilon_o} \sum_j \Delta n_j \left[\frac{\omega/\tau}{(\omega_o^2 - \omega^2)^2 + (\omega/\tau)^2} \right]_j \qquad (3\text{-}48)$$

so equation (3-47) may be rewritten

$$\Delta P_{abs} = 1/2E_e^2 \ \frac{e^2}{m^*} \sum_j \Delta n_j \left[\frac{\omega^2/\tau}{(\omega_o^2 - \omega^2)^2 + (\omega/\tau)^2} \right]_j \qquad (3\text{-}49)$$

Equation (3-49) may be further simplified in a manner identical to the simplication of $\Delta\varepsilon_r'$ earlier. For deep traps, $\omega_o >> \omega$, and the term in brackets in equation (3-49) reduces to

$$\Delta P_{abs} \propto \left[\frac{\omega^2/\tau}{\omega_o^2} \right] \qquad (3\text{-}50)$$

For shallower traps, $\omega/\tau > \omega_o^2$, and bracketed term becomes

$$\Delta P_{abs} \propto \left[\frac{\omega^2/\tau}{\omega^2/\tau^2} \right] = [\ \tau\ ] \qquad (3\text{-}51)$$

Thus it is evident that the relative power absorption rises from a very low value, when electrons are tightly bound, to a higher, constant value for more loosely bound electrons. Figure III-3 is a plot of the bracketed term in equation (3-49) using the representative values of parameters calculated earlier, and considering two values of τ. The variable is the trap energy E. It is seen that in the region corresponding to tightly bound electrons, all frequency dependence drops out of the expression for the power absorption, and power absorption data depends directly on E_e, Δn_j and τ. In the other region, the dependence is on ω_o. The curve applies only for the case of $\omega < 1/\tau$.

The case of a free electron may be solved by setting $\omega_o = 0$ in equation (3-49). This yeilds,

$$(\Delta P_{abs})_{\text{free electron}} \propto \left[\frac{\tau}{\omega^2\tau^2 + 1} \right] \qquad (3\text{-}52)$$

Fig. III - 3. Dependence of $\Delta\epsilon_r''$ on binding energy.

$\omega = 5 \times 10^9$

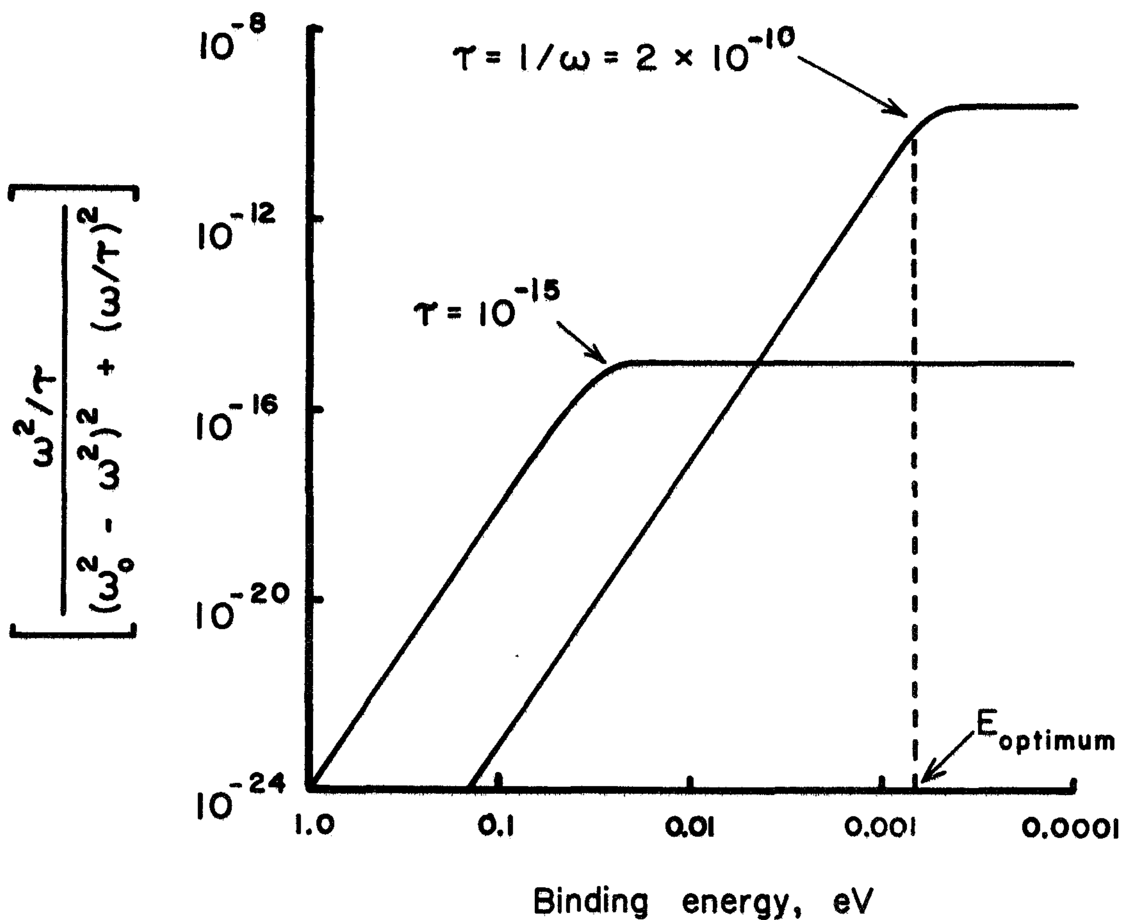

There are two limiting cases. If $\omega << 1/\tau$, we find

$$(\Delta P_{abs})_{f.e.} \propto [\ \tau\ ]\ , \qquad \omega << 1/\tau \qquad (3\text{-}53)$$

Alternately, if $\omega >> 1/\tau$, the expression becomes

$$(\Delta P_{abs})_{f.e.} \propto \left[\frac{1}{\omega^2\tau}\right]\ , \qquad \omega >> 1/\tau \qquad (3\text{-}54)$$

This latter expression is the dependence found by Arndt for the free carrier case. Here, it is obvious that absorption reaches its peak value for $\omega = 1/\tau$.

Further analysis shows that absorption is constant with respect to binding energy for any energy less than a certain value. To maximize absorption, the condition $\omega = 1/\tau$ should be met. Then $\Delta\varepsilon_r'$ is maximized for $\omega_o^2 = 2\omega^2$; this condition is represented by a dotted line on figure III-3. The corresponding energy $E_{optimum}$ represents the "best" possible trapping level, in terms of maximum frequency and power changes. An auxilliary requirement is that $\omega = 1/\tau$.

Comparison with the analysis of Arndt reveals general agreement. His conclusion, that power absorption due to bound electrons is many orders of magnitude less than power absorption due to conduction electrons, is valid only if the electrons are tightly bound. With loosely bound electrons, the relative power absorption is the same. An electron is considered loosely bound if $\omega/\tau > (\omega_o^2 - \omega^2)$.

Some discussion of the usefulness of power absorption data is in order. A comparison of equations (3-49), (3-45), and (3-20) shows that experimental curves of P_{abs} vs ψ and $\Delta\omega/\omega$ vs ψ should have the same form.

Thus, power absorption data can provide no new information about Δn_j but can give a value for either τ or E_e, provided the other value is known. Once these two parameters are evaluated, further analysis of power absorption data might provide a definite indication of whether free or bound carriers cause frequency changes.

Chapter 4

DETERMINATION OF ELECTRON TRAP ENERGY

To evaluate the accuracy of the photodielectric theory, values for the trap depths must be obtained for the sake of comparison. Of the many methods which exist, two which are easily performed and evaluated are thermally stimulated conductivity (TSC) and relative absorption measurements.

A. Thermally Stimulated Conductivity

The basic idea behind the thermally stimulated conductivity (TSC) technique is very simple. If an insulator has energy levels in the forbidden band which, at some low temperature, represent trapping centers rather than recombination centers, then these centers can be partially filled by light with an appropriate wavelength. Since the probability that an electron in a trap will escape from that trap in a given time is proportional to $e^{-E/kT}$ then it is obvious that as the temperature T is raised, the trapped electrons are more and more likely to gain enough thermal energy to escape to the conduction band, giving rise to an increase in the conductivity. Specifically, the rate equations for trapped and conduction electrons are,

$$dn_t/dt = - n_t N_c S v e^{-E/kT} + n_c(N_t - n_t)Sv \qquad (4\text{-}1)$$

$$dn_c/dt = - n_c/\tau_L - dn_t/dt \qquad (4\text{-}2)$$

Here, the subscripts t and c refer to trapping sites or the conduction band, n is an electron concentration, N is the effective density of states, S is the electron capture cross section, v is the conduction electron

thermal velocity, E is the absolute value of the energy difference between the trap and the conduction band, and τ_L is the free carrier lifetime.

The measurable quantity is the current through the photoconductor, which is proportional to n_c. Thus the dependence of n_c on T must be obtained. In order to simplify the math as much as possible, assume a linear heating rate b, such that

$$T = T_o + bt \tag{4-3}$$

There exist two limiting cases in which equations (4-1) and (4-2) have approximate solutions: 1) for slow retrapping, it is assumed that every electron released to the conduction band suffers recombination, and 2) for fast retrapping, there is effective thermal equilibrium between the traps and the conduction band. The first case is of little concern here, and therefore the results of the analysis of Haering and Adams[58] will be presented without discussion:

$$\sigma(T) = N_c Svq\mu\tau_L \exp\left[-E/kT - 1/b \int_{T_o}^{T} N_c Sve^{-E/kT} dT\right] \tag{4-4}$$

where σ is the conductivity, N_c is the effective density of conduction band states, S is the electron capture cross section for a trap, v is the thermal velocity in the conduction band, q is the electronic charge, μ is mobility, τ_L is the free carrier lifetime, and E is the trap energy. At the maximum of σ, the equation for E is

$$E = kT_m \ln\left[\frac{N_c vSkT_m^2}{bE}\right] \tag{4-5}$$

where T_m is the temperature at which σ is a maximum.

For the case of fast retrapping, let $n_c + n_t = n$. Since electrons in traps are in thermal equilibrium with the conduction band, we may write

$$\frac{dn}{dt} = -\frac{n_c}{\tau_L} \tag{4-6}$$

If $N_t >> N_c(T_m)e^{-E/kT_m}$, equation (4-6) becomes

$$\frac{dn}{dt} = -\frac{n}{\tau_L}\left(\frac{N_c}{N_t}\right)e^{-E/kT} \tag{4-7}$$

The solution of equation (4-7) is

$$n = n_o \exp\left[-\frac{1}{\tau_L b}\int_{T_o}^{T} \frac{N_c}{N_t} e^{-E/kT}\, dT\right] \tag{4-8}$$

If $E >> kT$, n_c is related to n by

$$n_c = e^{-E/kT} n(N_c/N_t)$$

$$= n_o(N_c/N_t) \exp\left[-E/kT - \frac{1}{N_t b\tau_L}\int_{T_o}^{T} N_c e^{-E/kT} dT\right] \tag{4-9}$$

The conductivity σ is given by

$$\sigma = n_c q\mu$$

$$= q\mu n_o (N_c/N_t) \exp\left[-E/kT - \frac{1}{N_t b\tau_L}\int_{T_o}^{T} N_c e^{-E/kT} dT\right] \tag{4-10}$$

To find E, it is necessary to set the derivative of $\ln \sigma$ equal to zero. Assuming $E >> kT$, the result is

$$e^{E/kT_m} = \frac{N_c k T_m^2}{N_t b \tau_L E} \qquad (4\text{-}11)$$

where T_m is the temperature at which $\sigma(T)$ reaches a maximum. Then

$$\sigma(T_m) = \sigma_o \exp\left[-\frac{E}{kT_m} - 1\right] \qquad (4\text{-}12)$$

where $\sigma_o = q\mu n_o N_c/N_t$. This equation applies only for $T = T_m$, and may be rewritten,

$$E = kT_m \left[\ln\left(\frac{\sigma_o}{\sigma(T_m)}\right) - 1\right] \qquad (4\text{-}13)$$

If $n_o/N_t \simeq 1$ such that the trap is nearly saturated, then $\sigma_o \approx N_c q\mu$. But $\sigma(T_m) = n_c q\mu$, so equation (4-13) becomes

$$E = kT_m \left[\ln\left(\frac{N_c(T_m)}{n_c(T_m)}\right) - 1\right] \qquad (4\text{-}14)$$

This is similar to the equation which Bube normally uses (in references 10, 34, 41 for example):

$$E_{Bube} = kT_m \left[\ln\left(\frac{N_c(T_m)}{n_c(T_m)}\right)\right] \qquad (4\text{-}15)$$

According to Haering and Adams[58], equation (4-15) is in error by at least $kT_m/2$.A comparison of equations (4-14) and (4-15) shows the error is kT_m when $n_o \simeq N_t$. In using equation (4-14), the calculated value of E will be high by 2.3 kT_m if $n_o = 0.1\ N_t$, and equation (4-15) will be in error by

$3.3\ kT_m$. For CdS, $E \simeq 20\ kT_m$, so the error is important, although it can be kept to a minimum by always filling the traps to near saturation.

The quantities of equation (4-14) may be found using the following relations. First,

$$n_c(T_m) = \frac{1}{\rho_m q \mu_m} = \frac{1}{q\mu_m} \frac{d}{RA} = \frac{I_m d}{q \mu_m V} \qquad (4\text{-}16)$$

where the subscript m indicates that the quantity is measured at the temperature at which the TSC peak occurs. Also ρ is the resistivity, $q = 1.6\times10^{-19}$ coulombs, μ is the mobility, d is the sample thickness, A is its effective electrical contact area, R is its resistance, I is the circuit current, and V is the bias voltage. All of these quantities except μ can be easily measured. According to Kulp[9] the mobility of CdS storage and tap crystals drops sharply as the temperature decreases below room temperature to a value of the order of 10 cm^2/volt-sec.

The relation for $N_c(T_m)$ is

$$N_c(T_m) = 2 \left(\frac{2\Pi m^* k T_m}{h^2}\right)^{3/2} = 4.83\times10^{21} \left(\frac{m^*}{m} \quad T_m\right)^{3/2} \quad \text{meters}^{-3} \qquad (4\text{-}17)$$

For CdS, $m_e^*/m = 0.2$ at $1.6^{\circ}K$ according to Hopfield and Thomas[18] and also

for $77^{\circ}K < T < 350^{\circ}K$, according to Zook and Dexter[19]. Using this value, equation (4-17) may be rewritten

$$N_c(T_m) = 4.32\times10^{20}\ T_m^{\ 3/2} \qquad (4\text{-}18)$$

The value of k is 8.62×10^{-5} eV/$^{\circ}$K.

B. Initial Rise of TSC Curve

The preceding describes how data near the peak of a TSC curve can be used to find the value of E, provided the traps are nearly saturated. If the traps are only partially filed, E can be found by an analysis of the initial rise of the TSC curve. A theoretical plot of $\ln \sigma(T)/\sigma_o$ vs E/kT is shown in figure IV-1. Note that the initial rise is given by

$$\sigma(T) \propto e^{-E/kT} \qquad (4\text{-}19)$$

Thus a plot of $\ln \sigma(T)$ vs 1/kT has a slope of -E, and this value may be compared with the value calculated by the earlier method.

C. Decayed TSC

The success of this initial rise method depends on whether or not only one trap is being filled by the optical stimulus. Figure IV-2 shows how the observed TSC curve should look when one trap is present, and Figure IV-3 shows how the shape of this curve is distorted as an increasing number of traps at other levels become filled. An obvious way to allow only one trapping level to appear is to only apply enough light to partially fill that level. This method succeeds because the deeper levels apparently

Fig. IV-1. Shape of theoretical TSC curve.

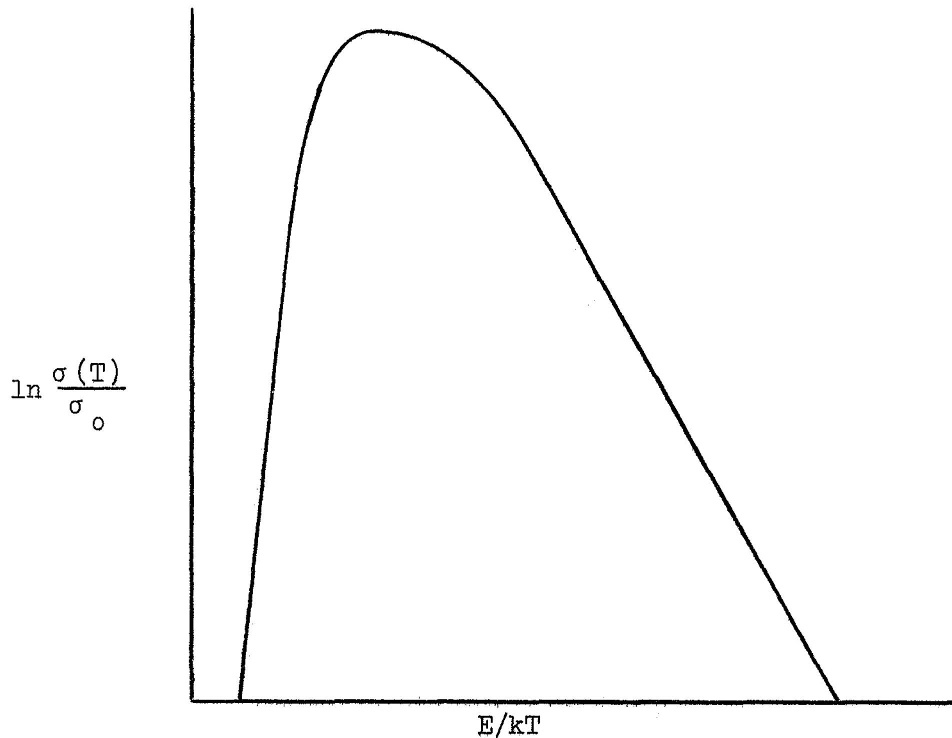

tend to be filled first. Unfortunately, only the deepest level can be observed in this manner. Another method is called decayed thermally stimulated conductivity. Here, all traps are saturated, then the temperature is raised enough to empty certain levels. Then the crystal is recooled, and subsequent heating shows the emptying of the remaining traps. Figure IV-4 illustrates the results of a typical decayed TSC experiment.

D. Relative Optical Absorption

There exists another method for determining the trapping level using the same apparatus as is used in the TSC tests; it will be

Fig. IV-2. Observed TSC peak for a single discrete trap.

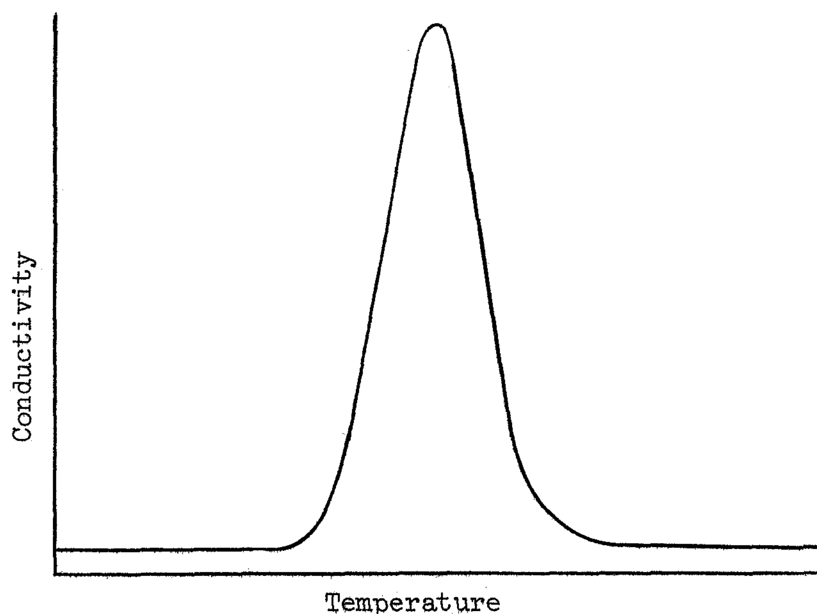

called the relative optical absorption method. The basic idea is to cool the photoconductor, apply light for a given length of time, and then perform a TSC experiment. The relative area under the TSC curve then gives a measure of the number of electrons which were trapped.

Before an electron can be trapped at a level with an energy E, it must absorb the energy of a photon whose wavelength is λ. The required relation between E and λ, as illustrated in figure IV-5 is

$$E_g = hc/\lambda + E \qquad (4\text{-}20)$$

Since conservation of energy must hold, the photon energy should be exactly $E_g - E$. A small amount of excess energy could be taken away by

Fig. IV - 3. Change in the shape of the TSC curve due to the emptying of more than one electron trap.

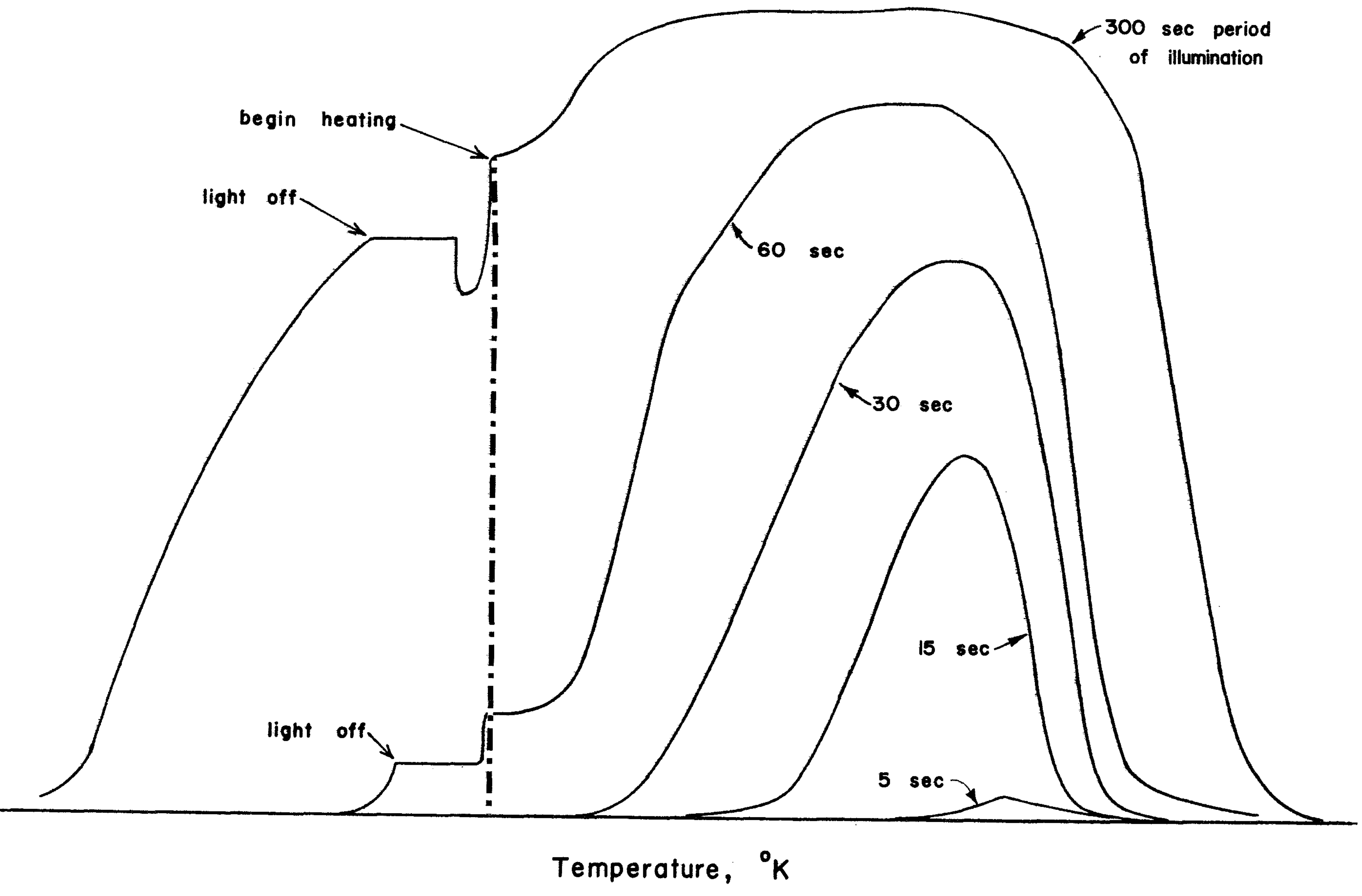

Fig. IV - 4. Comparison of normal and decayed TSC results.

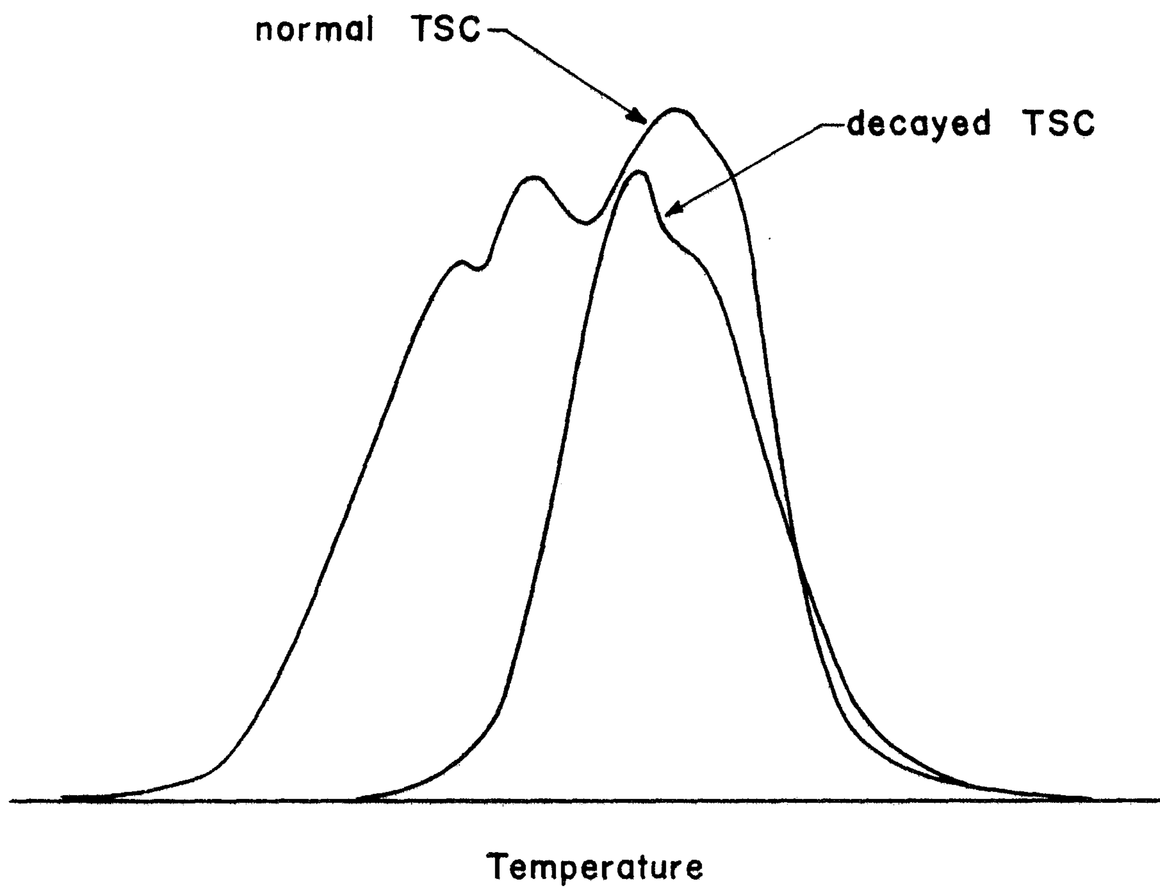

the creation or absorption of phonons, or the electron could come from slightly below the top of the valence band, but these circumstances are not the general case. In the case of CdS, conservation of momentum is not of concern, since the band to band transition is direct.

Thus, if light of wavelength λ is applied to CdS at a low temperature, carriers are excited directly to a trap with the energy E if equation (4-20) is satisfied. A TSC peak is observed only when this provision holds.

One minor complication arrises because the energy band picture of a semiconductor or insulator is a function of temperature. Therefore the proper value of E_g is the value which applies to the temperature at which the traps are filled. Hopfield and Thomas[18] give E_g = 2.5826 eV at 4.2°K and Colbow[23] gives a curve showing the variation of E_g with temperature;

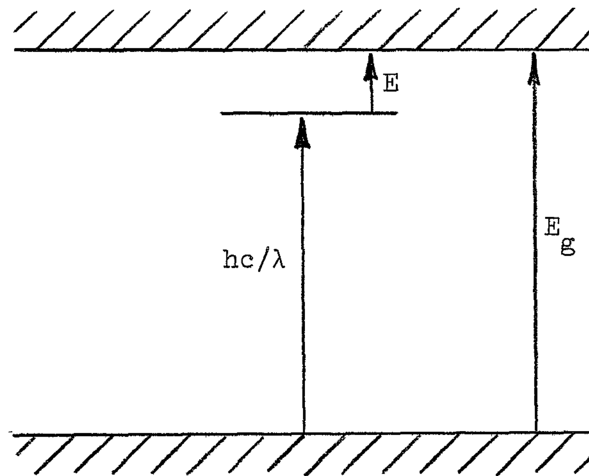

Fig. IV-5. Relation between photon energy and trap energy.

it is reproduced in figure II-2. On the other hand, Kulp[24] shows that the value of E is nearly constant for the temperature range below 100°K in CdS single crystals. This means that the values of E calculated at 77°K are valid at lower temperatures.

An example of the relative absorption method is given in figure IV-7. The curve is obtained by applying a given number of photons of some wavelength to the crystal at 77°K and noting the height of the resulting TSC curve, which is then plotted against wavelength. In this example, a absorption is high in the range $0.28 < E < 0.51$ eV. The curve has rounded corners, rather than square, due to slight differences in the nature of the traps and the phonon effects discussed earlier. This prevents the construction of a sharply defined energy band model; an approximate model based on the absorption curve of figure IV-7 is given in figure IV-6.

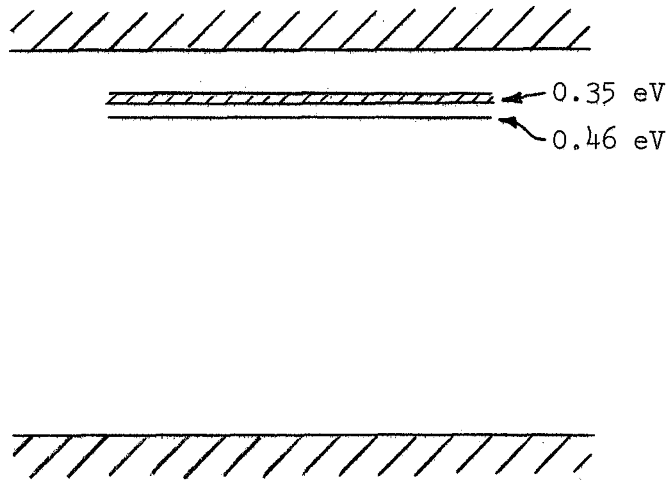

Fig. IV-6. Trap distribution derived from relative optical absorption measurement.

Fig. IV - 7. TSC peak current vs wavelength for cadmium sulfide sample 6.

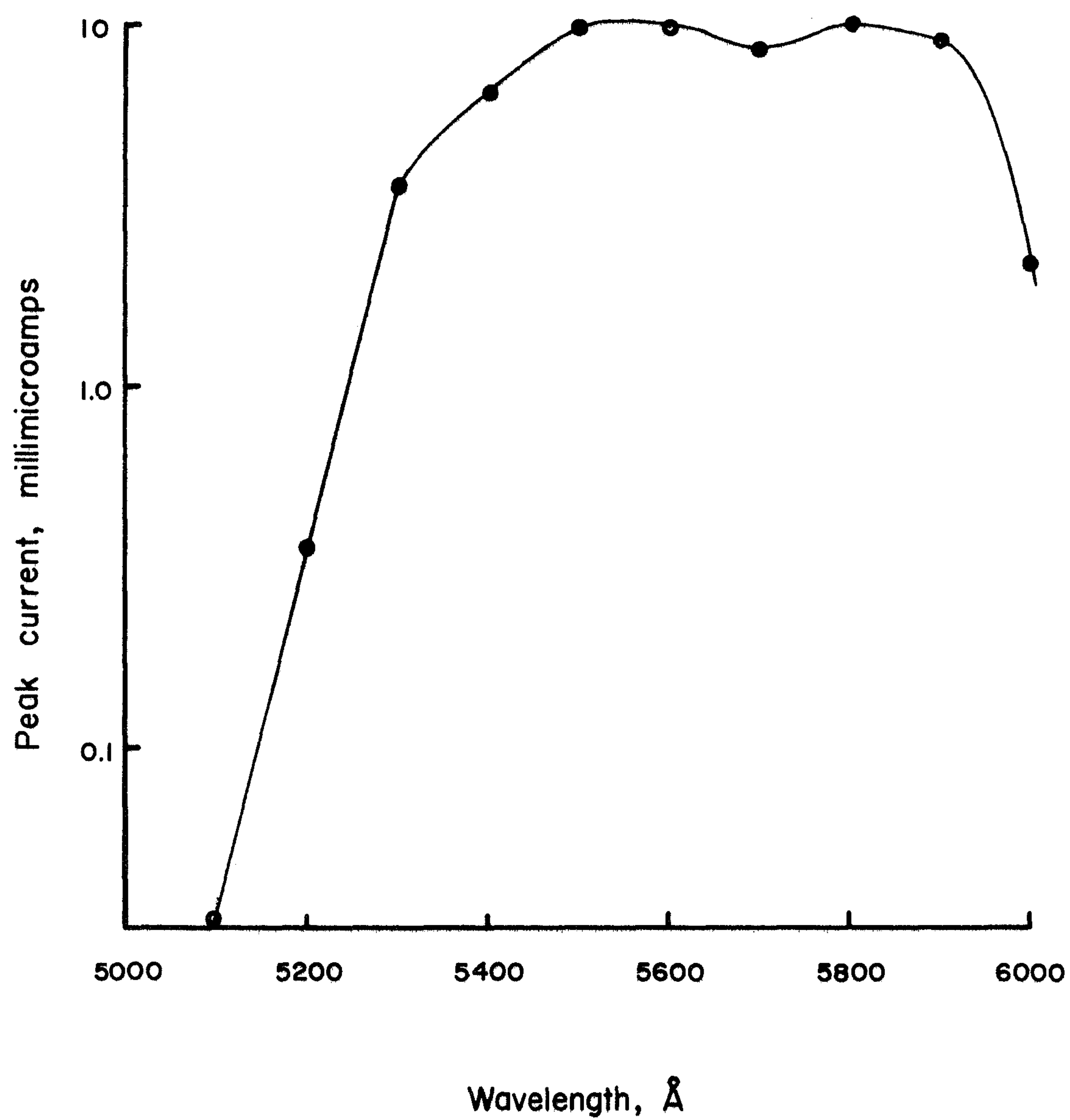

Chapter 5

EXPERIMENTAL TECHNIQUES

Many of the experimental techniques connected with the photodielectric effect in resonant cavities have been thoroughly described by Stone[5], and will only be briefly mentioned here. Techniques which are unique to experiments using CdS will be discussed more fully.

A. Preparing Cadmium Sulfide Samples

Cadmium sulfide is a soft, brittle material, and must be handled with extra care. Samples dropped from a height of about one foot tend to shatter, and samples subjected to any small bending moment tend to cleave. Thus any applied pressure, such as that required in lapping or making electrical contact, must be uniform to prevent breakage.

A diamond saw may be used to cut cadmium sulfide single crystals, but it is almost impossible to obtain wafers thinner than 1 mm. If the progress of the saw through the crystal is limited to several millimeters per minute, wafers one to two millimeters thick can be routinely cut without breakage. Faster cutting rates tend to shatter the crystal. During the cutting, the sample must be securely held in place on all sides, both to prevent shifting and to support the wafer. Best results are obtained by coating the crystal with white wax; black Apiezon wax should be avoided, as it is hard to clean off.

The wafer can then shaped with an ultrasonic grinder. Experience has shown that it is best not to cut too deeply into the crystal with the grinder; a net work of small surface cracks tends to develop when the

grinding tool approaches a depth of 1 mm. A satisfactory technique for cutting round samples of CdS from wafers 1 to 2 mm thick is outlined as follows. First, using the grinder, cut to a depth of about 1 mm with the circular tool. Then remove the wafer from the mounting plate to which it is attached. Remove any excess wax from the sample by boiling it in trichlorethylene. Place the sample on a clean flat surface, such as a stone-top bench, and slowly begin deepening the circular trough in the wafer with a sharp X-acto knife or similar tool. After this process has proceeded for a short period of time, the crystal will suddenly break along the groove. Repetition of this procedure around the circumference of the channel will yield a round sample with rough edges. The rough edges are then easily removed with coarse grit sand paper.

Cadmium sulfide samples can easily be given a glossy surface by lapping them. The lapping should be done by hand; this allows the lapper to feel the presence of small slivers of CdS which frequently break off during the polishing process. Since these slivers tend to scratch the sample, the grit should be washed away every minute or two, and replaced with fresh grit. Successive applications of #240, 400, and 600 grit yield a surface resembling frosted yellow glass. To achieve a glossy surface, use #600 grit and place a rubber sheet between the sample and a flat surface.

Following the polishing, the sample should be cleaned to remove any wax or oil left on the surface. This is accomplished by boiling the CdS in trichlorethylene. If an etch is desired, dilute HCl may be used, but this tends to dull the surface.

Samples to be used in photoconductivity or resistivity tests

should be provided with indium contacts. The only reliable method of applying permanent contacts is vacuum evaporation, although temporary contact may be made by pressing an indium circle against the CdS sample. It should be noted here that only indium and gallium always make ohmic contact with CdS.

Special care should be used in storing CdS samples. It was pointed out in Chapter II that water vapor and oxygen are readily adsorbed on the surface and therefore CdS crystals should be kept in a dry helium or nitrogen atmosphere when not in use. They should also be cushioned from shock and shielded from light.

It is usually desirable to measure the size of samples, as this information is normally required in the analysis of electronic properties of the material. The easiest way to obtain the area and volume of the sample is to measure its thickness and weight. Using the fact that the density of CdS is 4.82, the area and volume may then be quickly found.

B. Preparing the Cavity

The microwave cavity must first be electroplated with lead. This procedure is treated fully by Stone[5] and will not be treated here except to note that the plating solution appeared to give the best results when it had a pH of 0.4.

It was also found that an unused lead-plated cavity could be kept stain-free if stored in an air-tight container. The bottom of a coffee can was covered with anhydrous $CaSO_4$ crystals, which absorb water vapor. After placing the cavity inside, the can was filled with helium gas and closed with a plactic lid. The lead surfaces of circuits stored in this

manner suffered no noticable discoloration.

Various methods of attaching the CdS sample to the quarter-wave stub were attempted, and it was found that the only acceptable method was to employ a teflon collar. Indium-gallium and indium-mercury eutectics do not wet the CdS, and thus do not supply enough adhesion to keep the sample firmly in place. Various glues, such as Elmer's Glue and Duco Cement, have good adhesive properties, but differential expansion during the cooling process tends to break the CdS crystals.

For the best results, a CdS sample should be transferred from its storage box to the cavity in the dark, because optically induced effects in CdS frequently require days to decay. A measurement of the G factor at room temperature should not be made until the electrons reach their equilibrium energy states, as indicated by the stabilization of the cavity frequency. Generally, the frequency is invariable after about an hour if the crystal is properly shielded from the light.

The cooling procedure is outlined as follows. First, evacuate the vacuum space between the walls of the inner dewar. Next place the cavity assembly in the dewar and evacuate it. Liquid nitrogen is then transferred into the outer dewar and allowed to precool the cavity and inner dewar for about six hours. After refilling the liquid nitrogen jacket, the liquid helium may be transferred.

The process of transferring helium can be simple and quick provided the dewar has been properly precooled and evacuated. Best results are obtained when the gas pressure inside the helium storage dewar is kept at about 3 psi. Under these conditions, helium should begin to collect inside the dewar after about 1 minute. If no such collection is

observed after 1 1/2 minutes, the attempt to transfer should be abandoned, and the source of trouble should be sought. Noticable cooling of the transfer tube indicates its vacuum jacket is not sufficiently evacuated. If the transfer tube does not cool noticably, failure of the helium to condense indicates that the vacuum jacket of the inner dewar is not properly evacuated. If the helium level rises and then begins to drop, an additional possibility is that the helium storage dewar has been emptied.

Often it is desriable to quickly warm the apparatus after an experiment to facilitate a rapid sample change. After removing the cavity from the helium bath and allowing the liquid inside to evaporate, a slow flow of helium gas is maintained through the circuit to prevent the entrance of water vapor. The cavity is also placed in a flow of hot air from a heat gun. This produces warming to room temperature in about fifteen minutes, and prevents discoloration of the lead surface. It is not advisable to allow the cavity to reach room temperature slowly in a vacuum environment because this allows water vapor to enter through the spaces between the fibers in the light-pipe, damaging both the lead plate and light-pipe.

C. Photodielectric Effect Apparatus

A block diagram of the apparatus used to study the photodielectric effect is shown in figure V-1 and the equipment is shown in plate 1. The resonant cavity is operated as a high Q tuneable bandpass filter. The oscillator and receiver frequency are simultaneously adjusted to maximize the signal through the cavity, and the counter then determines the frequency of the oscillator. The receiver also provides a measure of the power

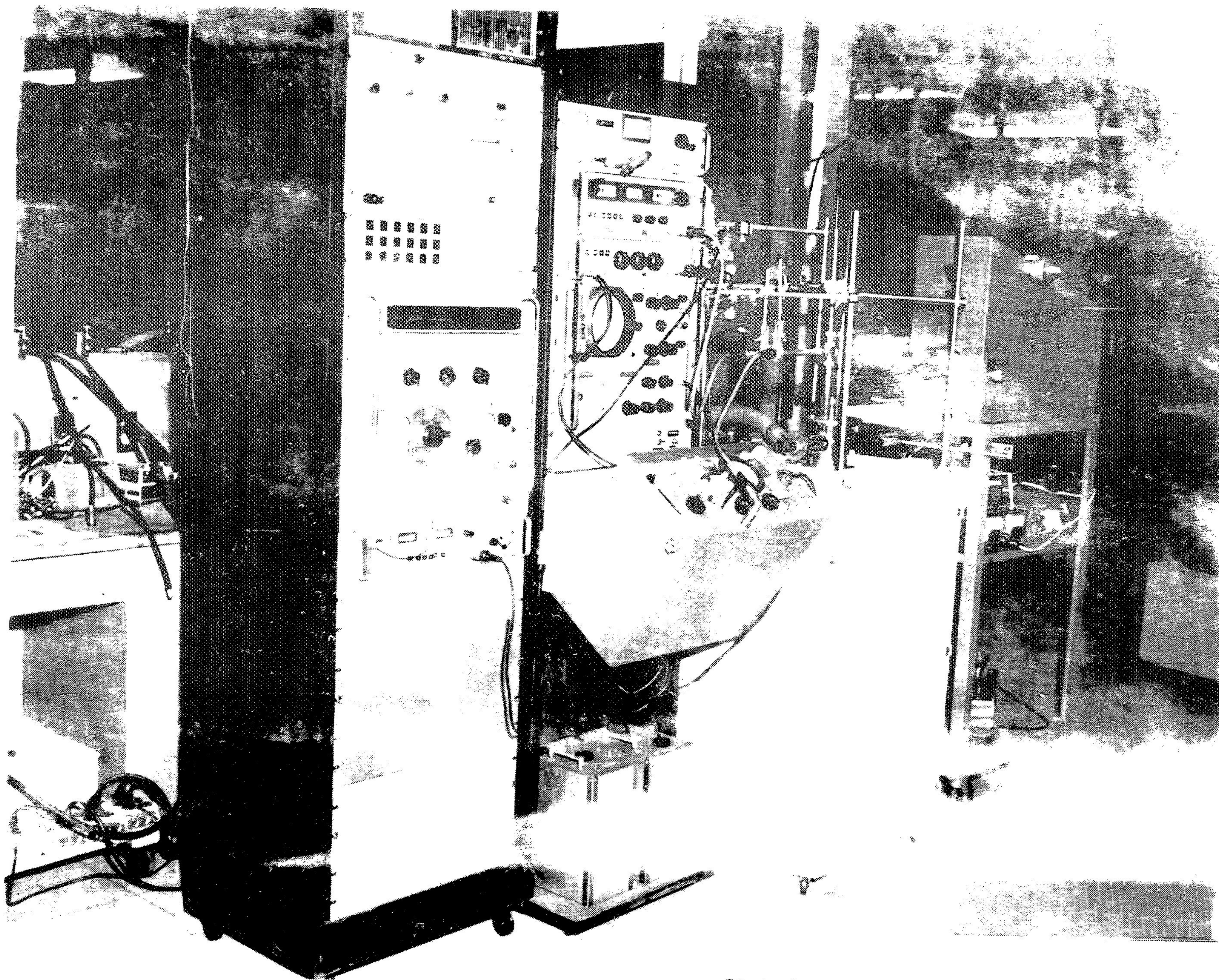

Plate 1 Photodielectric Effect Apparatus

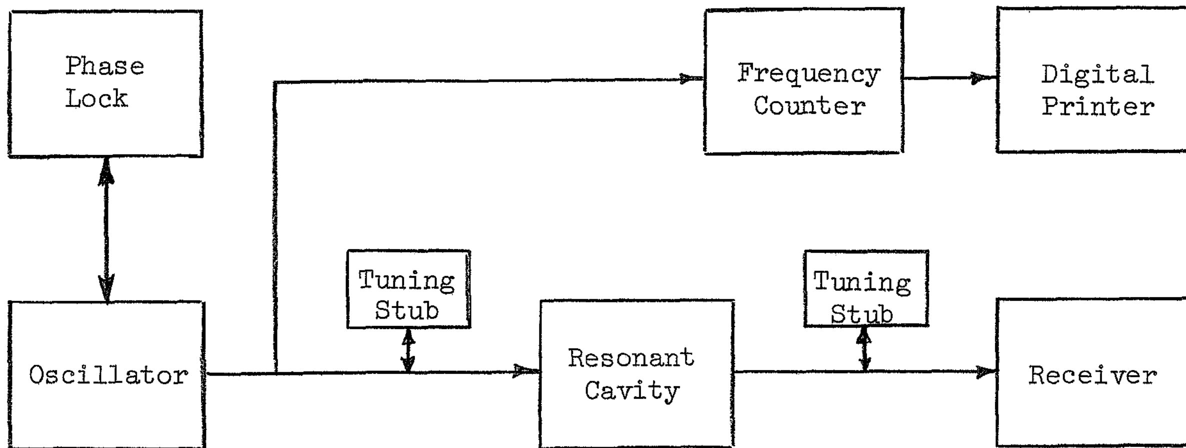

Fig. V-1. Block diagram of the apparatus used to study the photodielectric effect.

absorbed in the cavity. The tuning stubs provide matching between the cavity and the other equipment.

The cavity assembly consists of two sections; the header and the cavity itself. Figure V-2 shows the entire assembly in place in the dewar assembly, and plate 2 shows the disassembled cavity assembly.

The header suspends the cavity in the liquid helium. The three thin-walled stainless steel tubes contain the input and output probes and the fiber optic bundle. Stainless steel has a low thermal conductivity, and thus the thin-wall tubes minimize the conduction of heat into the dewar. The brass plate and brass scouring pad minimize the transfer of heat by convection currents in the helium gas. The probe supports are adjustable over a range of 2 inches, to provide variable coupling to the cavity. An inlet for pumping gas into the cavity is provided through one of the probe tubes. The

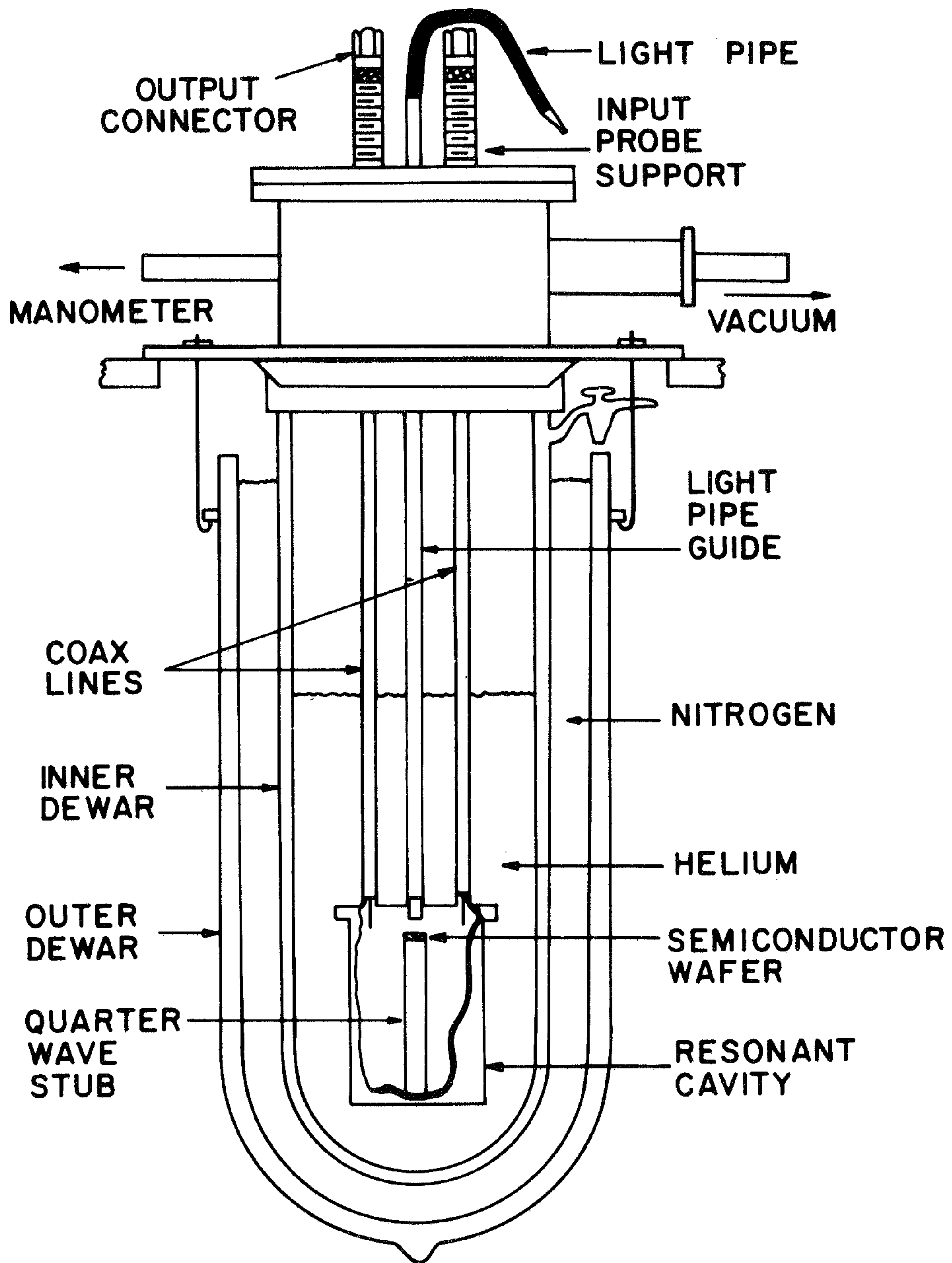

Fig. V-2 Cavity Assembly in Place in the Dewar Assembly

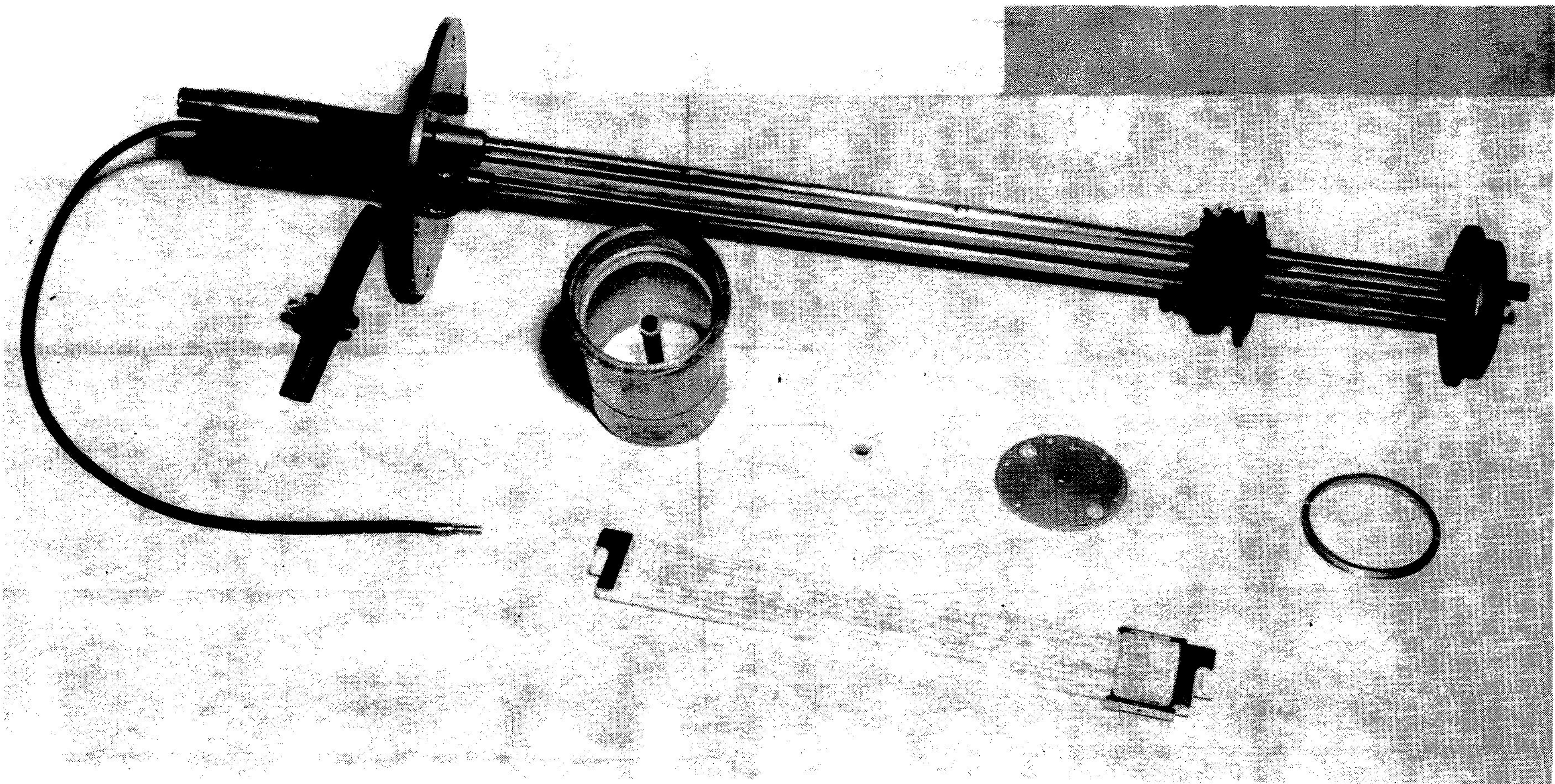

Plate 2 Disassembled Cavity Assembly

header is provided with vacuum-tight fittings so that the inside of the dewar may be evacuated.

The cavity consists of the radiation shield can, a tapered loading plate, and a locking ring. The loading plate is tapered and provided with small vent holes to facilitate the escape of any helium bubbles which may form inside the cavity. The locking ring securely attaches the loading plate to the can. The cavity is attached to the header with machine screws.

D. Light Source and Calibration

The light used in most tests is obtained from a Bausch and Lomb monochrometer, using incandescent lamps as sources. The lamp judged to be best is a 12 V automobile headlamp. It is preferred because of its steady, ripple-free output, ease of control, and freedom from cooling problems. For more intense light, a 200 W projection lamp is useful but somewhat inconvenient because it requires the use of a cooling fan.

The monochrometer provides a large range of wavelengths from 2000 to 7500 Å, plus a white light setting. The output wavelength has a linewidth of less than 50 Å, and the center wavelength is resettable to within one Å. The accuracy of the wavelength setting may be determined with the aid of a high pressure H_2 arc lamp, using the 6562.8 Å hydrogen line as a reference. The monochrometer has slits at both the input and output to vary the linewidth and intensity of the light.

An attachment for the monochrometer provides a shutter, f-stop, and condensing lens. A selection of lenses is available, and the light output is maximized by substituting lenses. The f-stop provides a variable diameter aperture measuring 5/8" to 1/16". The shutter has provisions for

1/25, 1/50, and 1/100 seconds, in addition to T and B settings.

The source of 9200 Å light is Texas Instruments SNX 100 galium arsenide light emitting diode, operated to give an output of about 10 milliwatts at 2 amps forward bias.

The fiber optic bundles were obtained from the Allied Radio Company and had transmission coefficients ranging from 40% to 70% depending on the length. A curve of the transmission coefficient vs λ for light pipes of this type is reproduced here as figure V-3. In all cases the light source is treated as the free end of the light pipe, and all light measurements are made at that point.

Light measurements are made with a silicon cell used in conjunction with a Hewelett-Packard 410 c VTVM. The silicon solar cell was selected to furnish the light calibration because of its high sensitivity, large area, and nearly equal response to photons in the visible region.

Treatments of solar cells are given by Bube[14], Prince[59], Burns[60], and Wolf[61]; the latter two go into more practical details, and are the source of most of the following discussion concerning silicon solar cells.

The collection efficiency η_c of a solar cell may be defined as the ratio of the number of electron-hole pairs separated by the electric field of the p-n junction to the total number of absorbed incident photons at a given wavelength. It depends on the band structure of the semiconductor material, the geometry of the cell, especially the location of the p-n junction, and of course the wavelength. Figure V-4 shows how η_c varies with λ for a typical, high efficiency silicon solar cell. It is seen that between 4500 Å and 7500 Å the curve is nearly linear and varies slowly with λ.

Fig. V - 3. Transmission coefficient for typical fiber optic bundles.

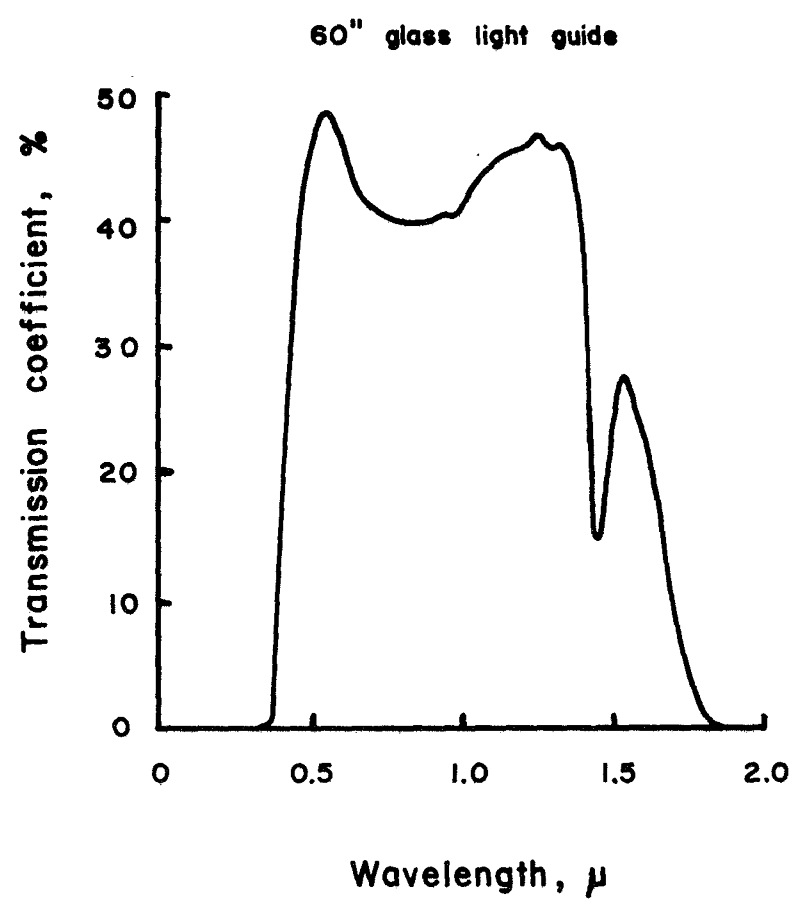

Fig. V - 4. Collection efficiency for a silicon solar cell.

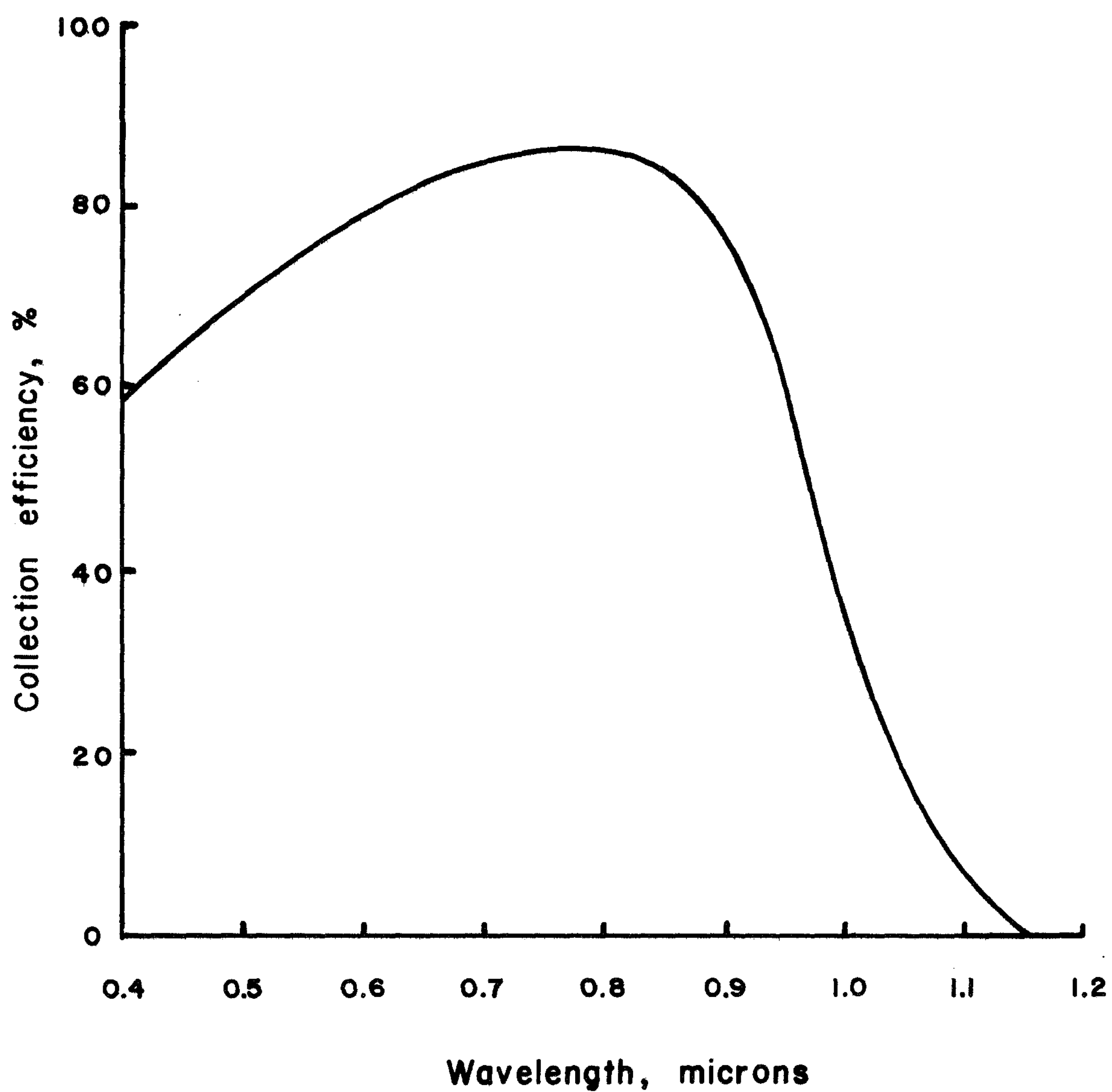

It may be shown[61] that the I-V characteristic of the solar cell may be expressed by the equation

$$I = I_o(e^{B(V - IR_s)} - 1) - I_L \qquad (5\text{-}1)$$

where I_o is the saturation current, $B = q/kT$, R_s is the series resistance of the cell, and I_L is the current due to, and directly proportional to, the light. This is merely the equation of a diode with I displaced by the amount I_L. For small values of I_L, the linear I-V characteristic of figure V-5 results, and if $IR_s << V$, $|I| = I_L$ at $V = 0$. Moreover, both V and I are directly proportional to I_L for this low light condition. The ideal measurement procedure would be to connect a zero-input-impedance ammeter to the cell. This would set $V = 0$, and the meter would read I_L directly. Unfortunately this is impossible since ammeters suitable for measuring low currents have appreciable input impedance, but a correction is easily made. In the circuit of figure V-6, the cell is represented by a current source I_L and a shunt resistance R_c, and the meter by a series resistance R_M and a zero-resistance ammeter. R_M varies according to the meter scale used. If the light is set at a constant level and the current is measured on a given meter scale, I_L may be found by the following well-known relation:

$$I_L = \frac{R_M + R_c}{R_c} I_M \qquad (5\text{-}2)$$

Thus, once R_c has been found, I_L may readily be determined from I_M. Once again it should be noted that this treatment only applies when the light is weak (i. e. $I_L << I_o$).

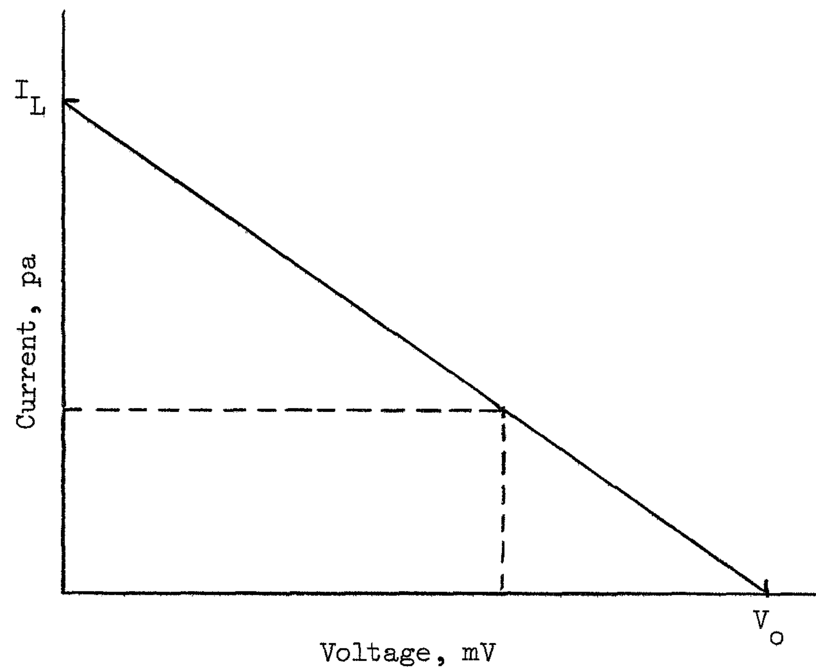

Fig. V-5. Current-voltage characteristic of a silicon solar cell for low light conditions.

A second efficiency term η_r must be introduced to take into account such things as reflection and errors in measuring the effective surface area of the cell. This term must be measured, and is assumed to be wavelength independent. First, the effective blackbody temperature of the light source must be measured. This is accomplished by measuring the I-V characteristics of the source, then finding $\rho(T)/\rho$ (300°K) for the filament, where $\rho(T)$ is the resistivity for the normal operating voltage. Reference to the Jones-Langmuir table[62] then gives the temperature of the filament. For convenience, the Jones-Langmuir table is reproduced here as table V-1.

Table V-1

SPECIFIC CHARACTERISTICS OF IDEAL TUNGSTEN FILAMENTS

(For a wire 1 cm long and 1 cm in diameter)

From H. A. Jones and I. Langmuir[62]

T, °K	$\rho(T)/\rho(273)$
500	1.924
600	2.41
700	2.93
800	3.46
900	4.00
1000	4.54
1100	5.08
1200	5.65
1300	6.22
1400	6.78
1500	7.36
1600	7.93
1700	8.52
1800	9.12
1900	9.72
2000	10.33
2100	10.93
2200	11.57
2300	12.19
2400	12.83
2500	13.47
2600	14.12
2700	14.76
2800	15.43
2900	16.10

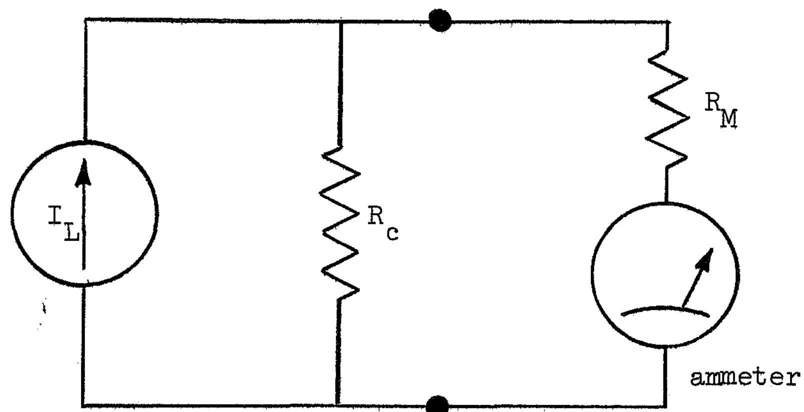

Fig. V-6, Circuit representation of a silicon solar connected to an ammeter.

The area, A_f, of the tungsten filament must also be measured. The Stefan-Boltzmann Law gives the power emitted from a black body as

$$\frac{P}{A_f} = \sigma T^4 \text{ watt m}^{-2} \tag{5-3}$$

where $\sigma = \frac{2\pi^5}{15} \frac{k^4}{h^3 c^3} = 5.67 \times 10^{-8} \text{ watt m}^{-2}\ {}^{\circ}K^{-4}$

If the total power emitted from an incandescent bulb is taken as the effective current times the effective voltage, and if T is known, then the area A_f is found from

$$A_f = \frac{P}{\sigma T^4} = \frac{IV}{\sigma T^4} \text{ square meters} \qquad (5\text{-}4)$$

The preceding calculations used the assumptions that emission from tungsten follows the T^4 law, and that power leaves the lamp only in the form of radiation. Although these assumptions are not exactly correct, experiments have shown that for the higher filament temperatures, any resulting errors may be ignored.

The photon flux as a function of wavelength may be found by using the calculated temperature and filament area in the following form of the blackbody radiation equation, which is given in cgs units:

$$\phi_p(\lambda) = \frac{2\Pi c\lambda^{-4} A_f}{e^{hc/k\lambda T} - 1} \text{ photon sec}^{-1} \text{ cm}^{-1}_{\Delta\lambda} \qquad (5\text{-}5)$$

This gives the expected distribution of photons leaving the lamp filament for a one cm wavelength interval centered at λ. This is easily converted to $\Delta\lambda = 1\text{Å}$, and is given by

$$\phi_p(\lambda) = \frac{2\Pi \times 10^{32}\, cA_f}{e^{hc/k\lambda T} - 1} [\lambda(\text{Å})]^{-4} \text{ photon sec}^{-1}\text{Å}^{-1} \qquad (5\text{-}6)$$

To obtain the number of photons from the lamp which actually impinge on the solar cell, $\phi_p(\lambda)$ must be multiplied by the geometry factor $A_c/4\Pi r^2$, where A_c is the area of the cell and r is the distance from the filament to the cell. This involves the assumption that the light is emitted from the lamp in a spherically symmetric distribution.

Thus, the final expression for the number of photons in a given wavelength range $\lambda_1 < \lambda < \lambda_2$ which impinge on the cell is

$$\phi(\lambda) = \int_{\lambda_1}^{\lambda_2} \frac{\phi_p(\lambda) A_c d\lambda}{4\Pi r^2}$$

$$= \int_{\lambda_2}^{\lambda_1} \frac{2\Pi \times 10^{32} \, c\lambda^{-4} A_f}{e^{hc/k\lambda T} - 1} \frac{A_c d\lambda}{4\Pi r^2} \text{ photons sec}^{-1} \qquad (5\text{-}7)$$

The number $\phi_{ehp}(\lambda)$ of photons which actually contribute to I_L differs from $\phi(\lambda)$ by the factor $\eta_r \eta_c$, due to reflection and incomplete conversion of photons to electron-hole pairs.

$$\phi_{ehp}(\lambda) = \eta_r \frac{A_c}{4\Pi r^2} \int_{\lambda_1}^{\lambda_2} \phi_p(\lambda) \eta_c d\lambda \qquad (5\text{-}8)$$

when η_r is assumed to be wavelength independent. Because of the unique shape of the η_c vs λ curve, a graphical integration is required to solve the preceding equation. The equation gives the carrier generation in the solar cell which is expected when a blackbody radiator is placed at at distance r from the cell. Comparison with experiment gives η_r, and this value was found to be 58.5% for the cell which was used.

It is now possible to find $\phi(\lambda)$ from the current indicated by the

ammeter. The current I_L at a discrete wavelength λ is given by

$$I_L(\lambda) = e\,\phi_{ehp}(\lambda)$$
$$= e\eta_r\eta_c(\lambda)\,\phi(\lambda) \qquad (5\text{-}9)$$

But I_L is related to the meter current by

$$I_L = \frac{R_M + R_c}{R_c} I_M \qquad (5\text{-}10)$$

Therefore,

$$\phi(\lambda) = \frac{R_M + R_c}{R_c} \frac{I_M}{e\eta_r\eta_c(\lambda)} \qquad (5\text{-}11)$$

To give an example of the preceding calculation, assume R_M = 9K, R_c = 18 K, η_r = 58.5%, and λ = 4800 Å. The current measured is 0.1457μa, and it is desired to convert the reading into a photon flux. Referring to the curve of η_c it is seen that η_c(4800) = 68%.

$$\phi(4800) = \frac{3}{2} \frac{0.1457 \times 10^{-6}}{1.6 \times 10^{-19} \times 0.585 \times 0.68} = 3.43 \times 10^{12}$$

Photons/sec.

This calculation corresponds to the actual case when the ammeter is the 1.5μa scale of the H-P 410c. For this case, we find a conversion factor of 2.35×10^{13} photons/sec - μa for λ = 4800 Å.

E. Thermally Stimulated Conductivity Apparatus

A block diagram of the TSC apparatus is given in figure V-7. Three separate current paths are required to give the sample current,

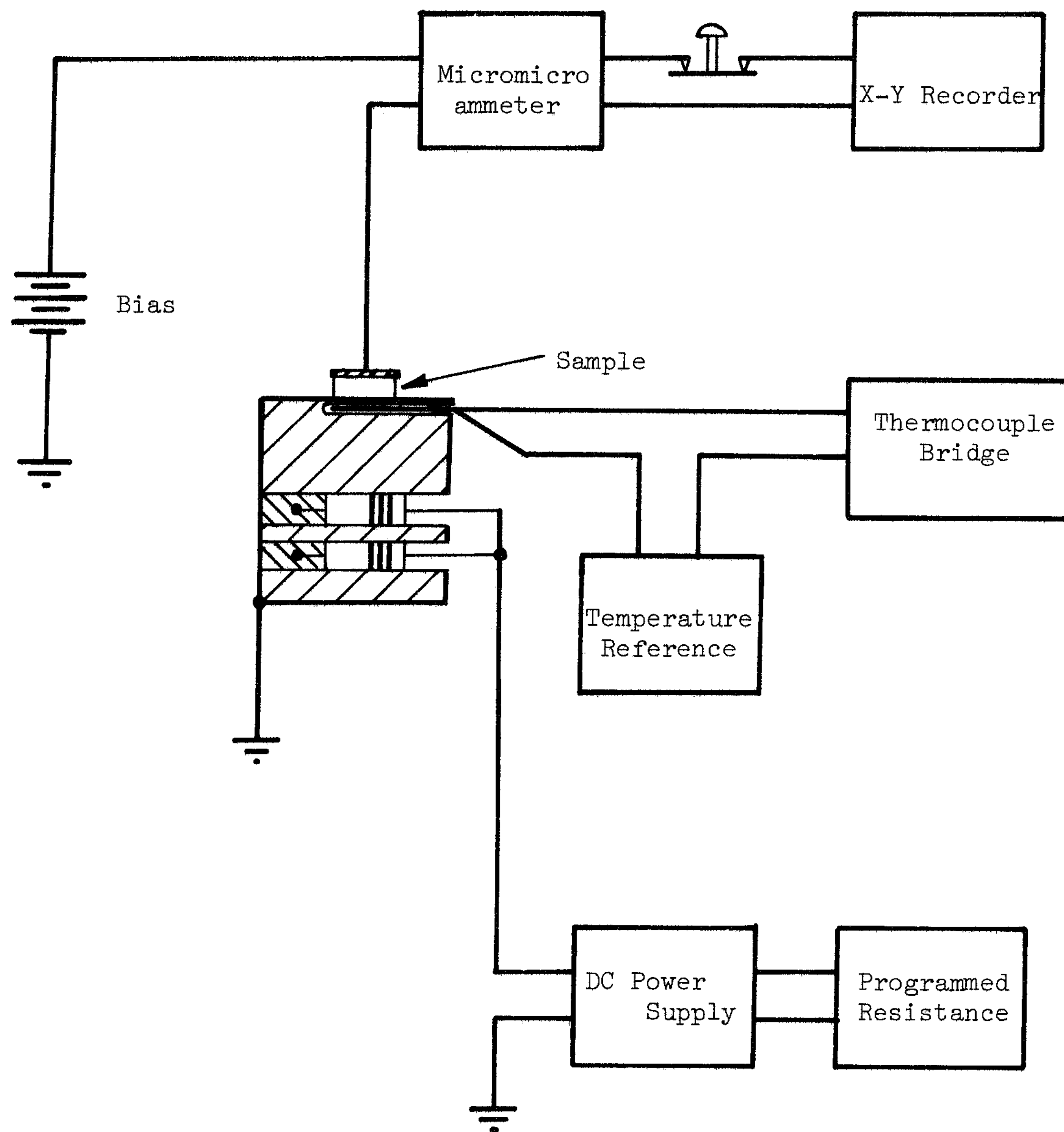

Fig. V-7. TSC apparatus.

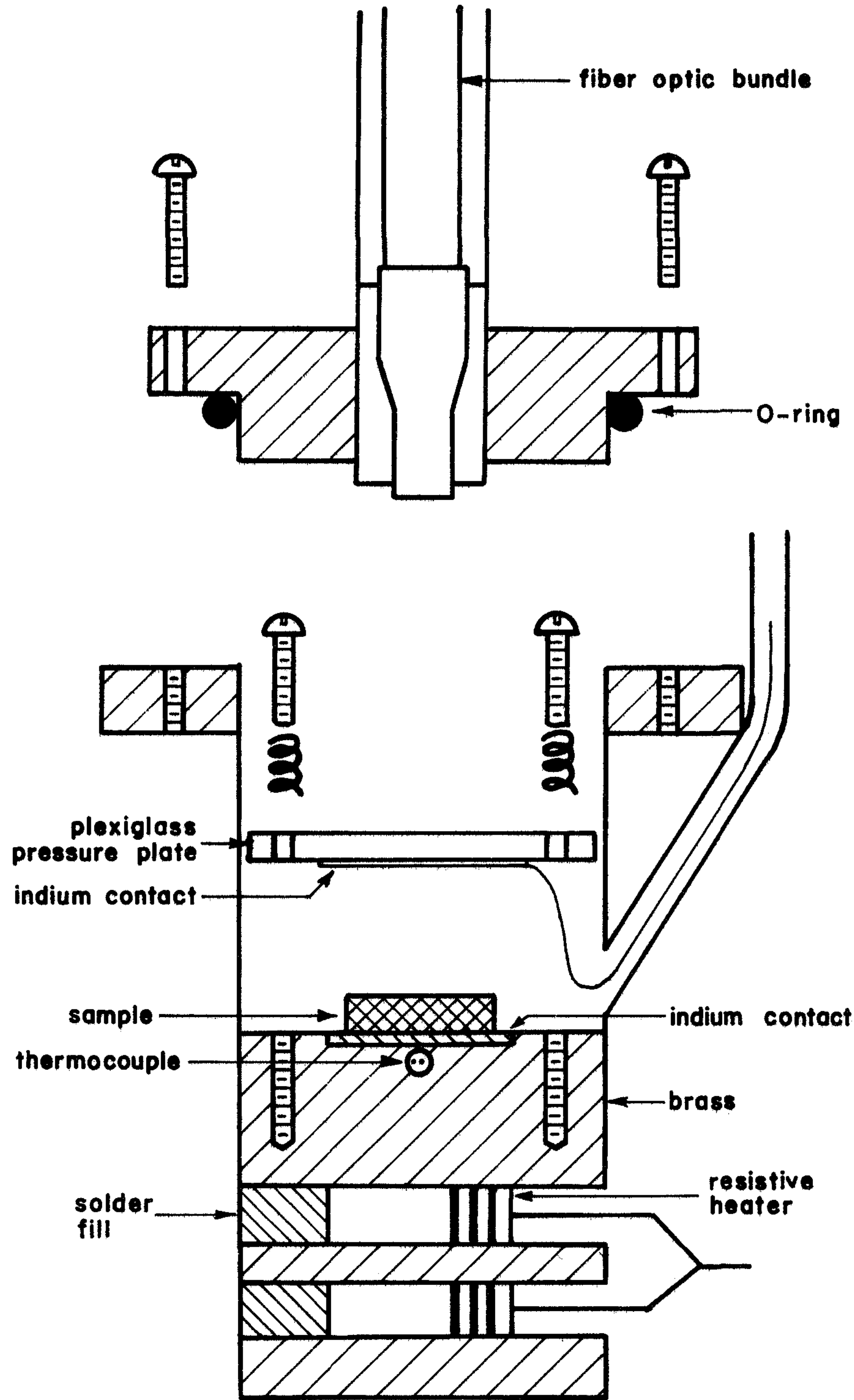

Fig. V-8. TSC sample holder.

Fig. V - 9. Heating rate for TSC apparatus.

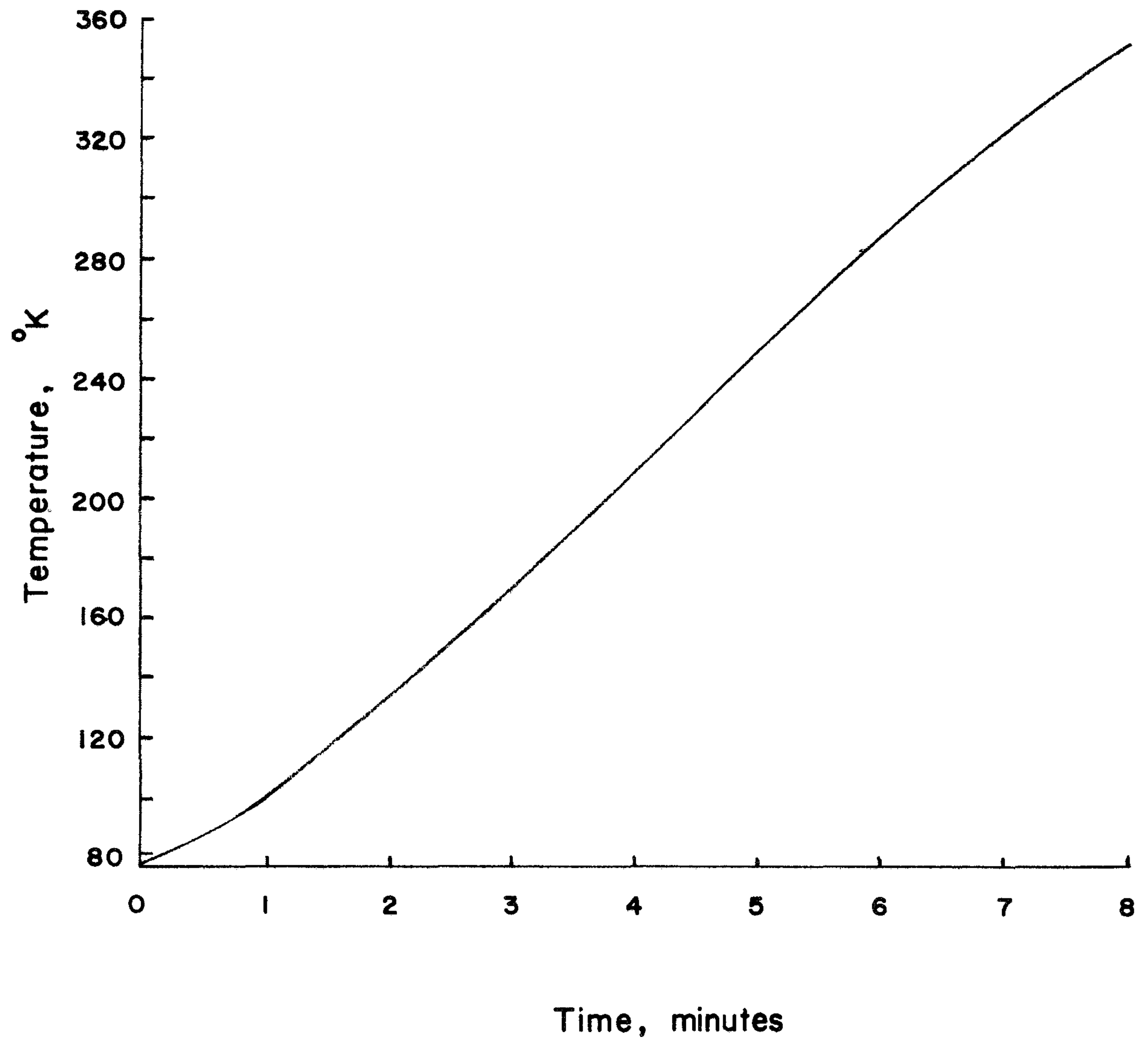

Chapter VI

RESULTS

A. The Photodielectric Effect

Four different samples of CdS and CdS:Al were used in the TSC and photodielectric tests; one was known to be high purity material, the second was nominally pure, and the other two were aluminum doped. The presence of some aluminum in two of the samples was discovered by placing portions in an evacuated quartz tube and heating it to more than 1100°C. This caused the sample to decompose, and the constituents could be observed when they condensed on different parts of the cool end of the tube. Neutron activation analysis confirmed the presence of aluminum in the samples.

The physical characteristics of the samples used in the photodielectric experiments are listed in table IV-1. All are about 1 cm in diameter and have polished surfaces.

1. Aluminum Doped Samples

The result of a typical photodielectric experiment with CdS:Al is shown in figure VI-1. Several features of the curve are significant. First, the frequency begins to drop immediately after the application of the light. Also, it is seen that up to the saturation point, the curve is quite linear. That is, the photodielectric apparatus with a CdS sample acts as an integrator of light. Third, the mechanical vibration during a liquid helium transfer process removed part of the frequency change, although it did not alter the rate of frequency change. Fourth, it is seen that when the light is turned off, the frequency change does not

Fig. VI-1. Typical photodielectric results.

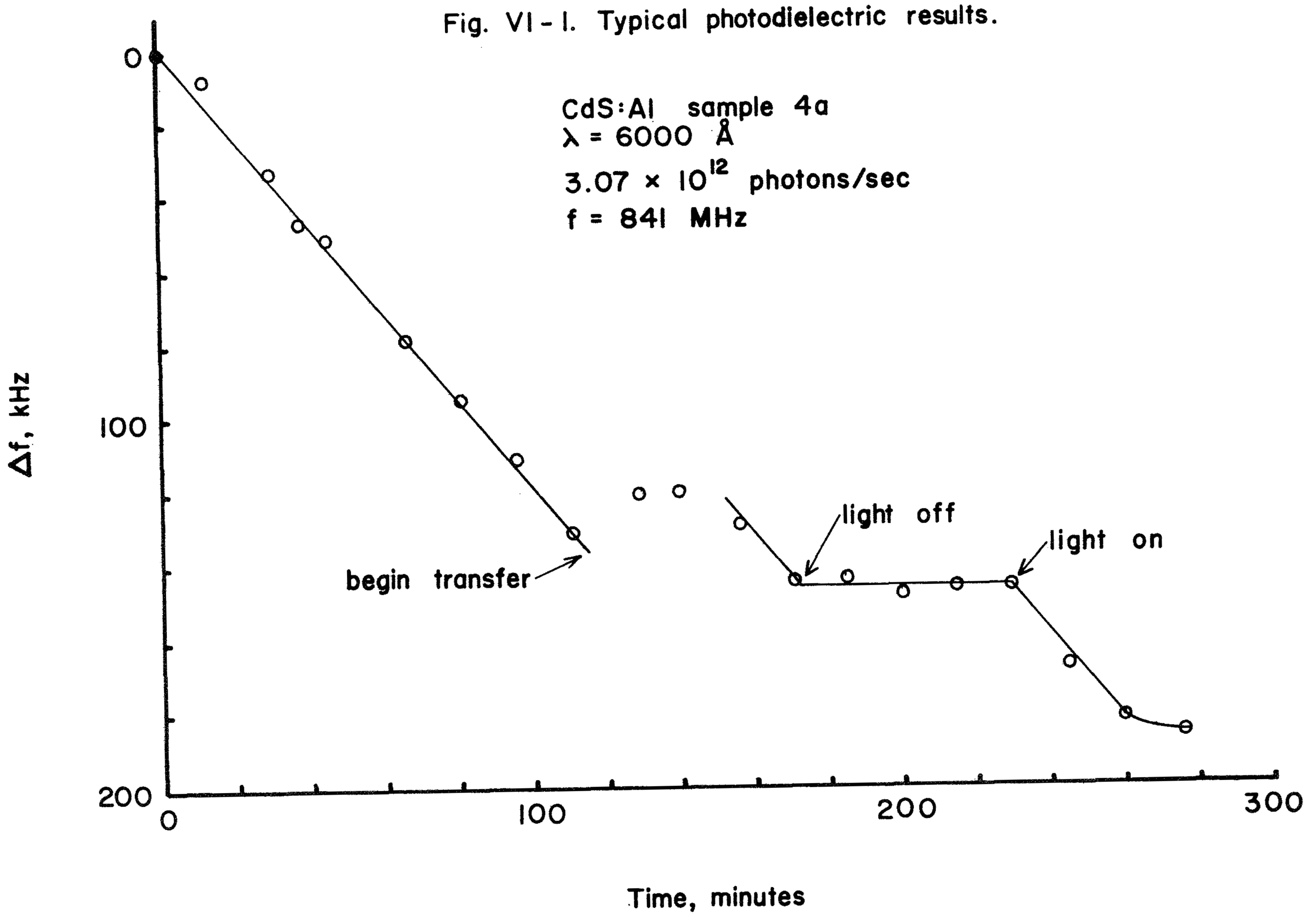

decrease, but remains constant. Finally, a definite saturation effect is noted, after which the frequency can not be changed significantly.

To determine whether any of these features were actually due to photoconductivity, the photoconductivity of the same samples was measured for the same conditions of temperature and light. The resulting curve showing the rise of conductivity for weak light in sample 4a at 4.2°K is shown in figure VI-2. Plotted on the same curve, for the sake of comparison, is the photodielectric response for the same sample and the same light. It is seen that no current can be measured until $n = \alpha/V_s \int \phi dt$ reaches 2×10^{16} electron-hole pairs per cm^3. Also, it may be noted that when n reaches 3×10^{17}, the photodielectric response begins to saturate, although the photoconductivity has only reached about 10% of its final value.

Table VI-1. Characteristics of photodielectric samples.

Sample	1	4a	4b	5	6
Type	Nominally Pure	Aluminum Doped	Aluminum Doped	High Purity	Aluminum Doped
Volume, cm^3	0.050	0.0716	0.0975	0.1125	0.143
Area, cm^2	0.597	0.723	0.80	0.75	0.742
Thickness, mm	0.838	0.99	1.22	1.5	1.93
G	0.018	0.0232	0.03155	0.033	0.0493
Electron Traps, eV	0.27 0.27*	0.15 0.176* 0.20 0.265 0.35 0.52	0.15 0.176* 0.20 0.265 0.35 0.52		0.127* 0.13 0.35 0.43

* - levels obtained with the photodielectric effect.

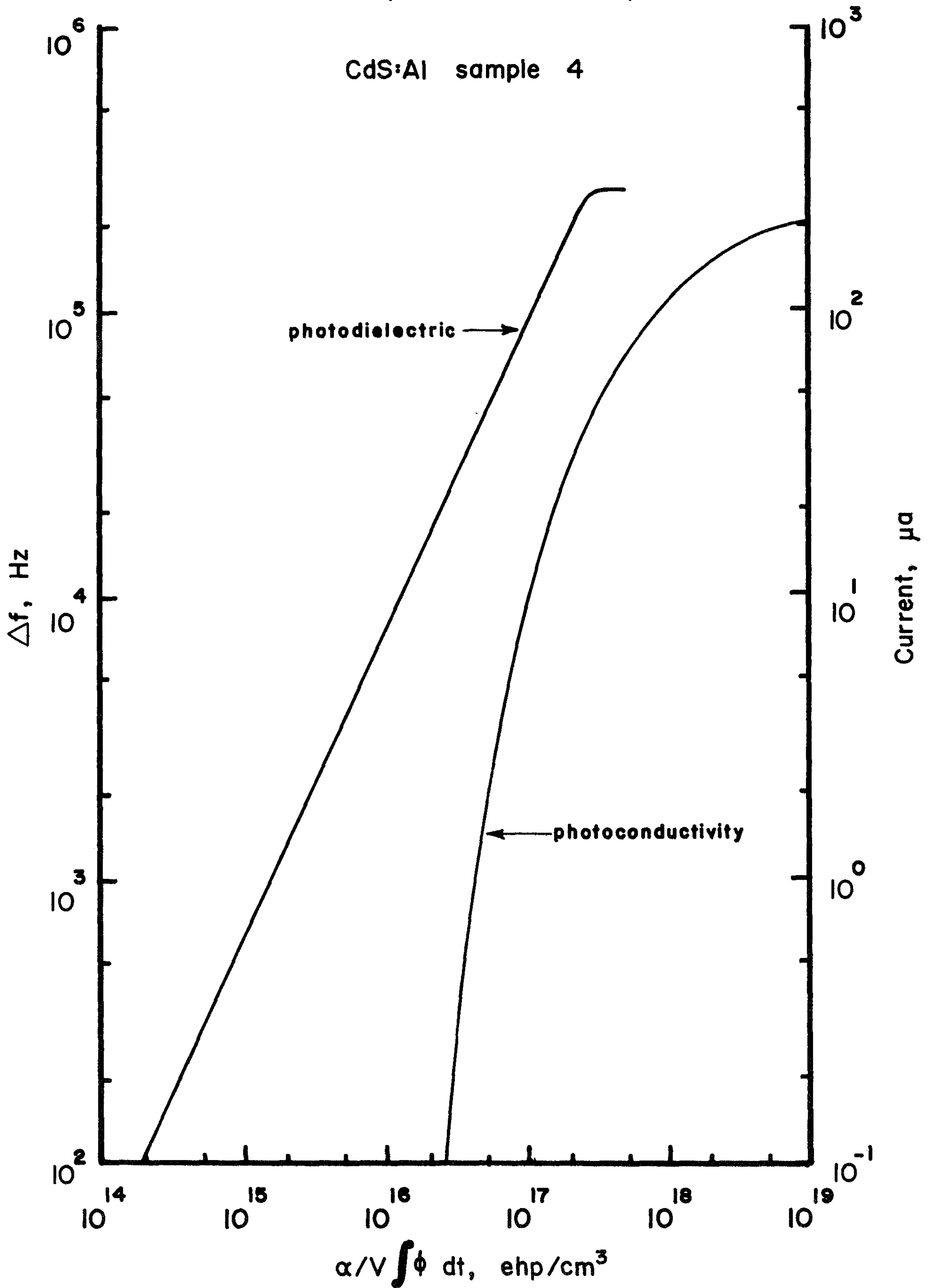

Fig. VI - 2. Comparison of photoconductivity and photodielectric responses.

Clearly, the photodielectric effect is not merely a reflection of the increasing photoconductivity.

A comparison of the shapes of the two curves shows that the photodielectric curve is linear, while the photoconductivity has regions varying approximately as n^5 initially, and later as $n^{1/2}$. Analysis of the photoconductivity curve is impossible without a more detailed energy level picture, but it may be supposed that the strange current variation is a result of a slight movement of the electron Fermi level. For example, if the Fermi level moved from 0.151 eV to 0.150 eV at $4.2^{\circ}K$, the result would be an increase by a factor of 15 in ther thermal exchange with the conduction band.

Considering figure VI-2 again, the features of the photodielectric curve may be explained with the aid of the energy model shown in figure VI-3. The excitation creates electron-hole pairs; the holes are

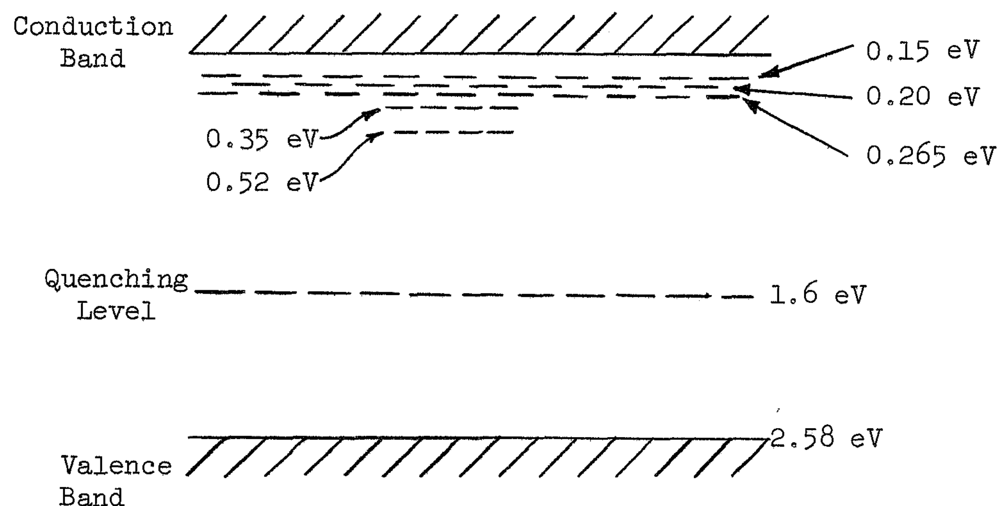

Fig. VI-3. Energy level model for CdS:Al sample 4.

immediately trapped at the quenching levels, while the electrons are transferred to the conduction band. Due to the negative charge at the quenching levels, the electrons do not recombine, but rather become trapped in one of the available trapping sites. TSC tests performed on samples 4 and 6 have shown that the deeper traps tend to fill first and that the densities of the 0.52 and 0.35 eV traps in sample 4 are small; less than 10^{15} cm^{-3} each. This number is estimated by measuring the length of time required to fill these deep traps with a given photon flux. For example, when ϕ was 2×10^{12} photons per second, $\alpha = 75\%$, and $V_s = 0.023$ cm^3, it was found that an excitation period of about 15 seconds was required to fill the 0.52 eV trap without appreciably filling the trap at 0.35 eV. Assuming all of the generated electrons were captured at the deepest trap, $(\alpha/V_s) \int \phi dt$ may be taken as the density of trapped carriers. A quick calculation shows that this number is $\sim 9.7 \times 10^{14}$ electrons. Any recombination which might have occurred would reduce this estimate to a lower value. The 0.52 and 0.35 eV traps always required about the same amount of time for filling, and thus there densities are thought to be approximately the same.

After the first 30 seconds of excitation, the two deep traps are essentially filled, and any subsequent excitation has the effect of filling the shallow traps. No detectable filling of the shallow traps occurred in that initial period of illumination. The peak thermally stimulated conductivity for the 0.15, 0.20, and 0.265 eV traps was about 10^2 to 10^5 higher than the peaks for the deeper traps. From figure VI-2, it is possible to estimate the density of shallow traps as about $3 \times 10^{17} cm^{-3}$, assuming the density is equal to $(\alpha/V_s) \int \phi dt$.

The linear frequency change in figure VI-2 is attributed to the filling of the distribution of shallow traps, and the associated effect on the dielectric constant of the crystal. TSC data for sample 4 indicates three closely spaced peaks at 0.15, 0.20, and 0.256 eV with approximately equal densities. Use of the equations of Chapter III and the data of figure VI-2 predicts the effective trap energy is 0.176 eV. The analysis leading to this number is given as follows.

First, it is noted that the undisturbed frequency change is linear and amounts to 262 kHz for a period of excitation of 185 minutes and a flux of 3.07×10^{12} photons/sec. Any tap effects are removed from the data by extrapolation. Setting f = 841 MHz, G = 0.0232, and $\varepsilon_{\ell} = 8.7$ (this is the ellipsoidal average of the relative dielectric constant, according to Neuberger[16]), and then employing equation (3-44), $\Delta\varepsilon_r$ is calculated to be 1.26. Since $\alpha = 75\%$, $V_s = 0.0716\ cm^3$, and $\phi = 3.07 \times 10^{12}$ photons/sec, equation (3-39) gives $n = 3.75 \times 10^{17}\ cm^{-3}$. Substituting $\Delta\varepsilon_r'$ and n into equation (3-20),with m*/m = 0.2, we then find $\omega_o^2 = 4.73 \times 10^{27}$. According to equation (3-30), this means that the trap energy is 0.176 eV.

It is seen that for the case of sample 4 the photodielectric experiment is not able to resolve the three peaks found by TSC methods. Instead, it gives an effective trap depth somewhat deeper than the shallowest of the three TSC levels. This might be expected; the E^{-3} dependence of the photodielectric effect on trap energy causes the shallow levels to be weighted more heavily than the deeper ones. TSC tests with sample 4 showed that the three shallow traps filled at the same time, so three different slopes, one for each level, were not observed in the photodielectric test.

Excitation of the sample at other wavelengths between 4800 Å and 6000 Å shows very little change in the preceding results, when compared on a per-unit-absorbed-photon basis. This is true for both photodielectric and photoconductivity experiments. The absorption of all of the samples dropped sharply for wavelengths above 6000 Å, and thus these wavelengths were not employed. Absorption was $\sim$75% for all $\lambda <$ 6000 Å; only reflection contributed significantly to the loss. The net effect, therefore, can be maximized by exciting the crystal at wavelengths of the maximum absorption region.

Photodielectric tests performed in the two aluminum doped samples yielded essentially the same results, except that with sample 6, a frequency change of over 700 kHz was achieved. This sample proved to have no 0.52 eV trap, but two well-defined traps at 0.43 and 0.35 eV, with concentration of about 10^{15} and 10^{16} cm^{-3} respectively, plus a single shallow trap at 0.13 eV with a concentration greater than 10^{17} cm^{-3}. The estimation of these densities preceded in the same manner as for sample 4. Using the equations of Chapter III, the photodielectric effect data in sample 6 predicts a trap at 0.127 eV with a concentration of 1.72×10^{17} cm^{-3}. The concentration is estimated as being approximately equal to $(\alpha/V_s) \int \phi dt$, as in the case of sample 4. The depth of the electron trap follows from the following experimental results: α = 0.75%, V_s = 0.143 cm^3, $\phi = 2.2 \times 10^{13}$ photons/sec, and t'= 125 minutes. Substitution into equation (3-39) gives $n = 1.72 \times 10^{17}$ cm^{-3}. In equation (3-44), Δf = 730 kHz, f = 831 MHz, G = 0.0495, and ε_ℓ = 8.7, so $\Delta\varepsilon_r' = 1.6$. Substitution of $\Delta\varepsilon_r'$ and n into equation (3-20) gives $\omega_o^2 = 1.71 \times 10^{27}$, so E = 0.127 eV. This agrees

quite well with the single shallow energy level at 0.13 eV found be TSC methods.

It should be noted that sample 6 proved to be about 1.5 times as sensitive as sample 4 when operated in the photodielectric mode and compared for equal volumes and light intensities. This difference is due to the fact that the major trap in sample 6 is slightly shallower than that in sample 4.

2. Nominally Pure Cadmium Sulfide

Sample 1, the nominally pure material, proved to be about one fifth as sensitive as the aluminum doped samples. TSC tests showed that sample 1 appears to have a large ($>10^{17}$ cm^{-3}) density of traps with a characteristic temperature greater than $340^{\circ}K$. The shallow traps found in CdS:Al are not seen in this sample. Low temperature measurements of absorption vs wavelength showed the absorption peaked at 4790 Å, instead of 5100 Å as was the case in the aluminum doped materials. This provides further proof of the lack of shallow traps. A sharp peak in the low temperature photoconductivity occurred at 5510 Å, indicating that the depth of the effective trap is 0.27 eV. Using the same sample under the same conditions, the photodielectric model predicts an energy level at 0.27 eV. This calculation uses the experimental values Δf = 30 kHz for t'= 50 minutes at $\phi = 3.5 \times 10^{12}$ photons/sec. Also, f = 847 MHz, $G = 0.0180$, $\varepsilon_{\ell} = 8.7$, $\alpha = 0.75$, and $V_s = 0.50$ cm^3. Here it is seen that the simple photodielectric model and theory accurately predict the depth of the 0.27 eV trap from frequency change data.

3. High Purity Cadmium Sulfide

Very little can be said about optical effects in sample 5, the high purity CdS, except that it is not a sensitive detector when operated in the photodielectric mode. For example, an average-sized sample was only able to produce an 18 kHz change in the cavity frequency before the effect saturated. Some traps in small concentrations were uncovered by the TSC procedure, but the location and density of the trap proved to be heavily dependent on the method of preparation of the sample, indicating the traps were probably due to some combination of surface defects and oxygen and water adsorption. This problem will have to undergo a great deal more study before the origins and locations of the traps can be accurately given.

It is interesting to compare some of the preceding results with the data of table II-1, which lists energy levels reported by other workers, along with the probable origins of the levels. This comparison suggests that the deeper traps at 0.52, 0.43, and 0.35 eV are due to either surface states or excess sulfur.

B. Power Absorption

The relative amount of power absorbed by the sample provides another indication of what processes are occurring the crystal. According to Chapter III, both free and bound carriers should contribute to the power absorption, but the relative contribution due to free carriers should be larger by some factor which depends on ω and τ, the momentum relaxation time.

In the experiments with the three sensitive crystals, the plot of

power absorption vs time always has the same form as the plot of frequency change, provided the photodielectric effect has not yet begun to saturate. This relation is illustrated in the figure VI-4 for sample 4. In all tests the ratio of Δf to ΔP was always approximately 50 kHz/db as long as the curve of Δf vs time was linear. A very revealing departure from this rule was observed when sample 4, already nearly saturated, was illuminated with an intense five second pulse of white light. The resulting changes in the frequency and absorbed power are shown in figure IV-5a. Here, it is seen that the power quickly dropped at least 2.1 db, and probably more, by the end of the pulse. The frequency, on the other hand, slowly decreased to a final change of 96 kHz. The power slowly recovered to a final change of 1.5 db, the value which might be expected to accompany the

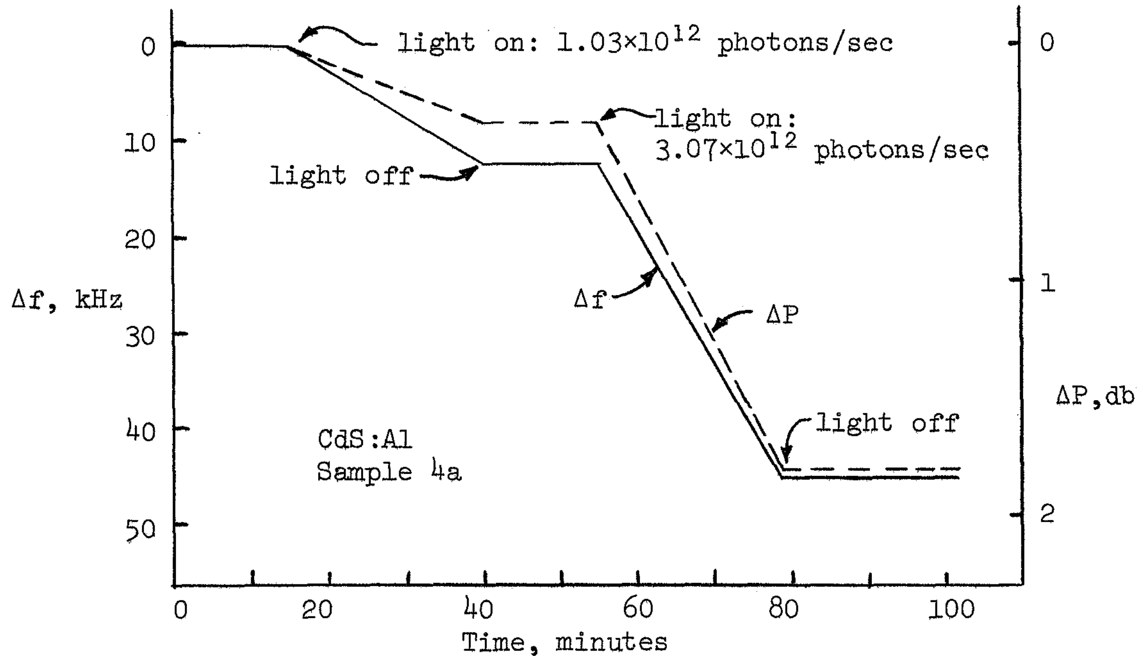

Fig. VI-4. Comparison of power absorption and frequency change.

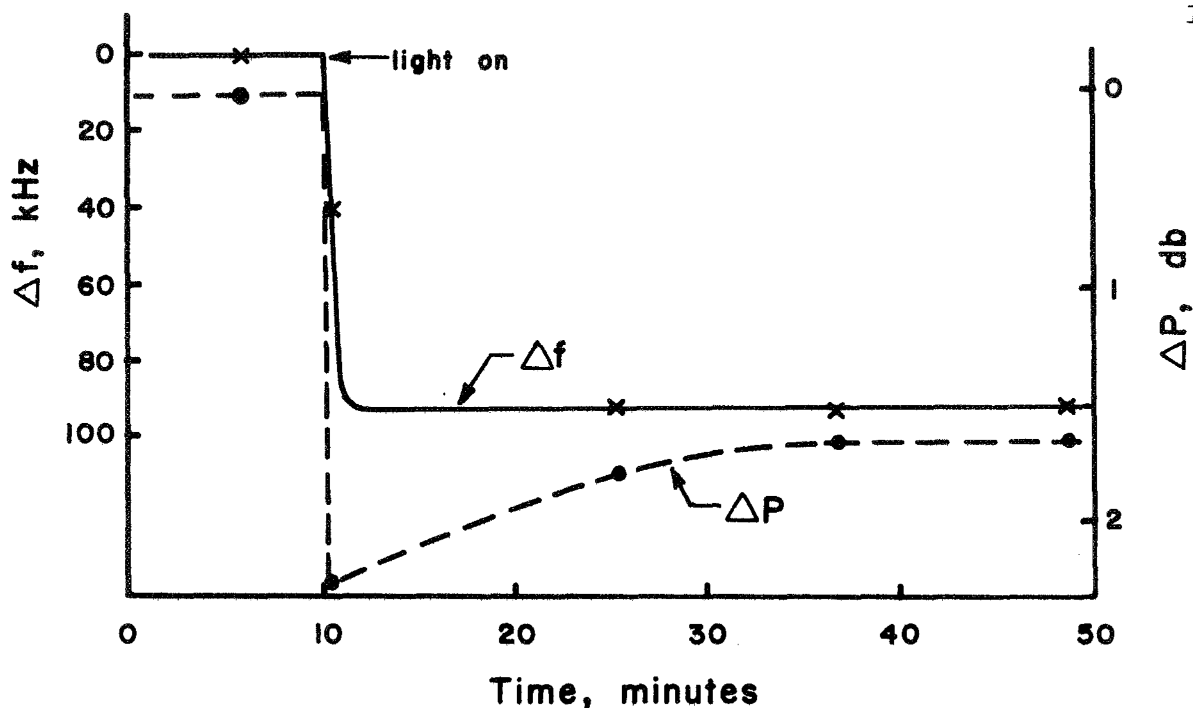

Fig. VI - 5a. Comparison of the changes in frequency and power absorption in CdS:Al sample 4 due to a single 5 sec pulse of 4 milliwatt white light.

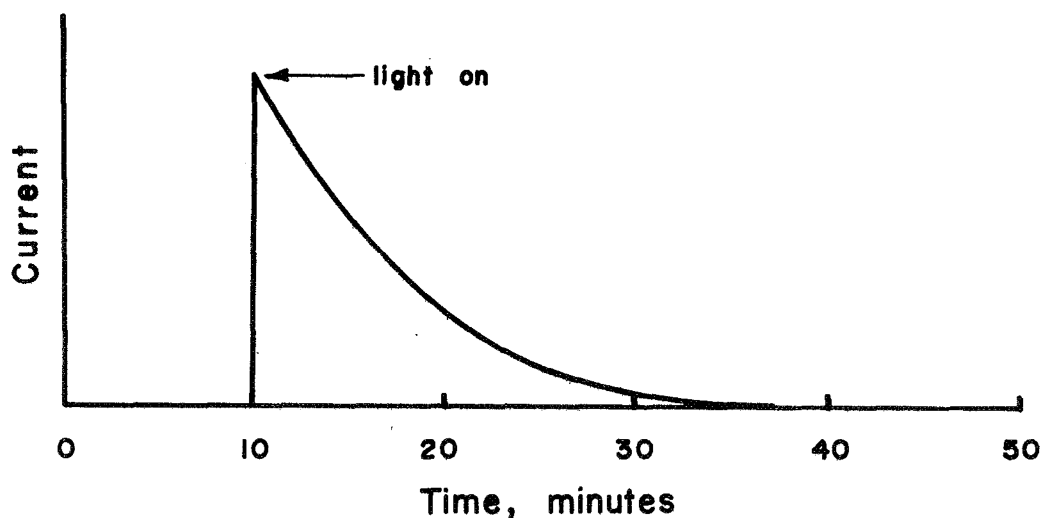

Fig. VI - 5b. Photoconductive response of sample 4 at 4.2 °K, predicted from power absorption data above.

frequency change. If the change due to trapped carriers is subtracted from the power absorption curve, the plot of figure VI-5b results. It has exactly the same shape as a plot of photoconductivity vs time for the same sample subjected to a very bright light. Thus, it is evident that the power absorption, when compared with the frequency change, may be used to separate free carrier effects from effects due to trapped carriers.

The same behavior is observed in a sample which is approaching saturation and is still being illuminated. Figure VI-6 shows Δf and ΔP for sample 4 under these conditions. This figure clearly indicates that at the time when the traps became saturated, there is an increase in the rate at which electrons are being added to the conduction band.

Since ΔP has the same dependence on n as Δf, it would be expected that the absorbed power should increase 3 db each time the value of n is doubled. This relationship was followed fairly closely by the experimental data in regions not close to saturation. Calculations of τ are not possible at this time, due to the inability to measure the absolute change in the power rather than the relative change.

C. The Tap Effect

During one photodielectric test with sample 4, it became necessary to transfer additional liquid helium. The light was left on during the transfer process. A plot of Δf vs time, shown in figure VI-1, shows that due to the small mechanical vibrations associated with the transfer process part of the frequency change was lost. According to the proposed model, this represents the freeing of holes in the quenching level, which then

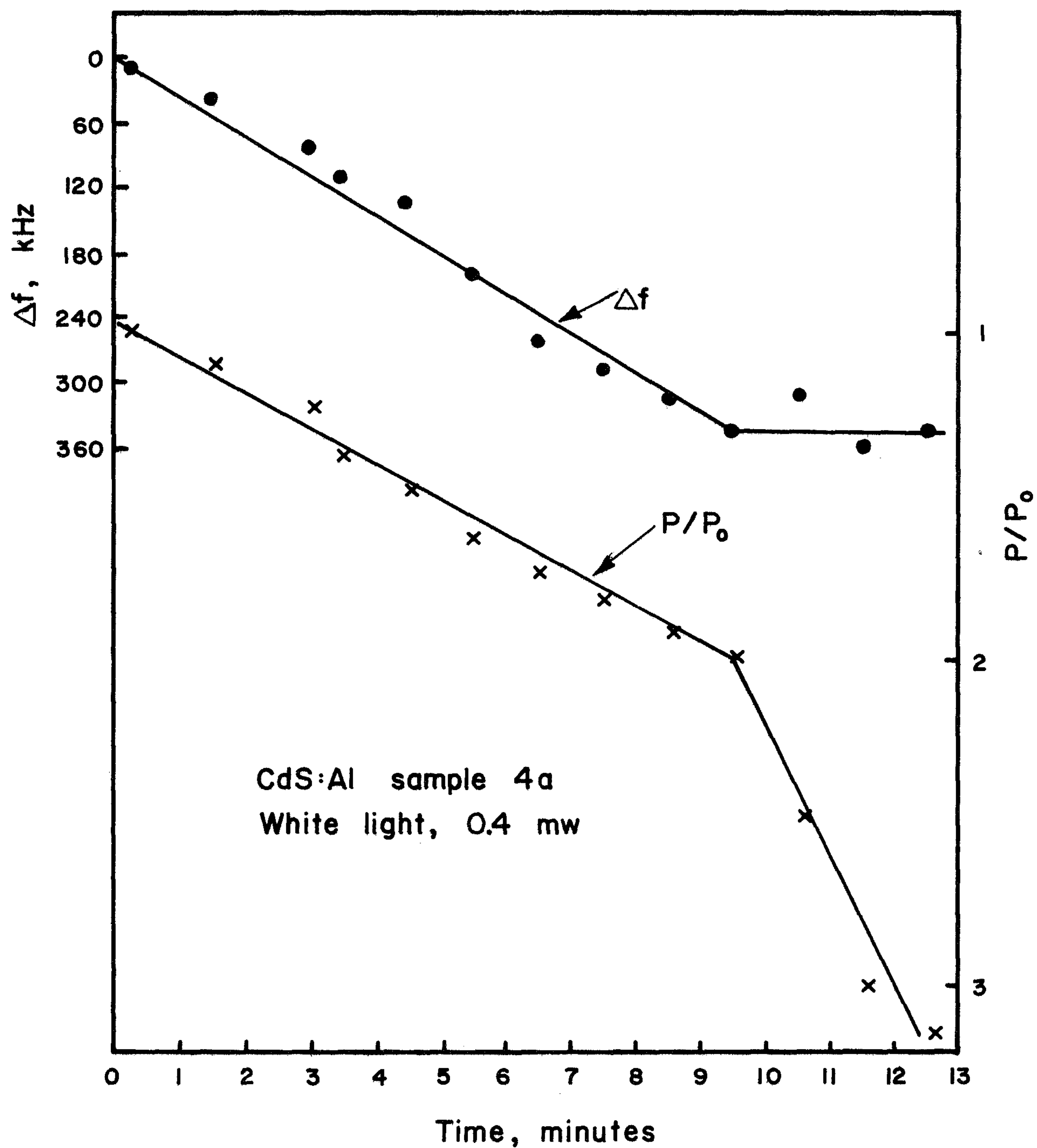

Fig. VI - 6. Comparison of the changes in absorbed power and frequency as trap saturation is approached.

recombine with electrons in the shallow traps. Such freeing has been confirmed using TSC tests; mechanical vibration has been shown to reduce the height of a current peak by orders of magnitude, or even remove it completely, depending on the amount of stimulation applied. The details of the mechanism of the tap effect are not well understood. Therefore it is possible that experiments using the photodielectric effect in CdS can be designed to yield more knowledge about the tap process.

The presence of the tap effect has one slight disadvantage: the apparatus must be protected from mechanical disturbances. In practice, it was judged to be sufficient to avoid touching the dewar module, and thus the disadvantage is certainly not a great one. The great advantage in having the tap effect, on the other hand, may be that it will provide a method of resetting the crystal without having to warm the entire cavity assembly to room temperature. More experimental work along these lines is necessary before the usefulness of the method can be evaluated.

D. Photodielectric Optical Detector

Due to the nature of the optical effects in CdS, the photodielectric detector is not easily compared to other detectors. For example, the minimum detectable power (MDP) depends on how long the experimenter is willing to integrate the light. The noise equivalent power (NEP), defined as

$$\mathrm{NEP} = \frac{\mathrm{MDP}}{(\mathrm{BW})^2} \qquad (6\text{-}1)$$

is undefinable in this case because the bandwidth, for low light levels, approaches zero.

To give an estimate of the photosensitivity of the photodielectric detector, one must set limits on several quantities. For example, assuming the minimum detectable frequency change to be 1 Hz, and the maximum allowable integration time to be one hour, the system used in these experiments should be able to detect about 1.31×10^{7} photons/sec, or about 5×10^{-12} watts, using sample 6. Any improvements in the system, obtained by using a higher frequency, larger sample, shallower traps, and so forth, would be expected to improve this figure.

The sensitivity is obviously a function of wavelength, and would be expected to vary in the same way as the absorption. When detecting white light, some filtering might be called for to remove certain infrared wavelengths to prevent quenching.

E. Summary and Recommendations

It has been shown that the photodielectric effect in a superconducting resonant cavity can be used to simultaneously study trap filling and photoconductivity in CdS samples. If the light flux and absorption coefficient of the sample are known, and if the electron traps are not grouped too closely, one photodielectric experiment yields the depth of the traps and their densities. Compared to thermally stimulated conductivity measurements, the photodielectric effect experiment is much easier to perform, consumes less time, and provides results which are more easily analyzed. Other advantages of the photodielectric approach are that no electrical contacts are required, and the only auxiliary physical measurements on the sample which are required are its weight and G factor.

Disadvantages are that closely spaced levels cannot yet be separated, and the method is relatively insensitive to deep traps.

It has also been seen that the photodielectric effect in CdS can be used to provide a sensitive photon counter for steady weak light. However, several improvements in the experimental apparatus should be implemented to improve the sensitivity and reduce the noise level of the detector. Making the cavity the frequency control element of an oscillator would be one such improvement. This would remove the experimenter's judgement from the list of factors which determine the resonant frequency. It would also allow a continuous plot of the cavity frequency to be made, thereby providing a great deal more resolution in the data.

Another improvement in the experimental apparatus would be to seal the cavity and keep it evacuated throughout the experiment, thereby preventing the formation of helium gas bubbles which cause the frequency of the cavity to vary.

An optical system to route the light into the cavity should be designed. In the current system, the light is attenuated by a factor of about 50% by passing through the fiber optic bundle. The light leaving the light pipe is not focused, which makes calibrations difficult, and the transmissivity of the glass fibers drops to zero at $\lambda = 2\mu$, hampering attempts to measure effects due to infrared light.

Assuming these improvements are made, many other experiments should be performed. In CdS, the effects of infrared quenching should be investigated, in order to form a more precise model for the optical effects and to study the usefulness of infrared quenching in resetting the cavity

frequency. With better resolution, more tests should be performed on samples 1, 4, and 6 to separate the effects of deep or closely spaced traps.

Methods of improving the sensitivity of CdS samples should be investigated. Many workers have reported improved photoconductive response after heating the sample in a vacuum. Dependence of the sensitivity on the adsorption of gases is also a well established fact. Samples with larger concentrations of shallow traps should be obtained and tested. Methods of resetting the crystal, such as the tap effect, infrared quenching, or high electric field effects, should be investigated to determine the degree of resetability possible and to provide more information on the nature of the traps.

The photodielectric effect in other II-VI compounds should be studied. If the optical processes are the same, the group of II-VI compounds could furnish sensitive optical detectors to cover the entire visible spectrum plus the near infrared. Other light-sensitive compounds such as Ge:Hg and InSb, should be investigated to determine whether the model and analysis presented here is useful outside the set of II-VI compounds.

BIBLIOGRAPHY

1. Arndt, G. D., W. H. Hartwig, and J. L. Stone, "Photodielectric Detector Using a Superconducting Cavity," (To be published.)

2. Hartwig, W. H., "Use of Photodielectric Response of Semiconductors to Detect Visible & Infrared Radiation," Air Force Contract Report 19(604)5717.

3. Genz, R. H., "Frequency Dependence of Reentrant Coaxial Cavities Upon Physical Properties of a Terminating Disc," Masters Thesis, The University of Texas, Austin, Texas, 1961.

4. Arndt, G. D., "Photodielectric Effect of Bulk Semiconductors in Resonant Cavities," PhD Dissertation, The University of Texas, Austin, Texas, 1965.

5. Stone, J. L., "A Unique Laser Detector Utilizing the Photodielectric Effect in Cooled Semiconductors," PhD Dissertation, The University of Texas, January, 1968.

6. Bube, R. H., _Photoconductivity of Solids_, New York, Wiley & Sons, 1960.

7. Lambe, John, "Recombination Processes in CdS," _Phys. Rev._ 98, 985 (1955).

8. Lambe, John, "CdS with Silver Activator," _Phys. Rev._ 100, 1586 (1955).

9. Kulp, B. A., "Defects In Cadmium Sulfide Crystals," _J. Appl. Phys._ 36, 553 (1965).

10. Bube, R. H., "Photoelectronic Properties of Imperfections in Cadmium Sulfo-Selemide Solid Solutions," _J. Appl. Phys._ 35, 586 (1964).

11. Kronenberg, S. and C. A. Accardo, "Dielectric Changes in Inorganic Phosphors," _Phys. Rev._ 101, 989 (1956).

12. Matthews, N. F. J. and P. J. Warter, "Transient Polarization in Insulating CdS," _Phys. Rev._ 144, 610 (1965).

13. Rose, A., _Concepts in Photoconductivity and Allied Problems_, Interscience Publishers, New York, 1963.

14. Aven, M. and J. S. Prener, _Physics and Chemistry of II-VI Compounds_, Interscience Publishers, New York (1967).

15. Smith, R. A., _Wave Mechanics of Crystalline Solids_, Chapman and Hall Ltd., London, 1963.

16. Neuberger, M., "Cadmium Sulfide," ASTIA AD 810354.

17. Czyzak, S. J., "The Study of the Properties of Single CdS and ZnS Crystals," ASTIA AD 242 787 (1960).

18. Hopfield, J. J. and D. G. Thomas, "Fine Structure and Magneto-Optic Effects in the Exciton Spectrum of CdS," Phys. Rev. 122, 35 (1961).

19. Zook, J. D. and R. N. Dexter, "Galvanomagnetic Effects in CdS," Phys. Rev. 129, 1980 (1963).

20. Dutton, D., "Fundamental Absorption Edge in Cadmium Sulfide," Phys. Rev. 112, 785 (1958).

21. Lempicki, A., "The Reflection Spectrum of Cadmium Sulfide," Proc. Phys. Soc. 74, 138 (1959).

22. Cardona, M. and G. Harbeke, "Optical Properties and Band Structure of Wurtzite-Type Crystals & Rutile," Phys. Rev. 137, A 1467 (1965).

23. Colbow, K., "Free-to-Bound and Bound-to-Bound Transitions in CdS," Phys. Rev. 141, 742 (1966).

24. Kulp, B. A., R. M. Detweiler and W. A. Anders, "Temperature Dependence of Edge Emission in Single-Crystal Cadmium Sulfide," Phys. Rev. 131, 2036 (1963).

25. Pedrotti, L. S. and D. C. Reynolds, "Energy Model for Edge Emission in CdS," Phys. Rev. 120, 1664 (1960).

26. Bueget, J. and G. T. Wright, "Electron Energy Levels in Cadmium Sulfide Single Crystals," British J. Appl. Phys. 16, 1457 (1965).

27. Lorentz, M. R. and H. H. Woodbury, "Double Acceptor Defect in CdTe," Phys. Rev. Letters 10, 215 (1963).

28. Bube, R. H. and L. A. Barton, "The Achievement of Maximum Photoconductivity Performance in Cadmium Sulfide Crystals," RCA Review 20, 564 (1959).

29. Woods, J. and K. H. Nichols, "Photochemical Effects in Cadmium Sulfide Crystals," British J. Appl. Phys. 15, 1361 (1964).

30. Brophy, J. and J. Robinson, "Frequency Factor and Energy Distribution of Shallow Traps in CdS," Phys. Rev. 118, 959 (1959).

31. Brophy, J. J., "Trapping and Diffusion in the Surface Region of CdS," Phys. Rev. 119, 591 (1960).

32. Lambe, John and Clifford C. Klick, "Model for Luminescence and Photoconductivity in the Sulfides," Phys. Rev. 98, 909 (1955).

33. Bube, R. H., G. A. Dussel, C. Ho and L. D. Miller, "Determination of Electron Trapping Parameters," J. Appl. Phys. 37, 21 (1966).

34. Bube, Richard H., "Infrared Quenching and a Unified Description of Photoconductivity Phenomena in CdS and CdSe," Phys. Rev. 99, 1105 (1955).

35. Bryant, F. J. and A. F. J. Cox, "Heat Treatment Effects in CdS," British J. Appl. Phys. 16, 1065 (1965).

36. Mark, P., "The Role of Chemisorption in Current Flow in Insulating Cadmium Sulfide Crystals," J. Phys. Chem. Solids 26, 959 (1965).

37. Litton, C. W. and D. C. Reynolds, "Edge Emission in CdS Crystals That Show Mechanically Excited Emission," Phys. Rev. 125, 516 (1962).

38. Wang, S., Solid State Electronics, McGraw-Hill, New York, 1966.

39. Bube, R. H. and H. E. MacDonald, "Effect of Photoexcitation on the Mobility in Photoconducting Insulators," Phys. Rev. 121, 473 (1961).

40. Woods, J., "Changes in Conductivity Resulting from Breakdown in CdS Single Crystals," Proc. Phys. Soc. 69, 975 (1956).

41. Bube, R. H., "Comparison of Surface-Excited and Volume-Excited Photoconduction in Cadmium Sulfide Crystals," Phys. Rev. 101, 1668 (1956).

42. Faeth, P. A., "On the Trapping Level Disposition in Cadmium Sulfide," J. Electrochem. Soc. 115, 440 (1968).

43. Shear, H., E. A. Hilson, and R. H. Bube, "Oxygen Chemisorption Effects on Photoconductivity in Sintered Layers," J. Electrochem. Soc. 112, 997 (65).

44. Robinson, Al, and R. H. Bube, "Photo-Hall Studies of Oxygen Adsorption Effects on Photoconductivity in Sintered", J. Electrochem. Soc. 112, 1002 (65).

45. Eastman, P. C., and Brodie, D. E. "CdS Films with Adjustable Carrier Density in any Given Sample," Proc. IEEE, 53, 512 (1965)

46. Garlick, G. F. J., and A. F. Gibson, "Electron Traps and Dielectric Changes in Phosphorescent Solids," Proc. Roy. Soc. A, 188, 485 (47)

47. Dussel, G. A. and R. H. Bube, "Electric Field Effects in Trapping Processes", J. Appl. Phys, 37, 2497 (1966).

48. Lambe, J. J., C. C. Klick, and D. L. Dexter, "Nature of Edge Emission in CdS," Phys Rev 103, 1715 (1956).

49. Kallman H, and P. Mark, "De-Excitation of ZnS and ZnCdS Phosphors by Electric Fields," Phys. Rev. 105, 1445 (1957)

50. Nozieres, P. and D. Pines, "Electron Interaction in Solids, General Formulation," Phys. Rev. 109, 741 (1958)

51. Nozieres, P. and D. Pines, "Electron Interaction in Solids. Collective Approach to the Dielectric Constant," Phys. Rev. 109, 762 (1958)

52. Levine, S. N., Quantum Physics of Electronics. MacMillan, New York, 1965

53. Kittel, C, Introduction to Solid State Physics, John Willey & Sons, New York, 1953.

54. Kallmann, H. Kramer, B, and Mark, P, "Impednace Measurements on CdS Crystals," Phys. Rev. 99, 1328 (1955)

55. Kallmann, H., B. Krammer, and G. Spruch, "AC Impedance Measurements on Insulated CdS Crystals," Phys. Rev. 119, 628, (59).

56. Broser, I. P. Brumm, and C. Reuber, "Der Photodielektrische Effekt in CdS - Einkristallen," Zeitschrift fur Physik 179, 367 (1964)

57. Garlick, G. F. J. and A. F. Gibson, "The Electron Trap Mechanism of Luminescence in Sulphdie and Silicate Phosphors," Proc. Phys. Soc. London 60A, 574 (48)

58. Haering, R. R. and E. N. Adams, "Theory and Application of Thermally Stimulated Currents in Photoconductors," Phys. Rev. 117, 451 (60).

59. Prince, M. B., "Silicon Solar Energy Converters," J. Appl. Phys. 26, 534 (1955)

60. Burns, J. W., "Research on Materials Exhibiting Photovoltaic Phenomona ASTIA AD 298 811

61. Wolf, M., "Limitations and Possibilities for Improvement of Photovoltaic Solar Energy Converters. Part I: Considerations for Earth's Surface Operation," Proc. IRE 48, 1246 (1960).

62. Jones, H. A., and I. Langmuir, "Specific Characteristics of Ideal Tungsten Filaments", G.E. Review, 30, 312 (1927)

ADDITIONAL REFERENCES

1. Anderson, Wm, "Maximizing the Performance of Photoconductors, C# AF 19-604-8353 ASTIA AD 278 050.

2. Auth, J., "The Influence of Temperature and Environmental Conditions on the Photodectromagnetic Effect in CdS," J. Phys. Chem Sol. 18, 261 (1961)

3. AuthJ. and E. A. Niekisch, "Charge Carrier Diffusion Length in CdS," Zeit Fuer Dat 10a, 1035 (1955)

4. Baer, W. S. and Dexter, R. N., "Electron Cyclotron Resonance in CdS Phys. Rev. 135, A1388 (1964)

5. Balkanski, M. and R. D. Waldron, "Internal Photoeffect and Exciton Diffusion in CdS and ZnS" Phys. Rev 112, 123 (1958)

6. Bancie-Grillot M, E. F. Gross, E. Grillot and B. S. Razbiran, "Linear Florescence and Adsorption of CdS at 4.2°K," Opt. and Spec. 6, 461 (1959)

7. Berlincourt, D. H. Jaffee, and L. Shiozawa, "Electroelastic Properties of the Sulfides, Selenides, and Tellurides of Zinc and Cadmium," Phys. Rev 129, 1009 (63)

8. Billups, R. R., et. at., "Preparation and Performance of Sintered CdS Phtoconductors," ASTIA AD 212 580 (59)

9. Bogdankevich, O. V., and A. G. Devyatkow and V. S. Orlor, "Mechanism of the Generation of Radiation in Electron Excited Cadmium Sulfide," Sov. Phys-Semicon. 1, 543 (1967)

10. Braunstein, R, and Ockman, N, "Optical Double Photon Absorption in CdS," Phys. Rev. 134, A499 (1964).

11. Brodin, M. S., S. V. Zakreskii, V. S. Mashkcvich and V. Ya. Reznichenko, "Mechanism of Generation of Laser Radiation in CdS_xCdSe_{1-x} Crystals in the Case of Two-Photon Excitation," Sov. Phys-Semicon. 1, 495 (1967).

12. Brophy, J. J., "Current Noise and Distributed Traps in CdS," Phys. Rev 122, 26 (1961).

13. Broser, I., "Luminescence (with Particular Reference to Inorganic Phosphors)," Bristish J. Appl. Phys, Supplement 4 (1955).

14. Broser, I. J. H. Maier and H. J. Schulz, "Fine structure of the Infrared Absorption and Emission Spectra of Cu^{++} in CdS," Phys. Rev 140, A2135 (1965)

15. Broser, I. and H. Kallman, "The Dissipation of Luminescence in Photo-materials by Alpha Particles," Zeit Frer. Nat. 5a, 381 (1950)

16. Browne, P. F., "Infrared Luminescence of Zinc and Cadmium Sulfide Phosphors," J. of Electronics 2, 1 (1956)

17. Bube, R. H. "Photoconductivity of the Sulfide,Selenide,and Telluride of Cd and Zn," Proc. IRE 43, 1936 (1955)

18. Bube, R. H., "Temperature Dependence of the Width of the Band Gap in Several Photoconductors," Phys. Rev 98, 431 (1955)

19. Bube, R. H., "Photoconductivity and Crystal Imperfections in CdS Crystals Determination of Characteristic Photoconductivity Quantities," J. Chem Phys 23, 18 (1955)

20. Bube, R. H. "Photoconductivity Speed of Response For High Intensity Excitation in CdS and CdSe," J. Appl. Phys. 27, 1237 (1956)

21. Bube, R. H., "Mechanism of Photoconductivity in Microcrystalline Powders," J. Appl. Phys. 31, 2239 (1960)

22. Bube, R. H.,"Imperfection Ionization Energies in CdS-type Materials by Photoelectric Techniques, Solid State Physics, Vol II, Academic Press, New York, 1960

23. Bube, R. H., "Cross-section Ratios of Sensitizing Centers in Photo-conductors," J. Appl. Phys. 32, 1707 (1961).

24. Bube, R. H. and A. B. Dreeben, "Dependence of the Hole Ionization Energy of Imperfections in CdS on Impurity Concentration," Phys Rev 115, 1578 (1959)

25. Bube, R. H., E. L. Lind and A. B. Dreeben,"Properties of CdS Crystals with High Impurity Concentrations," Phys. Rev, .28 532, (1962).

26. Bube, R. H. and S. M. Thomsen, "Photoconductivity and Crystal Imperfections in CdS Crystals," J. Chem Phys. 23, 15 (1955)

27. Cardoma, M, M. Weinstein, G. A. Wolff, "Ultraviolet Reflection Spectrum of CdS (Cubic)," Phys. Rev. 140, 633 (1965)

28. Cole, C. F., "The Dielectric Constant of a Semiconductor as Related to the Intrinsic Activation Energy," Proc. IRE 50, 1856 (62).

29. Degenford, J. E.and P. D. Coleman, "A Quasi-optics Perturbation Technique for Measuring Dielectric Constants," Proc. IEEE 54, 520 (1966)

30. DiDomenico, M. and L. K. Anderson, "Microwave Signal to Noise Performance of CdS Bulk Photoconductive Detectors," Proc. IEEE 52, 815, (1964)

31. Diemer G. et al, "An Analysis of Mixed Ambipolar and Excitation Diffusion in CdS Crystals," Phys. and Chem. Solids 8, 182 (1959)

32. Diemer G, and W. Hoogenstraaten, "Evidence for Hole Mobility in CdS," Physica 22, 172 (1956).

33. Diemer G, and W. Hoogenstraaten, "Ambipolar and Excitation Diffusion in CdS Crystals," Phys. and Chem. Solids 2, 118 (1957)

34. Dropkin, J. J., "Photoconduction in Phosphors," ASTIA AD 41 210

35. Drozd, L., and V. L. Levshin, "Location of Energy Levels in ZnS-CdS Phosphors," Opt. and Spect. 11, 348 (1961)

36. Dussel G. A., and R. H. Bube, " Further Considerations on a Theory of Superlinearity in CdS and Related Materials," J. Appl. Phys. 37, 12 (1966)

37. Eremenko, "Investigation of the Photoconductivity Response Spectrum of Mixed CdS - CdSe Monocrystals at 77 and 20 Degrees K," Sov. Phys. - Solid State, 2, 2320 (1961)

38. Furloug, L. R., and Ravilious, C. F., "Low Temperature Luminescence and Absorption of CdS," Phys. Rev. 98, 954 (1954)

39. Gildea, H. "Field Strength Effects in CdS Single Crystals," ASTIA AD 209 817 (58).

40. Gross, E. F. and B. V. Novikov, "Remarks on the Structure of the Spectral Curve of the Internal Photoeffect in CdS Crystals," Sov. Phys. Tech. Phys. 3, 729 (1958)

41. Gross, E. F., and B. V. Novikov, "The Fine Structure of Photoconductivity Spectral Response Curves for CdS Crystal," Sov. Phys. - Solid State 1, 321 (1959).

42. Gross, E. F., and B. V. Novikov, "The Effect of the Mechanical Treatment of the Surface on the Fine Structure of the Photoconductivity Response in CdS Crystals," Sov Phys. - Solid State 1, 1723 (1960)

43. Hadley, C. P. and E. Fisher, "Sintered CdS Photoconductive Cells," RCA Rev. 20, 635 (1959)

44. Hall, R. N., and J. H. Racett, "Band Structure Parameters Deduced from Tunneling Experiments," J. Appl. Phys. Supp. to V 32, 2078 (1961)

45. Halsted, R. E., E. F. Apple, and J. S. Prener, "Two Stages Optical Excitation in Sulfide Phosphors," Phys. Rev. Letters 2, 420 (1959)

46. Halsted, R. E., and B. Segal, "Double Acceptor Florescence in II-VI Compounds, " Phys. Rev. Letters 10, 392 (1963)

47. Handler, P., "Optical Properties of Space-Charge Regions," Phys. Rev. 137, A1862 (1965)

48. Henry, C. H., "Coupling of Electromagnetic Waves in CdS," Phys. Rev. 143, 627 (1966).

49. Jaszczyn-Kopec, P. J. Gallagher, H. Kallman, and B. Kramer, "Electron and Hole Trapping ZnS Phosphors," Phys. Rev. 140, 1309 (1965).

50. Kallmann, H., "Solid State Radiation-Induced Phenomena," ASTIA AD 277-734.

51. Kallmann, H, B. Kramer, and P. Mark, "De-Excitation of ZnS and ZnCdS Phosphors by Electric Fields," Phys. Rev. 109, 721 (1958)

52. Kallmann, H. B. Krammer, and A. Perlmutter, "Infrared Stimulation and Quenching of Photoconductivity in Luminescent Powders," Phys. Rev. 99, 391 (1955)

53. Kindig, N. B. and Spicer, W. E., "Band Structure of CdS - Photoemission Studies," Phys. Rev. 138, A561 (1965)

54. Kikuchi, M., and S. Iizima, "Avalanche Electroluminescence in CdS Single Crystals," J. Phys. Soc. Japan 14, 852 (1959).

55. Kikuchi, M. and S. Iizima, "Quenching Effect of the Photoconductivity Decay in CdS," J. Phys. Soc. Japan 14, 856 (1959)

56. Kitamura, S., "Effect of Oxygen upon Sintered CdS Photoconducting Films," J. Phys. Soc. Japan 15, 2343 (1960)

57. Kitorchenko, P. G. and V. I. Ustyanov, "Kinetics of Gamma Conductivity in CdS Crystals," Sov. Phys. - Solid State 4, 1241 (1963)

58. Klick, C. C., "Luminescence and Photoconductivity in CdS at the Absorption Edge," Phys. Rev. 89, 274 (1953)

59. Kroger, F. A, and H. J. G. Meyer, "Edge Emission of ZnS, ZnO, and CdS and Its Relation to the Lattice Vibrations of These Solids," Physica 20, 1149 (1954)

60. Kulp, B. A., K. A. Gale, and R. G. Schulze, "Impurity Conductivity of Single Crystal CdS," Phys. Rev. 140, 252 (1965)

61. Kulp, B. A., and R. H. Kelley, "P-type Photoconductivity and Infrared Quenching in Electron Bombarded CdS," J. Appl. Phys. 32, 1290 (1961)

62. Kushida, T. and A. H. Silver, "Nuclear Magnetic Resonance in Single Crystal of CdS," Phys. Rev. 137, A1591 (1965)

63. Langer, D. W., "Temperature and Pressure Dependence of the Index of Refraction of CdS," J. Appl. Phys. 37, 3530 (1966)

64. Liebson, S. H., "Surface Recombination of CdS," J. Chem. Phys. 23, 1732 (1955).

65. Litton, C. W. and D. C. Reynolds, "Double Carrier Injection and Negative Resistance in CdS," Phys. Rev. 133, A536 (1964).

66. Lorenz, M. R. Aven, M. and H. H. Woodbury, "Correlation between Irradiation and Thermally Induced Defects in II-VI Compounds," Phys. Rev. 132, 143 (1963)

67. Ludwig, W., "Photovoltaic Effects in CdS Single Crystals," Physics Statue Solidi 3, 1738 (1963)

68. Luyckx, A. "Electric Polarization of Cd Single Crystals and Photo-Magneto-Electric Effects," ASTIA AD 288 222

69. MacArthur, J. W., "Electron Mobility in CdS," Phys. Rev. 86, 615 (1952)

70. Marchenko, A. I., "Some Properties of Gold Doped CdS Monocrystals," Sov. Phys - Solid State 3, 1658, (1962)

71. Mark, P., "Ambipolar Diffusion of Free Carriers in Insulating CdS," Phys. Rev. 137, A203 (1965)

72. Marshall, R. and S. S. Mitra, "Optically Active Phonon Processes in CdS and ZnS," Phys. Rev. 134, A1019 (1964)

73. Masumi, T., "Dielectric Susceptibility Tensor in CdS," J. Phys. Soc. Japan 14, 1140 (1959)

74. McIrvine, E. C., "Phenomenology of Impurity Conduction in Semiconductors," J. Phys. Chem Solids 15, 356 (1960)

75. Medcalf, W. E. and R. H. Fahrig, "High-Pressure, High Temperature Growth of CdS Crystals," J. Electrochem. Soc. 105, 719, (1958)

76. Moore, A. R. and R. W. Smith, "Effect of Traps on Acoustoelectric Current Saturation in CdS," Phys. Rev. A1250 (1965)

77. Mort, J., and W. E. Spear, "Hole Drift Mobility and Lifetime in CdS Crystals," Phys. Rev. Letters 8, 314 (1962)

78. Muller, R. S. and B. G. Watkins, "Hall Effect Studies in Deposited CdS Thin Films," Proc. IEEE 52, 425 (1964).

79. Nelson, R. C., "Preparation of Photoconductive Films of CdS," J. Opt. Soc. Amer. 45, 774 (1955).

80. Nine, H. D., and R. Trvell, "Photosensitive-Ultrasonic Properties of CdS," Phys. Rev. 123, 799 (1961).

81. Nottingham, W. B., Preparation and Characteristics of Solid Luminescent Materials, Wiley, New York (1948).

82. Ogawa, T., "Measurement of the Electrical Conductivity and Dielectric Constant without Contacting Electrodes," J. Appl. Phys. 32, 583 (1961).

83. Ormont, B. F., and A. Nauk, "On the Relation between Energy, Electro-Physical, and Mechanical Properties of Semiconductors," Sov. Phys. - Doklady 124, 129 (1959).

84. Packard, J. R., D. A. Campbell and W. C. Tait, "Evidence for Indirect Annihilation of Free Excitons in II-VI Semiconductor Lasers," J. Appl. Phys. 38, 5255 (1967).

85. Paritskii, L. G., and S. M. Ryvkin, "Nonlinear Photoconductive Relaxation Processes in the Presence of Trapping Levels," Sov. Phys.-Solid State 3, 1631 (1962).

86. Pedrotti, F. L., and D. C. Reynolds, "Spin-Orbit Splitting in CdS:Se Single Crystals," Phys. Rev. 127, 1584 (1962).

87. Redfield, D., "Effect of Charged Surfaces on the Optical Absorption Edge," Phys. Rev. 140, A2056 (1965).

88. Reynolds, D. C., "Temperature Dependence of Edge Emission in CdS," Phys. Rev. 118, 478 (1960).

89. Reynolds, D. C., and C. W. Litton, "Edge Emission and Zeeman Effects in CdS," Phys. Rev. 132, 1023 (1963).

90. Rose, A., "Recombination Processes in Insulators and Semiconductors," Phys. Rev. 97, 322 (1955).

91. Ryvkin, S. M., and B. M. Konovalenko, "Dependence of Induced Conductivity in CdS on the Energy of Exciting Electrons," Sov. Phys.-Solid State 1, 1606 (1960).

92. Serdyuk, V. V., and T. Y. Seera, "The Long-Wavelength Photosensitivity and Infrared Quenching of Photocurrent in CdS Single Crystals," Sov. Phys. - Solid State 4, 761 (1962).

93. Shaw, D., "Photosensitivity and Speed of Response in CdS," British J. Appl. Phys. 12, 337 (1961).

94. Sheinkman, M. K., "Photoconductivity Mechanism in CdS Type Single Crystals," Sov. Phys. - Solid State 2, 1046 (1960).

95. Shenker, H., "Low-Field Breakdown, Non-Ohmic Conductivity, and Photoconductivity of CdS at Low Temperatures," J. Chem. Phys. Solids 19, 1 (1961).

96. Shirafugi, J., and Y. Invishi, "Effects of Vacancies on Pulse Photoconductions in CdS Single Crystals," J. Phys. Soc. Japan 16, 832 (1961).

97. Smith, R. W., "Edge Electroluminescence from CdS Crystals at Low DC Fields," Bull. Amer. Phys. Soc. Ser 1, 30, 30 (1955).

98. Smith,R.W., "Properties of Ohmic Contacts to Cds Single Crystals," Phys. Rev. 97, 1525 (1955).

100. Smith, R. W., "Low-Field Electroluminescence in Insulating Crystals of CdS," Phys. Rev. 105, 900 (1957).

101. Smith, R. W., "Properties of Deep Traps Derived from Space-Charge-Current Flow and Photoconductive Decay," RCA Rev. 20, 69 (1959).

102. Smith, R. W., and A. Rose, "Space-Charge Limited Currents in Single Crystals of CdS," Phys. Rev. 97, 1531 (1955).

103. Sokolskaya, I. L., and G. P. Shcherbakrov, "Study of Strong Field Effects in Field Emitting Crystals of CdS," Sov. Phys. - Solid State 3, 120 (1961).

104. Spear, W. E., and J. Mort, "Electron and Hole Transport in CdS Crystals," Proc. Phys. Soc. 81, 130 (1963).

105. Stupp, E. H., "Photoconductivity in CdS," J. Appl. Phys. 34, 163 (1963).

106. Svechnikov, S. V., "Characteristics of the Additional Conductivity Induced in Single Crystal CdSe by X-Irradiation," Sov. Phys.-Tech. Phys. 2, 2320 (1957).

107. Svechnikov, S. V., and V. T. Aleksandrov, "Certain Properties of CdSe and CdTe Monocrystals," Sov. Phys. - Tech. Phys. 2, 842 (1957).

108. Tait, W. C., J. R. Packard, G. H. Dierssen, and D. A. Campbell, "End-Pumped Laser Emission from Cadmium Sulfide Selenide Bombarded by an Electron Beam," J. Appl. Phys. 38, 3035 (1967).

109. Tell, B., T. C. Damen and S. P. S. Porto, "Raman Effect in CdS," Phys. Rev. 144, 771 (1966).

110. Thomas, D. G., and J. J. Hopfield, "Bound Exciton Complexes," Phys. Rev. Letters 7, 316 (1961).

111. Thomas, D. G., and J. J. Hopfield, "Fluorescence in CdS and Its Possible Use for an Optical Maser," J. Appl. Phys. 33, 3243 (1962).

112. Thomas, D. G., and J. J. Hopfield, "Optical Properties of Bound Exciton Complexes in CdS," Phys. Rev. 128, 2135 (1962).

113. Thomas, D. G., J. J. Hopfield, and M. Power, "Excitons and the Absorption Edge of CdS," Phys. Rev. 119, 570 (1960).

114. Thomson, S. M., and R. H. Bube, "High-Sensitivity Photoconductor Layers," Rev. Sci. Inst. 26, 664 (1954).

115. Tippins, H. H., and F. C. Brown, "Magnetoresistance of Silver Bromide," Phys. Rev. 129, 2554 (1963).

116. Van Gool, W., "Fluorescence and Photoconduction of Silver Activated CdS," Philips Res. Repts. 13, 157 (1958).

117. Vitrikhovskii, N. I., and I. B. Mizetskaya, "Mixed ZnS-CdS Monocrystals and Some of their Properties," Sov. Phys. - Solid State 2, 2301 (1961).

118. Wang, W. C., and J. Pau, "The Effect of Nonuniform Resistivity on Nonohmic Behavior in CdS," Proc IEEE 53, 330 (1965).

119. Wheeler, R. G., "Multiplet Structure of Excitons in CdS," Phys. Rev. Letters 2, 463 (1959).

120. Williams, R., "High Electric Fields in CdS. Field-Effect Constriction of Current flow and Breakdown," Phys. Rev. 123, 1645 (1961).

121. Woodbury, H. H., "Diffusion of Cd in CdS," Phys. Rev. 134, A492 (1964).